ANALYSIS AND COMPUTATION OF TRAVELING WAVE SOLUTIONS FOR BISTABLE NONLINEAR DIFFERENTIAL-DIFFERENCE EQUATIONS

by

Christopher Erhart Elmer

A thesis submitted to the Faculty and the Board of Trustees of the Colorado School of Mines in partial fulfillment of the requirements for the degree of Doctor of Philosophy (Mathematical and Computer Sciences).

Golden, Colorado
Date 9-2-98

Signed: 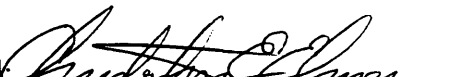
Christopher Erhart Elmer

Approved: 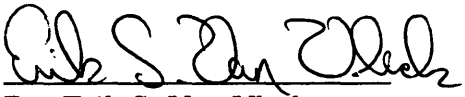
Dr. Erik S. Van Vleck
Thesis Advisor

Golden, Colorado
Date 9/2/98

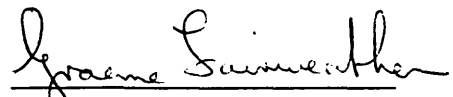
Dr. Graeme Fairweather
Professor and Head
Department of Mathematical and
Computer Sciences

ABSTRACT

We consider traveling wave solutions to bistable differential-difference equations obtained using both analytical and numerical techniques. The differential-difference equations of concern include spatially continuous and spatially discrete reaction-diffusion, damped wave, and wave equations. We explore these equations as constant coefficient problems and as variable diffusion and inhomogeneous equilibria state problems.

TABLE OF CONTENTS

LIST OF FIGURES

LIST OF TABLES

ACKNOWLEDGEMENTS

Many thanks go to my committee members, Dr. Steven Pruess, Dr. Graeme Fairweather, Dr. Mark Lusk, Dr. John Berger, and Dr. James Ely, for their careful and thorough proofreading of my thesis.

To the engineering faculty members, Dr. John Berger and Dr. Mark Lusk, I am grateful for their morel support as well as their tolerance of a mathematician.

I thank Dr. Graeme Fairweather for his fatherly support.

To Dr. Steven Pruess, Dr. Ardel Boes, Dr. William Law, Dr. Frank Hagin, Barbara Tinnes, Dr. Samuels, Dr. Dave Hale, and Dr. Erik Van Vleck I owe an immense debt and feel a deep sense of gratitude for seeing and showing me my potential.

I thank my advisor and mentor Dr. Erik Van Vleck for many things; in particular, the freedom given to work independently, the continual support and direction given throughout my graduate experience, and the foresite necessary to launch my career.

DEDICATION

To Loki the WonderPup and Princess the Beautiful, my very best friends, who make life a pretty good deal; and to all of my family, for their continual support and love.

Chapter 1

INTRODUCTION

We consider both analytically and numerically obtained traveling wave solutions of differential-difference equations of the form

$$\alpha\dot{u}(\eta,t)+\beta\ddot{u}(\eta,t)-\gamma\Delta u(\eta,t)$$
$$=L(u(\eta,t),u(\eta+r_1,t),...,u(\eta+r_N,t))-f(u(\eta,t),a). \qquad (1.1)$$

The left-hand side of (1.1) is the "differential" portion of the equation where Δ represents the Laplacian operator and " $\dot{}$ " indicates the derivative with respect to time. The operator L is a linear difference operator of a form that represents discrete diffusion. The function f is a nonlinear operator of bistable type which depends on a parameter a. The $r_i \in \mathbb{R}$, $i = 1, ..., N$, represent "shifts" of the solution function with respect to the spatial variable.

Throughout the modeling community interest is increasing in models of time de-

pendent differential equations that are discrete in space. In many areas of science, systems exhibit a spatially discrete structure. This spatially discrete structure is often the result of an underlying spatial lattice which affects the evolution and dynamics of the system. The representation in (1.1) allows the microscopic lattice structure of a system to have macroscopic effects on the solution behavior, in particular we note that the discrete Laplacian, L, allows the phenomena of anisotropy and propagation failure (phenomena that continuous Laplacian models fail to represent). Some of the fields of research in which we see the effects of a spatially discrete structure and can be modeled by equations of the form of (1.1) include material science (crystal growth and liquid-solid materials) [8], [18], [37], chemical reaction theory (chemical reactors) [24], [43], image processing and pattern recognition (cellular neural networks and optical memory) [27], [15], [16], [17], [51], [63], physics (relativistic quantum mechanics) [56], [57], [58], [62],and biology (myelinated nerve axons and myocardium) [5], [22], [41], [42], [65], [6], [23], [40].

Our interest in traveling wave solutions follows the extensive studies of traveling wave solutions to partial differential equations such as the reaction-diffusion equation

$$u_t = \alpha u_{xx} - f(u), \qquad u : (x,t) \to I\!R \quad \text{for} \quad x,t \in I\!R, \tag{1.2}$$

with $\alpha > 0$ and $f : \mathbb{R} \to \mathbb{R}$ defined as

$$f(u) = u(u-a)(u-1), \qquad 0 < a < 1, \tag{1.3}$$

where a is a detuning parameter. By traveling wave solution, $\phi : \mathbb{R} \to \mathbb{R}$, we mean solutions of the form

$$u(x,t) = \phi(x - ct) \tag{1.4}$$

where $c \in \mathbb{R}$ is the unknown wave speed which is found as part of the solution, [26]. Substituting the traveling wave ansatz (1.4) into the reaction-diffusion partial differential equation (1.2) we obtain

$$-c\phi'(\xi) = \phi''(\xi) - f(\phi(\xi)) \tag{1.5}$$

where $\xi = x - ct \in \mathbb{R}$. Equilibrium solutions to (1.2) and (1.5) are the simplest solutions to obtain. The solution types that are of interest in this work are solutions, waves, that connect the two "stable" equilibria, $u = 0, 1$. This requires imposing the boundary conditions

$$\phi(-\infty) \equiv \lim_{\xi \to -\infty} \phi(\xi) = 0, \qquad \phi(\infty) \equiv \lim_{\xi \to \infty} \phi(\xi) = 1.$$

If $x \in \mathbb{R}^n$ and we replace u_{xx} in (1.2) by $\Delta u = \sum_{k=1}^{n} D_{x_k x_k}$, we once again obtain

(1.5). The only difference is the traveling wave ansatz is now $u(x,t) = \phi(x \cdot \sigma - ct)$, where the vector $\sigma = (\sigma_1, \sigma_2, ..., \sigma_n)^T \in \mathbb{R}^n$, such that $\sum_{k=1}^{n} \sigma_k^2 = 1$, is normal to the traveling wave front. Equation (1.5) is independent of the direction vector σ and dimension n.

A spatially discrete analog of the partial differential equation (1.2) is the differential-difference equation

$$u_t(x,t) = \alpha[u(x+1,t) - 2u(x,t) + u(x-1,t)] - f(u), \tag{1.6}$$
$$u : (x,t) \to \mathbb{R} \quad \text{for} \quad x \in \mathbb{Z}, t \in \mathbb{R},$$

with bistable nonlinearity (1.3), which defines a countably infinite system of ordinary differential equations indexed by points on a spatial lattice. If we considered $x \in \mathbb{R}$ we would have an uncountably infinite number of such systems. Substituting the traveling wave ansatz $u(x,t) = \phi(x - ct)$ into (1.6) we obtain

$$-c\phi(\xi) = \alpha[\phi(\xi+1) - 2\phi(\xi) + \phi(\xi-1)] - f(u). \tag{1.7}$$

Now suppose that $x \in \mathbb{Z}^n$. Then the operator $[u(x+1,t) - 2u(x,t) + u(x-1,t)]$ is replaced by the n dimensional operator $\sum_{k=1}^{n}[u(x+e_k,t) - 2u(x,t) + u(x-e_k,t)]$ with e_k a unit vector of length n with 1 as the k^{th} element. The set of vectors $\{e_k\}_{k=1}^{n}$ form a basis for $\mathbb{R}^n$. This particular set of basis vectors represents a rectangular lattice.

Other choices of bases correspond to other lattices. Substituting the traveling wave ansatz $u(x,t) = \phi(x \cdot \sigma - ct)$ into the n dimensional version of (1.6), we obtain

$$-c\phi(\xi) = \alpha \sum_{k=1}^{n} [\phi(\xi + e_k \cdot \sigma) - 2\phi(\xi) + \phi(\xi - e_k \cdot \sigma)] - f(u), \tag{1.8}$$

which, unlike (1.5), does depend on the direction vector σ and on the dimension n. Another property that the traveling wave equations (1.7) and (1.8) exhibit, that their continuous counterparts do not, is propagation failure, failure of the traveling wave to propagate over a nontrivial interval of the detuning parameter a [10].

The class of equations (1.1) that we are interested in includes both (1.2) and (1.6). This class also includes equations that contain both a spatially discrete and spatially continuous diffusion term, i.e., both Δu and $\sum_{k=1}^{n}[u(x + e_k, t) - 2u(x,t) + u(x - e_k, t)]$. By treating the coefficients of our continuous and discrete diffusion terms as parameters, we are able to not only study solutions for the partial differential and infinite lattice system forms of the equation, but also to study how the two types of equations are related through various continuation paths. Including a second time derivative, $\beta\ddot{u}$, widens the class of equations and our results to include wave equations. While constant coefficient systems provide many interesting phenomena, equations with variable diffusion coefficients and equations with varying equilibrium states are also included.

If $\alpha \neq 0$ and $c \neq 0$, then (1.8) is a delay equation with both forward and backward delays, a functional differential equation of mixed type. Often in the modeling community, theory is developed based on the notion that phenomena have a local nature, that phenomena are independent of nonlocal information. Models are based on the variable and the local change of that variable. In reality, this is only a first approximation approach to many systems. Functional differential equations of mixed type often allow for a more realistic representation. The original foundation of studying the asymptotic behavior of delay equations which depend on energy functions can be traced back to Volterra. Very little work has been done on general systems of such mixed functional equations, except for the work of Rustichini [54], [55] and Mallet-Paret [46], [47]. Propagation failure for one dimension spatially discrete reaction-diffusion equations was studied by Keener [40], [41]. Zinner provided existence and stability of traveling wave solutions for spatially discrete reaction-diffusion equations [67], [68], [69]. In [30], Gao allowed the coefficients of the difference term to be directionally dependent. In [10], Cahn, Mallet-Paret, and Van Vleck provide propagation failure and lattice anisotropy results for traveling wave solutions of two dimensional spatially discrete reaction-diffusion equations with a linearized bistable nonlinearity. Mallet-Paret [47] looked at the global structure of solutions to lattice-differential reaction-diffusion equations. Shen's work includes (1.1) with $\beta = 0$ and nonlinearity $f(u,t)$ which is almost periodic in t [60], [61]. In [38] and [39], Johnston

studied bifurcation phenomena for several bistable nonlinearities. Other investigations into the solutions of mixed equations of the form (1.1) include the works [68], [36], [69], [67], and [14].

We are interested in bistable systems, systems where $f(u)$ can be represented by a (cubic-like) nonlinear function with "stable" zeros at 0 and 1, and an "unstable" zero at the detuning parameter $a \in (0,1)$. In this work we consider three nonlinearities $f(u)$ that are of bistable type which include varying degrees of smoothness. By bistable type we mean that $F(u)$ is double-welled, where $F'(u) = f(u)$. The nonlinearities that we investigate are:

$$f_1(u,a) = d_1 \begin{cases} u & u < a, \\ (u-1) & u > a, \end{cases} \qquad f_1(a) \in d_1[a-1, a], \tag{1.9}$$

$$f_2(u,a) = d_1 u(u-a)(u-1), \tag{1.10}$$

and

$$f_3(u,a) = d_1[a - u + d_2 \log\left(\frac{u(1-a)}{a(1-u)}\right)], \tag{1.11}$$

where $d_1, d_2 \in I\!R^+$. Figures 1.1 and 1.2 illustrate these nonlinearities along with their potential functions F_1, F_2, and F_3 for $a = 1/2$ and $a = 3/4$, respectively. In Figure 1.1 the detuning parameter $a = 1/2$ and we see that the wells in our double well potentials are of equal height. Figure 1.2 demonstrates what happens when a

is shifted away from $1/2$. Here $a = 3/4$ and we see that one well of the double well potential is raised above the other. This causes one phase to "flow" to the other, from 1 to 0 in Figure 1.2. In both figures, we see that the piecewise linear nonlinearity f_1 has no spinodal region. Considering the equilibrium solutions of

$$\dot{u}(\eta, t) = -f(u(\eta, t), a),$$

we see in all of the $F(u)$ curves that $F(0)$ and $F(1)$ lie at the bottom of a potential well and that $F(a)$ lies at a local maximum. Thus we refer to $u = 0$ and $u = 1$ as stable and we refer to $u = a$ as unstable.

This dissertation consists of five chapters, containing mainly original material, along with this introduction and a conclusion. Chapter 2 is an analytical and numerical study of equations of the form

$$\alpha\dot{u}(\eta, t) + \beta\ddot{u}(\eta, t) = \gamma\Delta u(\eta, t) + L_D u(\eta, t) - f(u(\eta, t), a), \tag{1.12}$$

a constant coefficient equation with both a spatially discrete and a spatially continuous diffusion operator, and second time derivative operator. The study of equations that contain both spatially discrete and spatially continuous diffusion operators is virtually nonexistent, as is examining traveling wave solutions to damped wave equations. Section 2.2 consists of our analytical derivation of a solution along with our

$f(u)$

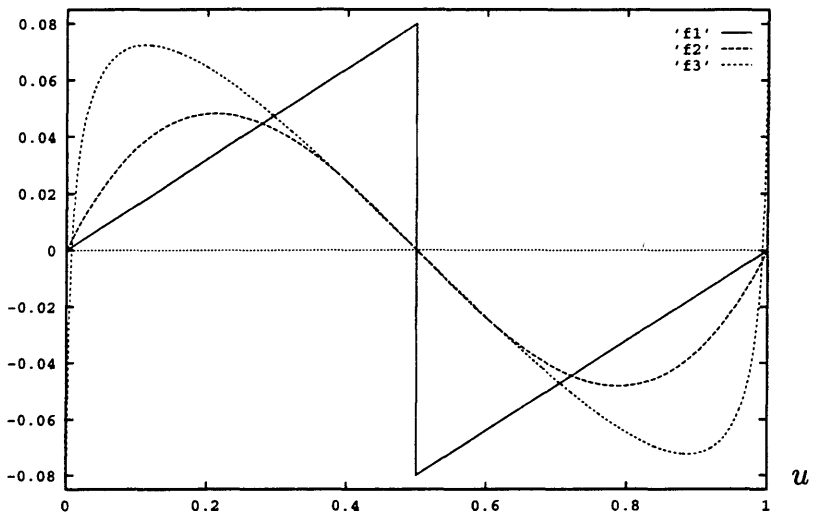

$$f_1(u, 0.5) = 0.16 \begin{cases} u, & u < a \\ u - 1, & u > a \end{cases} \qquad f_2(u, 0.5) = u(u - a)(u - 1)$$

$$f_3(u, 0.5) = 0.4[a - u + 0.1 \log\left(\tfrac{u(1-a)}{a(1-u)}\right)]$$

$F(u)$

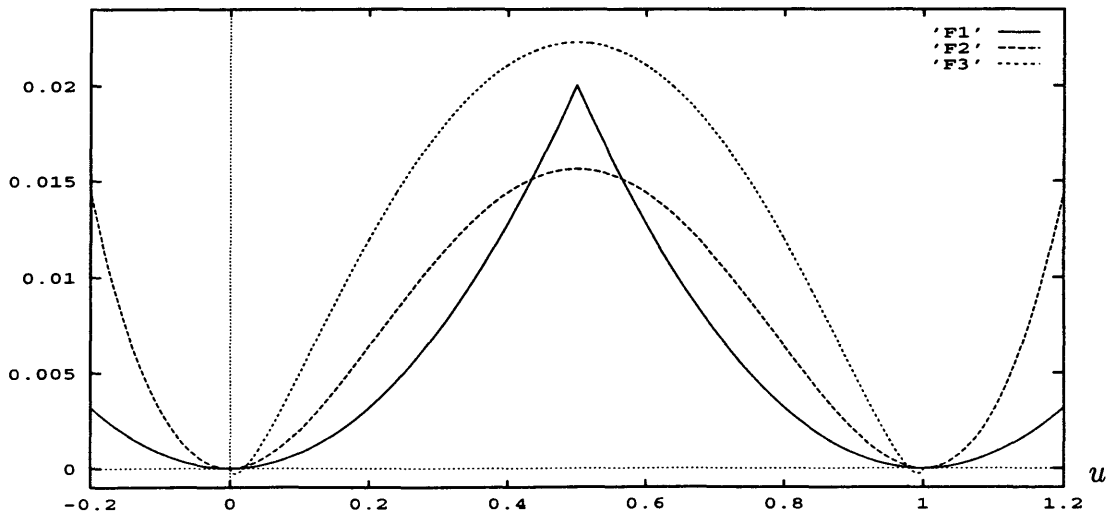

Figure 1.1: Bistable Nonlinearities, $a = 0.5$.

$f(u)$

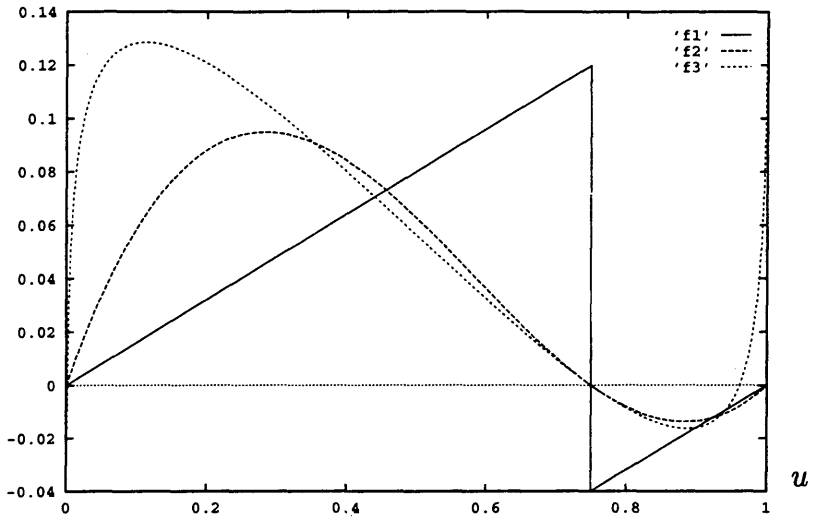

$$f_1(u, 0.75) = 0.16 \begin{cases} u, & u < a \\ u - 1, & u > a \end{cases} \qquad f_2(u, 0.75) = u(u - a)(u - 1)$$

$$f_3(u, 0.75) = 0.4[a - u + 0.1 \log\left(\tfrac{u(1-a)}{a(1-u)}\right)]$$

$F(u)$

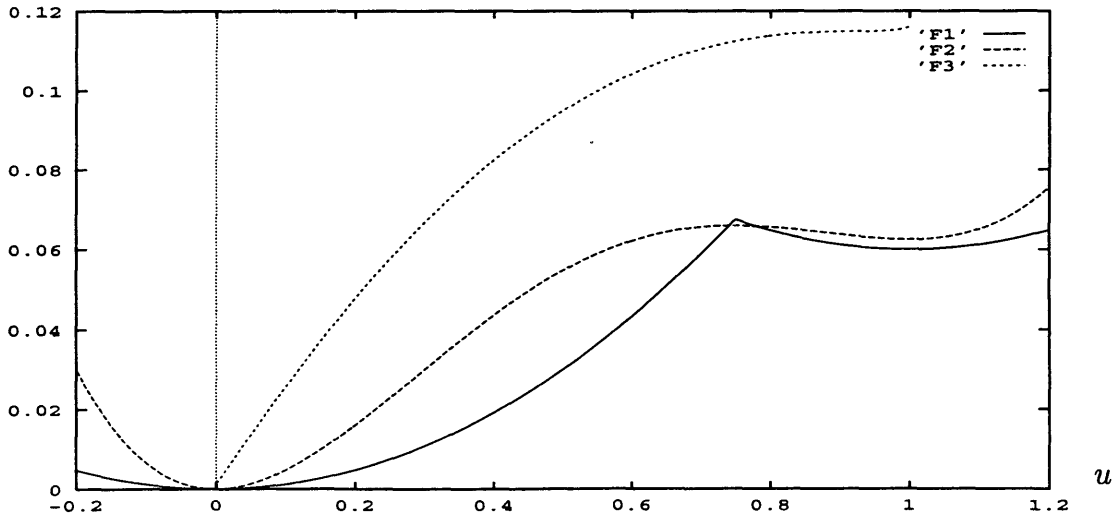

Figure 1.2: Bistable Nonlinearities, $a = 0.75$.

analytically derived results. First we give a complete definition of the problem. This includes discussing boundary conditions and a phase condition. Next we derive a solution including results about monotonicity and smoothness. Even though the equation we are studying contains equations that others have examined, few researchers present explicit solutions to their functional differential equations. We then present the relation between the wave speed of the traveling wave solution and the detuning parameter, $a(c)$, and use it to derive results about the phenomenon of propagation failure and the restriction of the interval for a. The study of propagation failure due to a difference term is relatively new ground. We also provide plots of the $a(c)$ relation. Section 2.3 is dedicated to the numerical solution of our traveling wave equation. Detailed graphical representations of the functional differential equations that this equation encompasses are nonexistent. We first define a numerical method, and then present plots of numerically obtained waveforms. This includes a presentation of the impact of the spatially discrete versus the spatially continuous Laplacian, and a presentation of the solutions in terms of the three classifications, reaction-diffusion, damped wave, and undamped wave. We finish this section with a summary of how the numerical and analytical solutions support each another. Section 2.4 consists of summary remarks.

In Chapter 3 we study equations of the form

$$\dot{u}(\eta,t) = L_D u(\eta,t) - f(u(\eta,t),a),$$

$$L_D u(\eta,t) = \alpha(\eta+1)[u(\eta+1,t) - u(\eta,t)] + \alpha(\eta)[u(\eta-1,t) - u(\eta,t)],$$

where the diffusion coefficient α varies with respect to the spatial lattice. We first derive a solution for periodic $\alpha(\eta)$. This consists of redefining the differential-difference equation with respect to the period of α. Because of the unwieldy nature of the algebra involved in the general periodic solution, we present a detailed example for periodic diffusion of period two. This includes a look at the $a(c)$ relation for this problem. We then discuss an application of the periodic diffusion differential-difference equation, laminate materials.

In Chapter 4 we present a numerical method, a variation on Newton's method. The method is defined and convergence proven for a much larger class of functional differential equations than we study in this work. Our primary tools are results from linear Fredholm operator theory for both differential and difference operators.

In Chapter 5 we present several numerical examples. We show that solutions obtained using nonlinearities f_2 and f_3 exhibit propagation failure and step-like solutions just like the solutions obtained with nonlinearity f_1. We show bifurcation points occurring in an $a(c)$ curve, and we solve problems with inhomogeneous equilibria states.

Chapter 2

ANALYSIS AND COMPUTATION OF TRAVELING WAVE SOLUTIONS FOR BISTABLE CONSTANT COEFFICIENT WAVE, DAMPED WAVE, AND REACTION-DIFFUSION LATTICE DIFFERENTIAL EQUATIONS

In this chapter we consider analytically and numerically obtained traveling wave solutions of lattice-differential equations of the form

$$\alpha\dot{u}(\eta,t) + \beta\ddot{u}(\eta,t) = \gamma\Delta u(\eta,t) + L_D u(\eta,t) - f(u(\eta,t),a), \tag{2.1}$$

where $u(\eta,t)$ maps $\mathbb{R}^n \times \mathbb{R} \to \mathbb{R}$, $\alpha,\beta,\gamma \in \mathbb{R}^+ \cup 0$, $a \in (0,1)$, Δ is the continuous Laplacian operator $\sum_{i=1}^{n} D_{\eta_i,\eta_i}$, and "$\cdot$" and "$\cdot\cdot$" denote differentiation with respect to t. We let L_D be a discrete Laplacian operator defined with respect to an integer

lattice of the form

$$L_D u(\eta, t) = \sum_{k=1}^{n} \varepsilon_k [u(\eta + e_k, t) - 2u(\eta, t) + u(\eta - e_k, t)],$$

where $\varepsilon_k \in \mathbb{R}^+$ and e_k is the unit vector whose kth element equals 1, for $k = 1, ..., n$. The set $\{e_k\}_{k=1}^n$ forms a basis for $\mathbb{R}^n$. Using an ε_k for each dimension allows us to vary the directional dependence, and using e_k for our forward and backward shifts on an integer lattice is equivalent to using a nearest neighbor representation for L_D. Throughout this chapter, we use the piecewise linear representation f_1, (1.9), for f.

Let σ be a vector in $\mathbb{R}^n$ such that $\sum_{i=1}^n \sigma_i^2 = 1$. A solution $u(\eta, t) = \varphi(\eta \cdot \sigma - ct)$ of (2.1), where $\varphi : \mathbb{R} \to \mathbb{R}$, "$\cdot$" denotes the Euclidean dot product, and $c \in \mathbb{R}$ is the unknown constant wave speed, is called a traveling wave solution. Substituting the traveling wave ansatz into (2.1), we obtain the spatially discrete ordinary differential equation

$$-c\alpha\varphi'(\xi) + c^2\beta\varphi''(\xi) = \gamma\varphi''(\xi) + L_T\varphi(\xi) - f(\varphi(\xi), a),$$

or

$$-\kappa_c\varphi'(\xi) - \delta_c\varphi''(\xi) = L_T\varphi(\xi) - f(\varphi(\xi), a), \tag{2.2}$$

where $\delta_c = \gamma - c^2\beta$, $\kappa_c = c\alpha$, $\xi = \eta \cdot \sigma - ct$, and

$$L_T\varphi(\xi) = \sum_{k=1}^{n} \varepsilon_k[\varphi(\xi + e_k \cdot \sigma) + \varphi(\xi - e_k \cdot \sigma) - 2\varphi(\xi)].$$

We present traveling wave solutions for δ_c nonnegative when $\kappa_c \neq 0$ and δ_c positive when $\kappa_c = 0$. The unit vector σ is normal to the wavefront and indicates the direction of the traveling wave with respect to the lattice.

Equation (2.1) includes the continuous and spatially discrete nonlinear wave, damped wave, and reaction-diffusion equations. We present a description of the family of traveling wave solutions defined by (2.1), equivalently (2.2). The parameters in (2.1) allow for continuation between the discrete and continuous Laplacian terms.

We present both analytically and numerically obtained solutions implementing each solution method independent of the other. The analytically obtained solutions are produced using classical methods. Using relaxation, continuation, and fixed point iteration, the numerically obtained solutions are produced using a standard boundary value problem solver. Since the phenomenon uncovered is verified with both solution methods, we have a natural basis for comparison of the two solution techniques. From our analytically obtained solution, we derive a relation between the detuning parameter a, in (1.9), and the wave speed c, from which we generate $a(c)$ plots to help illustrate phenomena we discuss. For all our results, we incorporate the classical

phase condition $\varphi(0) = a$.

For $\kappa_c \in \mathbb{R}$, $\delta_c \geq 0$, with κ_c and δ_c not both equal to zero, we show that a solution $\varphi(\xi)$ of (2.2), with nonlinearity (1.9) and boundary conditions $\varphi(-\infty) = 0, \varphi(\infty) = 1$, exists for all $\xi \in \mathbb{R}$ and is strictly monotone increasing on $\mathbb{R}$. The solution $\varphi(\cdot) \in C(\mathbb{R})$ with $\varphi(\cdot) \in C^1(\mathbb{R})$ if and only if $\delta_c > 0$. The discontinuity in φ' when $\delta_c = 0$ comes from the discontinuity in the nonlinearity that we are using and produces "kinks" in the numerical solution plots. Because of the spatially discrete Laplacian term in (2.1) and (2.2), it is possible for the wave speed c to equal zero for a nontrivial interval of the detuning parameter a (the interval of propagation failure). In fact, there exists an interval of propagation failure if and only if the coefficient of the spatially discrete Laplacian, $\sum_{k=1}^{n} \varepsilon_k$, is not zero and the coefficient on the spatially continuous Laplacian, γ, is zero. Also, for $\gamma = 0$, as $\sum_{k=1}^{n} \varepsilon_k \to 0$, the interval of propagation failure expands to $(0, 1)$. Information about the interval of propagation failure comes from letting c go to zero in the $a(c)$ relation. We also study the $a(c)$ relation in general, when we are not taking $c \to 0$. The relation $a(c)$ is odd and analytic in c for all c if $\delta_c > 0$, and odd and analytic in c for all $c \neq 0$ if $\delta_c = 0$. The relation $a(c) = 1/2$ holds if and only if $\kappa_c = 0$, thus $a(c) = 1/2$ when $\alpha = 0$. For $\kappa_c \neq 0$, the $a(c)$ relation is strictly increasing. If we are solving the reaction-diffusion equation, $\beta = 0$, then $c \in (-\infty, \infty)$ and $a \in (0, 1)$, but if we are solving the damped wave equation, $\beta > 0$, then c is restricted to a proper subinterval of $\mathbb{R}$ and

through the $a(c)$ relation, we see that a is restricted to a proper subinterval of $(0, 1)$. In fact, the range of a for the damped wave equation is symmetric about $a = 1/2$ and the lowest upper and greatest lower bounds can be found with the $a(c)$ relation by setting $c = \sqrt{\gamma/\beta}$ for the upper bound and by setting $c = -\sqrt{\gamma/\beta}$ for the lower bound. As $|c| \to \sqrt{\gamma/\beta}$ the spatially mixed damped wave equation approaches the spatially discrete reaction-diffusion equation. This indicates that these lowest upper and greatest lower bounds on a for the spatially mixed damped wave equation can be found using the $a(c)$ relation for the spatially discrete reaction-diffusion equation with the same α, ε_k's, and σ values. Let's suppose $\delta_c \to 0$, $\kappa_c \to 0$, and that the elements of the direction vector σ are rationally related. Then the solution φ approaches a step function in the limit. For our phase condition a jump discontinuity between steps occurs at $\xi = 0$. The step to the right of $\xi = 0$ is equal to the least upper bound of the interval of propagation failure and the step to the left of $\xi = 0$ is equal to the greatest lower bound of the interval of propagation failure. Hence the jump between steps at $\xi = 0$ is equal in length to the interval of propagation failure. In addition to the above results, the numerical plots of the solution demonstrate the differences in traveling wave solutions of the reaction-diffusion, damped wave, and the undamped wave equation, and the impact of the spatially discrete and the spatially continuous Laplacian terms. We also present contour plots in the κ_c versus δ_c parameter space and the α versus β parameter space which show the level set of a.

Section 2.1 consists of our analytical derivation of a solution along with our analytically derived results for (2.2). First we complete the definition the problem. This includes discussing boundary conditions and a phase condition. Next we derive a solution to (2.2) when κ_c and δ_c are not both zero, including results about monotonicity and smoothness. Then we present the $a(c)$ relation and use it to derive results about the phenomenon of propagation failure and the restriction of the interval for a. We also provide plots of the $a(c)$ relation. For completeness, a brief outline of results when κ_c and δ_c both approach zero is included. The importance of this case is that our traveling wave equation becomes a difference equation. We also show a relation between the function that is produced in the limit and the interval of propagation failure. Section 2.2 is dedicated to the numerical solutions of our traveling wave equation. We first define the numerical method. We then present plots of numerically obtained waveforms. This includes a presentation of the impact of the spatially discrete versus the spatially continuous Laplacian, and a presentation of the solutions in terms of the three classifications, reaction-diffusion, damped wave, and undamped wave. We finish this section with a summary of how the numerical and analytical solutions support one another. Section 2.3 consists of a summary of this chapter. A list of the $a(c)$ plots can be found in Table 2.1 and a list of the solution plots can be found in Table 2.2.

2.1 Analytical Results

We complete the definition of the traveling wave equation (2.2), find an analytical solution to the traveling wave equation, and investigate the phenomena of propagation failure, solution "kinks", restrictions on the wave speed and the detuning parameter, and lattice induced anisotropy.

2.1.1 Background

Because $\varphi = 0$ and $\varphi = 1$ are zeros of $f_1(\varphi)$, in (1.9), it is natural to impose the boundary conditions

$$\varphi(-\infty) = 0, \quad \varphi(\infty) = 1 \tag{2.3}$$

to (2.2). Solutions to (2.2) with (2.3) are only unique up to a phase shift, i.e., if $\varphi(\xi)$ is a solution to (2.2) with (2.3) then so is $\varphi(\xi + b)$, thus we need to choose a phase for uniqueness. Assuming that φ is strictly monotone increasing, $\varphi(\xi) = a$ for only one value of ξ; call it ξ_0. Without loss of generality, we may assume $\xi_0 = 0$. Later we will justify these assumptions and our choice of a phase condition. This choice of phase condition implies

$$\varphi(\xi) < a, \qquad \xi < 0, \qquad \text{and} \qquad \varphi(\xi) > a, \qquad \xi > 0.$$

Thus, for the Heaviside function defined by

$$h(x) = \begin{cases} 1 & x > 0, \\ 0 & x < 0, \end{cases}$$

$h(\varphi(\xi) - a) = h(\xi)$ for $\xi \neq 0$. Therefore, $f_1(\varphi(\xi))$ in (1.9) becomes

$$f(\varphi(\xi)) = \varphi(\xi) - h(\varphi(\xi) - a) = \varphi(\xi) - h(\xi) \qquad \text{for} \quad \xi \neq 0. \tag{2.4}$$

This form of the nonlinearity incorporates the phase condition into our problem.

Thus for any function φ the right-hand side of (2.2) becomes $L_T\varphi(\xi) - \varphi(\xi) + h(\xi)$. Taking the limits from the left and right of ξ as it approaches 0 we see that

$$\begin{aligned} \lim_{\xi \to 0-} \quad & [L_T\varphi(\xi) - \varphi(\xi) + h(\xi)] = L_T\varphi(0) - \varphi(0) \\ \neq \quad & L_T\varphi(0) - \varphi(0) + 1 = \lim_{\xi \to 0+} [L_T\varphi(\xi) - \varphi(\xi) + h(\xi)]. \end{aligned}$$

This in turn implies for any function φ that satisfies (2.2) with (2.4) and (2.3) that

$$\lim_{\xi \to 0-} (-\kappa_c\varphi'(\xi) - \delta_c\varphi''(\xi)) \neq \lim_{\xi \to 0+} (-\kappa_c\varphi'(\xi) - \delta_c\varphi''(\xi)). \tag{2.5}$$

2.1.2 An Analytic Solution and the $a(c)$ Relation

We now derive the solution of the continuous/discrete traveling wave equation (2.2) with $\kappa_c = c\alpha$, $\delta_c = \gamma - c^2\beta$, $\delta_c \geq 0$ when $\kappa_c \neq 0$, $\delta_c > 0$ when $\kappa_c = 0$, the boundary conditions (2.3), and the piecewise linear function f (2.4). From our derived solution, we obtain a relationship between the detuning parameter, a, and the wave speed, c. Also, from this solution and the $a(c)$ relation, we present results concerning propagation failure. In order to construct our solution, we use the Fourier transform. This is the reason for using a "linearized" nonlinearity f.

This section begins with the construction of a solution, $\varphi(\xi)$, for (2.2). Our construction follows the construction in [10] and [47] for traveling wave solutions to spatially discrete reaction-diffusion equations. The construction consists of defining a function $\varphi_\varepsilon(\xi) = e^{-\varepsilon\xi}\varphi(\xi)$ and transforming (2.2). To the $\varphi_\varepsilon(\xi)$ version of the continuous/discrete equation, we apply the Fourier transform, and after some manipulation, we derive a formula for $\varphi(\xi)$. We then show that this solution, $\varphi(\xi)$, is continuous in both ξ and κ_c, and is analytic in κ_c for $\kappa_c \neq 0$. We also show that $D_{\kappa_c}\varphi(\xi)$ is bounded. From the formula for $\varphi(\xi)$, we next derive a relation between a and c, called Γ. The function Γ is odd in κ_c, analytic in κ_c, and discontinuous at $\kappa_c = 0$ if and only if $\gamma = 0$. When $\gamma = 0$, the discontinuity in Γ is a jump discontinuity and is called the range of propagation failure.

We then show that $\varphi(\xi)$ is strictly increasing on the real line. The last key result of

this section is that c depends analytically on a for a outside the interval of propagation failure. This is not true for a in the interval of propagation failure. We begin our derivation of a solution with a preliminary lemma.

Lemma 2.1.1 *Let φ be a solution of (2.2) for $\kappa_c \neq 0, \delta_c \geq 0$ or $\kappa_c = 0, \delta_c > 0$. Then there exists an $\varepsilon_0 > 0$ such that, for some $K > 0$,*

$$|\varphi(\xi)| \leq Ke^{\varepsilon_0 \xi} \quad \text{for} \quad \xi \leq 0. \tag{2.6}$$

Proof. Let $\psi(\xi) = \varphi(-\xi)$. Then (2.2) becomes

$$-\delta_c \psi''(\xi) = -\kappa_c \psi'(\xi) + L_T \psi(\xi) - \psi(\xi)$$

for all $\xi > 0$. From the boundary conditions, $\psi(\xi) \to 0$ as $\xi \to \infty$.

Let $\hat{\psi}$ be the Laplace transform of ψ:

$$\hat{\psi}(s) = \int_0^\infty e^{-s\xi} \psi(\xi) d\xi,$$

which is analytic for $\mathrm{Re}(s) > 0$. If $\kappa_c \neq 0$, integrating by parts once gives

$$\begin{aligned}\hat{\psi}(s) &= \frac{\psi(0)}{s} + \int_0^\infty \frac{e^{-s\xi}}{s}\psi'(\xi)d\xi \\ &= \frac{\psi(0)}{s} + \int_0^\infty \frac{e^{-s\xi}}{\kappa_c s}(\delta_c\psi''(\xi) + L_T\psi(\xi) - \psi(\xi))d\xi.\end{aligned}$$

If $\kappa_c = 0$, $\delta_c > 0$, integrating by parts twice gives

$$\begin{aligned}\hat{\psi}(s) &= \frac{\psi(0)}{s} + \frac{\psi'(0)}{s^2} + \int_0^\infty \frac{e^{-s\xi}}{s^2}\psi''(\xi)d\xi \\ &= \frac{\psi(0)}{s} + \frac{\psi'(0)}{s^2} + \int_0^\infty \frac{e^{-s\xi}}{(-\delta_c)s^2}(-\kappa_c\psi'(\xi) + L_T\psi(\xi) - \psi(\xi))d\xi.\end{aligned}$$

Integrating either of these relations, we obtain

$$P(s)\hat{\psi}(s) = q(s), \tag{2.7}$$

where

$$P(s) = \kappa_c s - \delta_c s^2 + 1 - H,$$

and

$$q(s) = (\kappa_c - \delta_c s)\psi(0) - \delta_c\psi'(0) - J(s),$$

with

$$H = \sum_{k=1}^{n} \varepsilon_k (e^{e_k} + e^{-e_k} - 2),$$

and

$$J(s) = \sum_{k=1}^{n} \varepsilon_k (e^{e_k \cdot \sigma} \int_0^{e_k \cdot \sigma} e^{-s\xi} \psi(\xi) d\xi - e^{-e_k \cdot \sigma} \int_{-e_k \cdot \sigma}^{0} e^{-s\xi} \psi(\xi) d\xi).$$

Integrating by parts,

$$\int_0^b e^{-s\xi} \psi(\xi) d\xi = -\frac{e^{-s\xi} \psi(\xi)}{s} \Big|_{\xi=0}^{b} + \frac{1}{s} \int_0^b e^{-s\xi} \psi'(\xi) d\xi.$$

Thus the integrals in (2.7) are of order $O(|s|^{-1})$. This implies that

$$q(s) = (\kappa_c - \delta_c s)\psi(0) - \delta_c \psi'(0) + O(|s|^{-1}).$$

As $|\mathrm{Im}(s)| \to \infty$, $\kappa_c s - \delta_c s^2$ dominates $1 - H$ (where $\mathrm{Im}(s)$ is the imaginary part of s). This follows from the fact that $\sum_{k=1}^{n} \varepsilon_k < \infty$. Thus,

$$\hat{\psi}(s) \;=\; \frac{\psi(0)}{s} - \frac{\delta_c \psi'(0)}{\kappa_c s - \delta_c s^2} + O(|s|^{-2}) \quad \text{as} \quad |\mathrm{Im}(s)| \to \infty.$$

Consequently, we can shift the integration contour around singularities on the imag-

inary axis. Therefore

$$\psi(\xi) = \frac{1}{2\pi i}\int_{\varepsilon_0-i\infty}^{\varepsilon_0+i\infty} e^{s\xi}\hat{\psi}(s)ds = \frac{1}{2\pi i}\int_{-\varepsilon_0-i\infty}^{-\varepsilon_0+i\infty} e^{s\xi}\hat{\psi}(s)ds + \frac{1}{2\pi i}\sum_{\mathrm{Im}(s)=0} e^{s\xi}\mathrm{Res}(\hat{\psi}, s) \tag{2.8}$$

$$= \frac{1}{2\pi i}\int_{-\varepsilon_0-i\infty}^{-\varepsilon_0+i\infty} e^{s\xi}\left(\hat{\psi}(s) - \frac{\psi(0)}{s} + \frac{\delta_c\psi'(0)}{\kappa_c s - \delta_c s^2}\right)ds + \frac{1}{2\pi i}\sum_{\mathrm{Im}(s)=0} e^{s\xi}\mathrm{Res}(\hat{\psi}, s),$$

where $\varepsilon > 0$ is sufficiently small, $\mathrm{Res}(g, z)$ denotes the residue of a meromorphic function g at a point z, and the sum in (2.8) is taken over all poles of $\hat{\psi}$ on the imaginary axis, if any exist. The limits of integration denote contour integrals along the vertical lines $t \to \pm\varepsilon_0 + it$, for $t \in \mathbb{R}$.

Some explanation may be in order to help justify (2.8). The first equality in (2.8) is due to the Laplace inversion formula. We can use this since $\hat{\psi}$ has no poles in the right half of the complex plane. The second equality in (2.8) comes from shifting the contour of integration, the vertical axis, around any poles of $\hat{\psi}$ on the imaginary axis, and $\varphi_0 > 0$ is small enough that $\hat{\psi}$ has no poles in the strip $-\varepsilon_0 \leq \mathrm{Re}(s) < 0$. The third equality in (2.8) follows from the identities

$$\frac{1}{2\pi i}\int_{\varepsilon-i\infty}^{\varepsilon+i\infty}\frac{e^{s\xi}}{s}ds = \begin{cases} 1, & \varepsilon > 0, \\ 0, & \varepsilon < 0, \end{cases}$$

and

$$\frac{1}{2\pi i}\int_{\varepsilon-i\infty}^{\varepsilon+i\infty}\frac{e^{s\xi}}{s-a}ds=\begin{cases}e^{a\xi}, & \varepsilon>0,\\ 0, & \varepsilon<0,\end{cases}$$

for $\xi > 0$.

The third integral in (2.8) satisfies

$$\left|\frac{1}{2\pi i}\int_{-\varepsilon_0-i\infty}^{-\varepsilon_0+i\infty}e^{s\xi}\left(\hat{\psi}(s)-\frac{\psi(0)}{s}+\frac{\delta_c\psi'(0)}{\kappa_c s-\delta_c s^2}\right)ds\right|\leq Ke^{-\varepsilon_0\xi}\quad\text{for}\quad\xi\geq 0,$$

for some $K > 0$; in particular, this term approaches zero as $\xi \to \infty$. Recall that $\psi(\xi) \to 0$ as $\xi \to \infty$ by assumption. Each of the residues in the summation vanishes, i.e.

$$\text{Res}(\hat{\psi}, s) = 0 \quad \text{for} \quad \text{Im}(s) = 0.$$

Therefore, $|\psi(\xi)| \leq Ke^{-\varepsilon_0\xi}$ for $\xi \geq 0$, which is equivalent to (2.6). ■

Now we are ready to construct our solution to the traveling wave equation (2.2) with boundary conditions $\varphi(-\infty) = 0$ and $\varphi(+\infty) = 1$, and reaction term f given by (1.9). First, let $\varphi_\varepsilon(\xi) = e^{-\varepsilon\xi}\varphi(\xi)$, with $\varepsilon > 0$, ε small. By Lemma 2.1.1, if φ is a solution to (2.2), then, as $\xi \to -\infty$,

$$\varphi_\varepsilon(\xi) = e^{-\varepsilon\xi}\varphi(\xi) \leq |e^{-\varepsilon\xi}||\varphi(\xi)| \leq |Ke^{(\varepsilon_0-\varepsilon)\xi}| \to 0 \quad \text{for} \quad 0 < \varepsilon < \varepsilon_0.$$

Also as $\xi \to \infty$,

$$\varphi_\varepsilon(\xi) = e^{-\varepsilon\xi}\varphi(\xi) \to 0$$

since $\varphi(+\infty) = 1$. This implies that $\varphi_\varepsilon(-\infty) = 0$ and $\varphi_\varepsilon(+\infty) = 0$. Substituting $\varphi(\xi) = e^{\varepsilon\xi}\varphi_\varepsilon(\xi)$ into (2.2), we obtain

$$-\kappa_c e^{\varepsilon\xi}(\varepsilon\varphi_\varepsilon(\xi)+\varphi'_\varepsilon(\xi)) = \delta_c e^{\varepsilon\xi}(\varepsilon^2\varphi_\varepsilon(\xi)+2\varepsilon\varphi'_\varepsilon(\xi)+\varphi''_\varepsilon(\xi))+e^{\varepsilon\xi}L_\varepsilon\varphi_\varepsilon(\xi)-e^{\varepsilon\xi}\varphi_\varepsilon(\xi)+h(\xi),$$

which rearranges to

$$(-\kappa_c - 2\delta_c\varepsilon)\varphi'_\varepsilon(\xi) = \delta_c\varphi''_\varepsilon(\xi) + L_\varepsilon\varphi_\varepsilon(\xi) - (1 - \kappa_c\varepsilon - \delta_c\varepsilon^2)\varphi_\varepsilon(\xi) + e^{-\varepsilon\xi}h(\xi), \quad (2.9)$$

where

$$L_\varepsilon\varphi_\varepsilon(\xi) = \sum_{k=1}^{n} \varepsilon_k(e^{\varepsilon e_k\cdot\sigma}\varphi_\varepsilon(\xi + e_k\cdot\sigma) + e^{-\varepsilon e_k\cdot\sigma}\varphi_\varepsilon(\xi - e_k\cdot\sigma) - 2\varphi_\varepsilon(\xi)).$$

Now let's apply the Fourier transform

$$\hat{\varphi}_\varepsilon(s) = \int_{-\infty}^{\infty} e^{-is\xi}\varphi_\varepsilon(\xi)d\xi,$$

where $\varepsilon > 0$ is sufficiently small, to both sides of (2.9). Then

$$\hat{\varphi}_\varepsilon(s) = \int_{-\infty}^{\infty} e^{-is\xi}\varphi_\varepsilon(\xi)d\xi = -\int_{-\infty}^{\infty} \frac{i}{s}e^{-is\xi}\varphi'_\varepsilon(\xi)d\xi$$

$$= \frac{i}{s(\kappa_c + 2\delta_c\varepsilon)}\int_{-\infty}^{\infty}[e^{-is\xi}\delta_c\varphi''_\varepsilon(\xi) + e^{-is\xi}L_\varepsilon\varphi_\varepsilon(\xi)$$

$$-e^{-is\xi}(1 - \kappa_c\varepsilon - \delta_c\varepsilon^2)\varphi_\varepsilon(\xi) + e^{-is\xi}e^{-\varepsilon\xi}h(\xi)]d\xi$$

or

$$(-is(\kappa_c + 2\delta_c\varepsilon) + 1 - \kappa_c\varepsilon - \delta_c\varepsilon^2 - E(s) + \delta_c s^2)\hat{\varphi}_\varepsilon(s) = \frac{1}{(is + \varepsilon)},$$

where

$$E(s) = \sum_{k=1}^{n} \varepsilon_k(e^{\varepsilon e_k\cdot\sigma}e^{ise_k\cdot\sigma} + e^{-\varepsilon e_k\cdot\sigma}e^{-ise_k\cdot\sigma} - 2).$$

This implies that

$$\hat{\varphi}_\varepsilon(s) = \frac{1}{(is + \varepsilon)R(s - i\varepsilon)},$$

where

$$R(q) = -i\kappa_c q + 1 - G(q) + \delta_c q^2, \tag{2.10}$$

with

$$G(q) = \sum_{k=1}^{n} \varepsilon_k(e^{iqe_k\cdot\sigma} + e^{-iqe_k\cdot\sigma} - 2) = 2\sum_{k=1}^{n} \varepsilon_k[\cos(qe_k\cdot\sigma) - 1].$$

The following lemma is a simple extension of Lemma 4.4 in [10].

Lemma 2.1.2 *For $\kappa_c \neq 0$, $\delta_c \geq 0$ or $\kappa_c = 0$, $\delta_c > 0$, the function R, in (2.10), possesses a simple root $q = -iz_0$ with $z_0 > 0$. Moreover, there exists an $\epsilon_0 > 0$ such that if $q \in \mathbb{C}$ is any other root of R satisfying $Im\ q \leq 0$, then in fact $Im\ q < -z_0 - \epsilon_0$.*

Remark 2.1.1 *If $\delta_c < 0$ when $\kappa_c = 0$, there exists additional singularities to R for q real.*

The Fourier inversion theorem gives

$$\varphi(\xi) = e^{\varepsilon\xi}\varphi_\varepsilon(\xi) = \frac{1}{2\pi}\int_{-\infty}^{+\infty} e^{(is+\varepsilon)\xi}\hat{\varphi}_\varepsilon(s)ds,$$

which is absolutely convergent. This implies

$$\varphi(\xi) = \frac{1}{2\pi}\int_{-\infty}^{+\infty} \frac{e^{(is+\varepsilon)\xi}}{(is+\varepsilon)R(s-i\varepsilon)}ds = \frac{1}{2\pi i}\int_{-i\varepsilon-\infty}^{-i\varepsilon+\infty} \frac{e^{is\xi}}{sR(s)}ds.$$

Because of the simple pole at $s = 0$, we break up the integral into

$$\varphi(\xi) = \frac{1}{2\pi i}\left(\int_{C_\epsilon} + \int_{S_\epsilon}\right)\frac{e^{is\xi}}{sR(s)}ds, \tag{2.11}$$

where C_ε is $(-\infty, -\varepsilon]$ and $[+\varepsilon, +\infty)$ on the real axis, and S_ε is the half-circle at the origin. This would not be true if $\kappa_c = 0, \delta_c < 0$. First consider the C_ε integral. For $\kappa_c \neq 0, \delta_c \geq 0$ we have

$$\begin{aligned}
\frac{1}{2\pi i}\int_{C_\varepsilon} \frac{e^{is\xi}}{sR(s)}ds &= \frac{1}{2\pi i}\left(\int_{-\infty}^{-\varepsilon} + \int_{+\varepsilon}^{+\infty}\right)\frac{e^{is\xi}}{sR(s)}ds \\
&= \frac{1}{2\pi i}\int_{+\varepsilon}^{+\infty}\left[\frac{e^{is\xi}}{sR(s)} - \frac{e^{-is\xi}}{sR(-s)}\right]ds \\
&= \frac{1}{\pi}\int_{+\varepsilon}^{+\infty}\frac{A(s)\sin(s\xi)}{s(A^2(s)+\kappa_c^2 s^2)}ds + \frac{\kappa_c}{\pi}\int_{+\varepsilon}^{+\infty}\frac{\cos(s\xi)}{A^2(s)+\kappa_c^2 s^2}ds,
\end{aligned} \tag{2.12}$$

where

$$A(s) = 1 + \delta_c s^2 + 2\sum_{k=1}^{n}\varepsilon_k[1 - \cos(se_k \cdot \sigma)]. \tag{2.13}$$

If $\kappa_c = 0, \delta_c > 0$, (2.12) reduces to

$$\frac{1}{2\pi i}\int_{C_\varepsilon}\frac{e^{is\xi}}{sR(s)}ds = \frac{1}{\pi}\int_{+\varepsilon}^{+\infty}\frac{\sin(s\xi)}{sA(s)}ds.$$

For $s \in I\!R$, $A(s) = \mathrm{Re}[R(s)]$.

For the S_ε integral, we have

$$\frac{1}{2\pi i}\int_{S_\varepsilon}\frac{e^{is\xi}}{sR(s)}ds = \frac{1}{2\pi i}2\pi i\frac{1}{2}\mathrm{Res}\left(\frac{e^{is\xi}}{sR(s)}, 0\right) = \frac{1}{2}. \tag{2.14}$$

Combining the integral results (2.12) and (2.14) in (2.11), and letting $\varepsilon \to 0$, we obtain an explicit formula for $\varphi(\xi)$. From (2.11), we have the following formula for the solution of (2.2) for $\kappa_c \neq 0$:

$$\varphi(\xi) = \frac{1}{2} + \frac{1}{\pi}\int_0^\infty \frac{A(s)\sin s\xi}{s(A^2(s)+\kappa_c^2 s^2)}ds + \frac{\kappa_c}{\pi}\int_0^\infty \frac{\cos s\xi}{A^2(s)+\kappa_c^2 s^2}\,ds. \tag{2.15}$$

When $\kappa_c = 0$, $\delta_c > 0$;

$$\varphi(\xi) = \frac{1}{2} + \frac{1}{\pi}\int_0^\infty \frac{\sin s\xi}{sA(s)}ds.$$

Remark 2.1.2 *i) Noting that*

$$1-\varphi(-\xi,-\kappa_c) = \frac{1}{2} - \frac{1}{\pi}\int_0^\infty \frac{-A(s)\sin(s\xi)}{s(A^2(s)+\kappa_c^2 s^2)}ds - \frac{-\kappa_c}{\pi}\int_0^\infty \frac{\cos(s\xi)}{A^2(s)+\kappa_c^2 s^2} = \varphi(\xi,\kappa_c),$$

we see that, for $\varphi(\xi) = \varphi(\xi,\kappa_c)$, we have the symmetry property

$$\varphi(\xi,\kappa_c) = 1-\varphi(-\xi,-\kappa_c).$$

ii) Recalling that

$$\varphi(\xi) = \frac{1}{2\pi i}\int_{-i\varepsilon-\infty}^{-i\varepsilon+\infty} \frac{e^{is\xi}}{sR(s)}ds,$$

we can see that as $\xi \to -\infty$, $\varphi(\xi) \to 0$. Our symmetric property then gives

$\varphi(+\infty) = 1$. *This confirms our choice of boundary conditions.*

Proposition 2.1.1 *Let $\varphi(\xi, \kappa_c)$ denote the solution function (2.15). Then $\varphi(\xi, \kappa_c)$ is continuous in both ξ and κ_c, and is analytic in κ_c, for $\kappa_c \neq 0$. In addition, for $\kappa_c \neq 0$, the derivative of $\varphi(\xi, \kappa_c)$ with respect to κ_c,*

$$\psi(\xi) = \psi(\xi, \kappa_c) = D_{\kappa_c}\varphi(\xi, \kappa_c),$$

is bounded as $\xi \to \pm\infty$. For $\xi \neq 0, \psi(\xi)$ satisfies the equation

$$-\varphi'(\xi) + 2\frac{c}{\alpha}\beta\varphi''(\xi) + (c^2\beta - \gamma)\psi''(\xi) - \kappa_c\psi'(\xi) = L_T\psi(\xi) - \psi(\xi),$$

which is the derivative of the equation with respect to κ_c.

Proof. For any compact subset of $\{\kappa_c \in \mathbb{R} | \kappa_c \neq 0\}$, there exists a uniform lower bound

$$|A^2(s) + \kappa_c^2 s^2| \geq K_1(1 + s^2) \quad \text{for} \quad s \geq 0, \tag{2.16}$$

and thus, there exists a uniform lower bound for the denominators of the solution $\varphi(\xi)$ (2.15). If κ_c is pure imaginary, then $A^2(s) + \kappa_c^2 s^2 = 0$ for some $s > 0$. This in turn yields an upper bound of the form $K_2(1 + s^2)^{-1}$, for bounded ξ, for the two integrands in (2.15). This, and the analyticity of the integrands in κ_c and continuity

in (ξ, κ_c) for each s, imply the analyticity and continuity of φ.

The boundedness of ψ is easily proved by differentiating the formula for φ, (2.15), with respect to κ_c, i.e.,

$$\begin{aligned}
\psi(\xi, \kappa_c) &= D_{\kappa_c}\varphi(\xi, \kappa_c) \\
&= -\frac{2c\beta}{\alpha\pi}\int_0^\infty \frac{s\sin(s\xi)}{(A^2(s)+\kappa_c^2 s^2)}ds + \frac{2c(\beta-\alpha^2)}{\alpha\pi}\int_0^\infty \frac{sA(s)\sin(s\xi)}{(A^2(s)+\kappa_c^2 s^2)^2}ds \\
&\quad + \frac{1}{\pi}\int_0^\infty \frac{\cos(s\xi)}{(A^2(s)+\kappa_c^2 s^2)}ds + \frac{2c^2(\beta-\alpha^2)}{\pi}\int_0^\infty \frac{s^2\cos(s\xi)}{(A^2(s)+\kappa_c^2 s^2)^2}ds.
\end{aligned}$$

Using the bound (2.16), each integral is bounded and hence ψ is bounded.

Differentiating (2.2), we obtain

$$-\varphi'(\xi) - \kappa_c D_{\kappa_c}\varphi'(\xi) + 2\frac{c}{\alpha}\beta\varphi''(\xi) + (c^2\beta-\gamma)D_{\kappa_c}\varphi''(\xi) = D_{\kappa_c}L_T\varphi(\xi) - D_{\kappa_c}\varphi(\xi).$$

Along with $\psi(\xi, \kappa_c) = D_{\kappa_c}\varphi(\xi, \kappa_c)$, this implies that

$$-\varphi'(\xi) - \kappa_c\psi'(\xi) + 2\frac{c}{\alpha}\beta\varphi''(\xi) + (c^2\beta-\gamma)\psi''(\xi) = L_T\psi(\xi) - \psi(\xi),$$

as desired. ■

Remark 2.1.3 *As discussed earlier, $\varphi(\xi) = a$ for only one value of ξ, say $\xi = 0$. This then gives us the following relations between a and c:*

$$\varphi(0) = a = \frac{1}{2} + \frac{\kappa_c}{\pi}\int_0^\infty \frac{ds}{A^2(s) + \kappa_c^2 s^2}, \quad when \quad \kappa_c \neq 0, \tag{2.17}$$

and

$$\varphi(0) = a = \frac{1}{2} \quad when \quad \kappa_c = 0.$$

Now that we have derived a solution $\varphi(\xi)$, we need to justify the assumption that the solution to (2.2), with (2.4) and (2.3) is monotone increasing. The proof of the following remark follows the proofs of Corollary 4.5 and Theorem 4.6 from [10] if we recall that $\varphi''(\xi) = \lim_{\epsilon\to 0}(1/\epsilon)[\varphi(\xi+\epsilon) + \varphi(\xi-\epsilon) - 2\varphi(\xi)]$ and that $-\kappa_c\varphi'(\xi) = 0$ when $\kappa_c = 0$.

Remark 2.1.4 *The solution φ, (2.15), of (2.2) with (2.4) and (2.3), is strictly increasing for $\xi \in \mathbb{R}$.*

Lemma 2.1.3 *For $\kappa_c \neq 0$ and $\delta_c \geq 0$, the derivative $\varphi'(\xi)$ of (2.15) is continuous if and only if $\delta_c > 0$. In addition, if $\delta_c > 0$,*

$$\lim_{\xi\to 0-} \varphi''(\xi) - \lim_{\xi\to 0+} \varphi''(\xi) = \frac{1}{\delta_c},$$

and, if $\delta_c = 0$,

$$\lim_{\xi \to 0-} \varphi'(\xi) - \lim_{\xi \to 0+} \varphi'(\xi) = \frac{1}{\kappa_c}.$$

Proof. We note that by (2.2) with (2.4), any difficulty in smoothness occurs at $\xi = 0$. Taking the difference of (2.2) with (2.4) as ξ approaches zero from the left and from the right, we obtain

$$\lim_{\xi \to 0-} (-\kappa_c \varphi'(\xi) - \delta_c \varphi''(\xi)) - \lim_{\xi \to 0+} (-\kappa_c \varphi'(\xi) - \delta_c \varphi''(\xi)) = -1 \tag{2.18}$$

since φ is continuous on $\mathbb{R}$. Suppose $\delta_c = 0$. Then (2.18) implies

$$\lim_{\xi \to 0-} \varphi'(\xi) - \lim_{\xi \to 0+} \varphi'(\xi) = \frac{1}{\kappa_c}.$$

Thus φ' is discontinuous at $\xi = 0$.

Now suppose $\delta_c > 0$. Taking the derivative of $\varphi(\xi)$ with respect to ξ in (2.15), we see that $\lim_{\xi \to 0-} \varphi'(\xi) = \lim_{\xi \to 0+} \varphi'(\xi)$. Thus (2.18) implies that

$$\lim_{\xi \to 0-} \varphi''(\xi) - \lim_{\xi \to 0+} \varphi''(\xi) = \frac{1}{\delta_c}.$$

■

We now address exactly what is meant by a solution to (2.2). To solve (2.2), it is sufficient to regard both $f(\varphi)$, (2.4), and $h(\xi)$ as set valued functions, with f and h singleton sets for $\varphi \neq a$ and $\xi \neq 0$, and $f(a) = [a-1, a]$ and $h(0) = [0, 1]$. This amounts to filling in the jump discontinuities in the graphs of f and h. By a solution to (2.2) we mean that $\varphi \in C(\mathbb{R})$ and the differential inclusion

$$-\kappa_c \varphi'(\xi) - \delta_c \varphi''(\xi) \in L_T \varphi(\xi) - \varphi(\xi) + h(\xi).$$

holds for $\xi \in \mathbb{R}$.

2.1.3 Propagation Failure

We now analyze the relationship between the wave speed c and the detuning parameter a. We are particularly interested in the phenomenon of propagation failure, the existence of a nontrivial interval for a such that the wave speed is zero. Throughout this subsection, we include plots of the $a(c)$ relation calculated from (2.17) using the three point Gaussian quadrature algorithm *adapt* of [59]. Table 2.1 lists the $a(c)$ plots which appear. An $*$ indicates a quantity that is varied.

Set

$$\Gamma(\kappa_c, \delta_c) := \varphi(0) - \frac{1}{2} = a - \frac{1}{2} = \frac{\kappa_c}{\pi} \int_0^\infty \frac{ds}{A^2(s) + \kappa_c^2 s^2}, \qquad \kappa_c \neq 0, \tag{2.19}$$

a(c)	Figure	α	β	γ	$(\varepsilon_1, \varepsilon_2, \varepsilon_3)$	σ
Reaction-Diffusion	2.1	*	0	10	$(1,0,0)$	$(1,0,0)$
	2.2	*	0	0	$(1,0,0)$	$(1,0,0)$
	2.6	1	0	10^{-3}	*	$(\frac{\sqrt{2}}{2}, \frac{\sqrt{2}}{2}, 0)$
	2.7	1	0	0	$(1,1,1)$	*
	2.8	1	0	10^{-4}	$(1,1,1)$	*
Damped Wave	2.3	*	0.1	10	$(1,0,0)$	$(1,0,0)$
	2.4	10^{-6}	0.1	*	$(1,1,0)$	$(\frac{\sqrt{2}}{2}, \frac{\sqrt{2}}{2}, 0)$
	2.5	0.1	0.1	*	$(1,0,0)$	$(1,0,0)$

Table 2.1: The $a(c)$ plots. $*$ indicates that quantity is varied.

where

$$A(s) = 1 + \delta_c s^2 + 2\sum_{k=1}^{n} \varepsilon_k [1 - \cos(s e_k \cdot \sigma)]. \tag{2.20}$$

From a change in variables in (2.19) we obtain

$$\Gamma(\kappa_c, \delta_c) = \frac{\operatorname{sgn}(\kappa_c)}{\pi} \int_0^\infty \frac{ds}{A^2(s/\kappa_c) + s^2}, \qquad \kappa_c \neq 0. \tag{2.21}$$

Remark 2.1.5 *i)* $\Gamma(\kappa_c, \delta_c) \neq 0$ *when* $\kappa_c \neq 0$.

ii) For $\sigma_k \neq 0$, $\Gamma(\kappa_c, \delta_c) \to 0$ *as* $\varepsilon_k \to \infty$, $k = 1, ..., n$.

iii) Recall $a - 1/2 = 0$ *when* $\kappa_c = 0$.

iv) For $\alpha = 0$, *the* c *versus* a *curve is* $a(c) = 1/2$ *for all* c.

Lemma 2.1.4 *For* $\kappa_c \neq 0$, *the function* $\Gamma(\kappa_c, \delta_c)$ *in (2.19) is strictly increasing in* κ_c.

Proof. The case when $\delta_c = 0$ is proved in Theorem 4.7 of [10]. For $\delta_c > 0$, the application of the Mel'nikov method in the style of Theorem 4.7 of [10] proves the lemma. In this application it is important to recall that

$$\lim_{\xi \to 0-} (-\kappa_c \varphi'(\xi) - \delta_c \varphi''(\xi)) \neq \lim_{\xi \to 0+} (-\kappa_c \varphi'(\xi) - \delta_c \varphi''(\xi))$$

and that $\varphi'(\xi)$ is continuous at $\xi = 0$. ∎

We now show that Γ is bounded and that Γ is odd and analytic in κ_c. The proofs of these results follow after a brief discussion.

Theorem 2.1.1 *Let $\varphi(\xi)$ be a solution to (2.2) with (2.4) and (2.3). Thus $\Gamma(\kappa_c, \delta_c)$ is defined by (2.19) with $\kappa_c \neq 0$. Then Γ is odd and analytic in κ_c. In addition, if $\beta = 0$,*

$$|\Gamma(\kappa_c, \delta_c)| < \frac{1}{2} \qquad \textit{and} \qquad \lim_{|\kappa_c| \to \infty} |\Gamma(\kappa_c, \delta_c)| = \frac{1}{2}. \tag{2.22}$$

If $\beta > 0$, then κ_c is restricted to the interval $[-d, d]$,

$$|\Gamma(\kappa_c, \delta_c)| \leq \Gamma(d, 0), \qquad \textit{and} \qquad \lim_{|\kappa_c| \to d} |\Gamma(\kappa_c, \delta_c)| = \Gamma(d, 0), \tag{2.23}$$

where $d = \alpha\sqrt{\gamma/\beta}$.

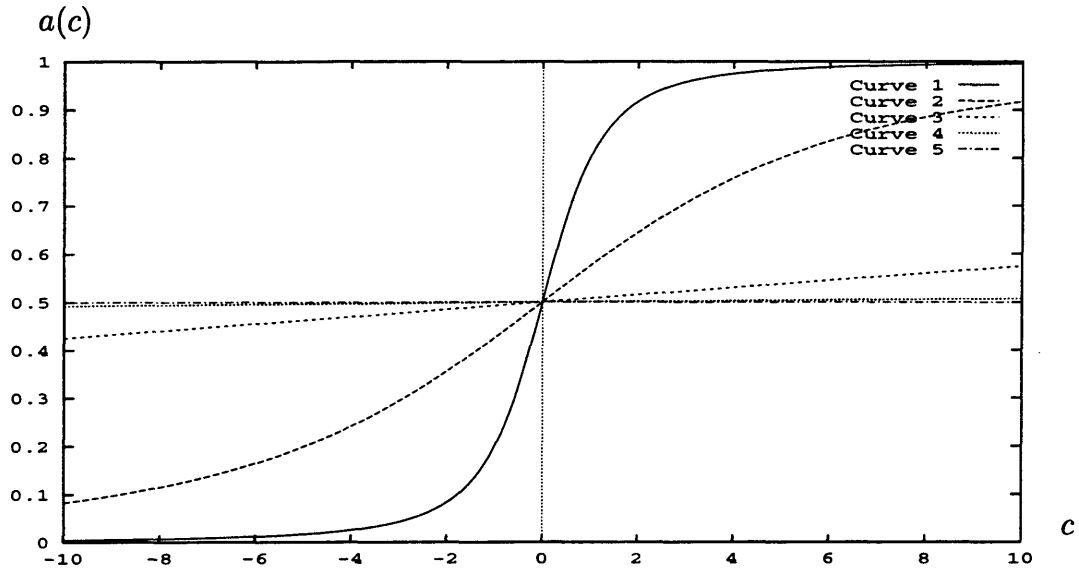

Curve	1	2	3	4	5
α	5	1	10^{-1}	10^{-2}	10^{-5}

Fixed Parameters	β	γ	$(\varepsilon_1, \varepsilon_2, \varepsilon_3)$	σ
	0	10	(1,0,0)	(1,0,0)

Figure 2.1: An $a(c)$ plot for the reaction-diffusion equation for various α.

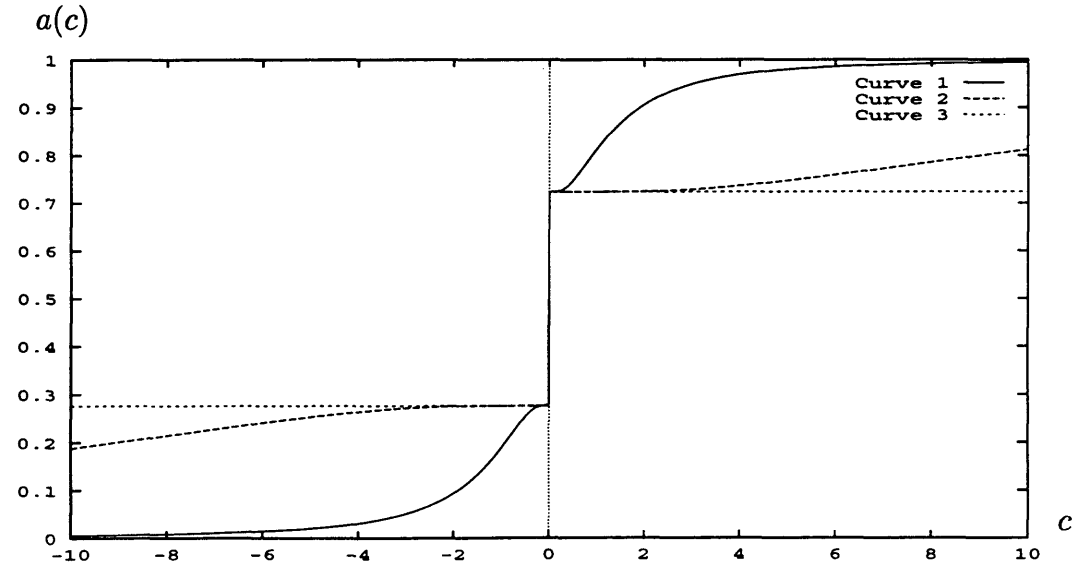

Curve	1	2	3
α	1	0.1	0.01

Fixed Parameters	β	γ	$(\varepsilon_1, \varepsilon_2, \varepsilon_3)$	σ
	0	0	(1,0,0)	(1,0,0)

Figure 2.2: An $a(c)$ plot for the reaction-diffusion for various α.

Remark 2.1.6 *Let's consider the damped wave equation, i.e.* $\alpha > 0$ *and* $\beta > 0$. *Let's pick* $|c|$ *as large as possible for this case, let* $c = -\sqrt{\gamma/\beta}$ *and* $c = \sqrt{\gamma/\beta}$. *For these values of* c, $\delta_c = 0$, *(2.2) becomes the traveling wave form of a spatially discrete reaction-diffusion equation, and* $|\Gamma| = \Gamma(d, 0)$, *the* Γ *of the spatially discrete reaction-diffusion equation. Thus the range of values of* a *for the damped wave equation is* $[1/2 - \Gamma(d,0), 1/2 + \Gamma(d,0)]$. *(see Figures 2.2, 2.3, 2.4, and 2.5).*

We see in Figures 2.1, 2.2, and 2.3 that as α increases, $|\Gamma(\kappa_c, \delta_c)|$ increases toward its upper bound of 1/2. This agrees with both (2.22) and (2.23). Figures 2.1, 2.2, 2.6, 2.7, and 2.8 illustrate (2.22), while Figures 2.3, 2.4, and 2.5 illustrate (2.23).

Theorem 2.1.2 *Let* $\Gamma(\kappa_c, \delta_c)$ *be defined by (2.19) with* $\kappa_c \neq 0$ *and let* $\varrho(\delta_c) \equiv \lim_{|\kappa_c| \to 0+} |\Gamma(\kappa_c, \delta_c)|$ *for* $\delta_c \geq 0$. *Then*

$$\varrho(\delta_c) = \begin{cases} \lim_{T\to\infty} \frac{1}{2T} \int_0^T \frac{ds}{A(s)} & \delta_c = 0, \\ 0 & \delta_c > 0. \end{cases} \tag{2.24}$$

Remark 2.1.7 *i) Since* $\kappa_c \to 0+$ *and* $\delta_c \to \gamma$ *as* $c \to 0+$, *when* $\gamma = 0$, $(1/2 - \varrho(0), 1/2 + \varrho(0))$ *is the range for the detuning parameter* a *for which the solutions to (2.2) exhibit propagation failure.*

ii) The interval $[1/2 - \Gamma(d,0), 1/2 + \Gamma(d,0)]$, *in Remark 2.1.6, is equal to the interval of propagation failure when* $\gamma = 0$. *(See Figures 2.2, 2.3, 2.4, and 2.5).*

Let's examine the case when $\kappa_c \to 0+$ because $\alpha \to 0+$. Suppose $\beta = 0$ and we are solving the reaction-diffusion equation. When $\gamma \neq 0$, $|a - 1/2| = \varrho(\delta_c) = \varrho(\gamma) = 0$ as $\alpha \to 0+$ for all c. Figure 2.1 is an $a(c)$ plot showing how $a \to 1/2$ as $\alpha \to 0+$ in the mixed (spatially continuous/discrete) reaction-diffusion model. When $\gamma = 0$, $|a - 1/2| = \varrho(0) > 0$ as $\alpha \to 0+$ for all c. Figure 2.2 is an $a(c)$ plot showing how $a \to 1/2 \pm \varrho(0)$ as $\alpha \to 0+$ in the spatially discrete reaction-diffusion model. We have propagation failure in this case. The interval of propagation failure is the interval of the jump discontinuity in Figure 2.2.

Now suppose $\beta > 0$ and $\alpha > 0$ and we are solving the damped wave equation. When $\alpha > 0$, $\delta_c \geq 0$, we have seen that the bound for c, $|c| \leq \sqrt{\gamma/\beta}$, implies a bound on a. Figure 2.3, for a mixed damped wave model, is an $a(c)$ plot where the bound on $|c|$ is $\sqrt{\gamma/\beta} = 10$. Figure 2.3 also shows the upper bound (at $c = 10$) and lower bound (at $c = -10$) on the detuning parameter a for different values of α. Now notice in Figure 2.2 that the values of a at $c = -10$ and $c = 10$ for the same values of α. We see the two sets of values of a (in Figure 2.2 and Figure 2.3) are the same. Notice in Figure 2.3 how the range of a depends on α. As $\alpha \to 0+$, the $a(c)$ curve approaches $1/2$ for $|c| < \sqrt{\gamma/\beta}$ and $a(\pm\sqrt{\gamma/\beta})$ approaches $1/2 \pm \varrho(0)$. Figure 2.4 also shows

this result for various values of γ. Figure 2.5 shows explicitly the restriction of the range of a. Here we present $a(c)$ plots for various γ (the sigmoid curves) along with the $a(c)$ curve for the spatially discrete reaction diffusion equation with the same σ, $(\varepsilon_1, \varepsilon_2, \varepsilon_3)$, and α.

Suppose $\alpha = 0$ so that $\kappa_c = 0$ and we have the undamped wave equation. Then, regardless of the choice of the other parameters, $a(c) = 1/2$ for all $c \in \mathbb{R}$.

Proof of Theorem 2.1.1.

The oddness of Γ follows directly from (2.19). Analyticity follows from Proposition 2.1.1.

Let $\kappa_c \neq 0$. Suppose $\beta = 0$. Then

$$A(s/\kappa_c) = [1 + \delta_c/\kappa_c^2 s^2 + 2\sum_{k=1}^{n} \varepsilon_k(1 - \cos((s/\kappa_c)e_k \cdot \sigma)] \geq 1$$

and

$$\lim_{|\kappa_c|\to\infty} A(s/\kappa_c) = \lim_{|\kappa_c|\to\infty} [1 + \delta_c/\kappa_c^2 s^2 + 2\sum_{k=1}^{n} \varepsilon_k(1 - \cos((s/\kappa_c)e_k \cdot \sigma)] = 1$$

for $s > 0$. Thus

$$|\Gamma(\kappa_c, \delta_c)| = \frac{1}{\pi}\int_0^\infty \frac{ds}{A^2(s/\kappa_c) + s^2} \leq \frac{1}{\pi}\int_0^\infty \frac{ds}{1 + s^2} = \frac{1}{2},$$

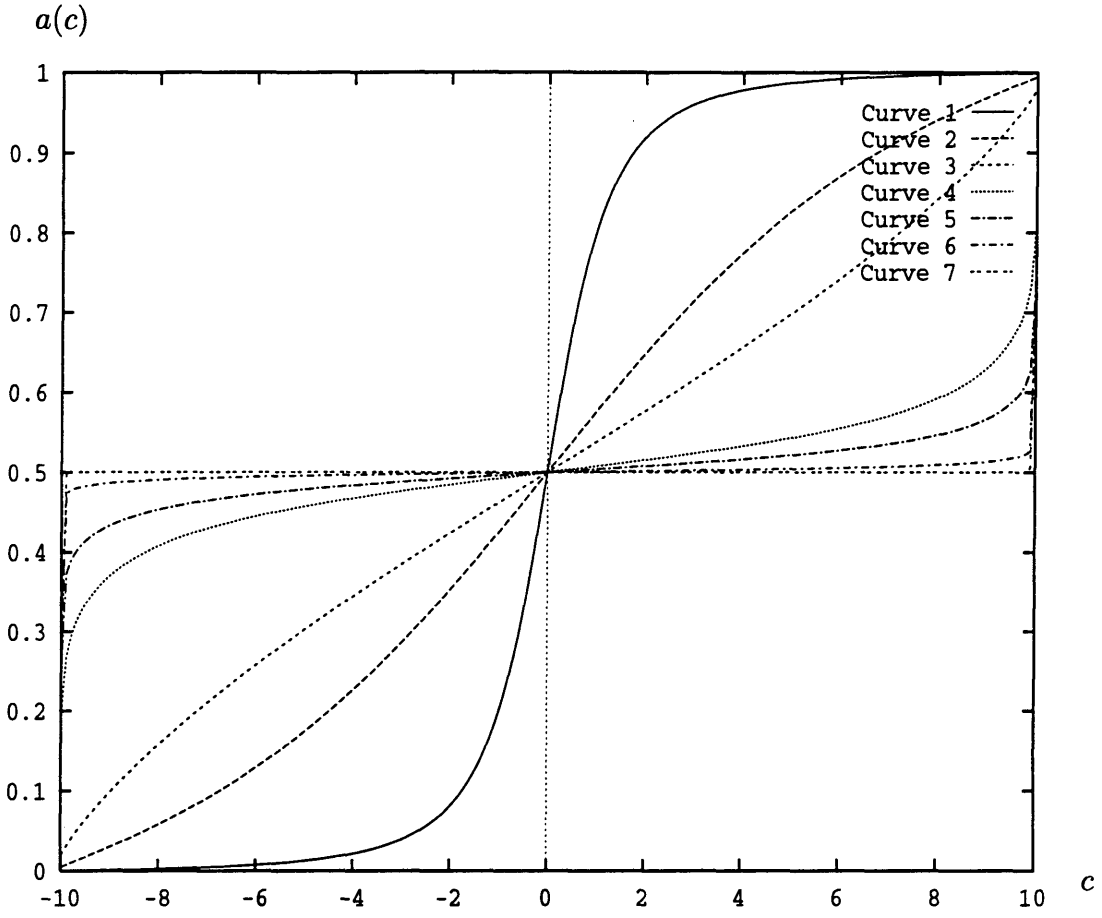

Curve	1	2	3	4	5	6	7
α	5	1	5×10^{-1}	10^{-1}	5×10^{-2}	10^{-2}	10^{-5}

Fixed Parameters	β	γ	$(\varepsilon_1, \varepsilon_2, \varepsilon_3)$	σ
	0.1	10	$(1,0,0)$	$(1,0,0)$

Figure 2.3: An $a(c)$ plot for the damped wave equation for various α.

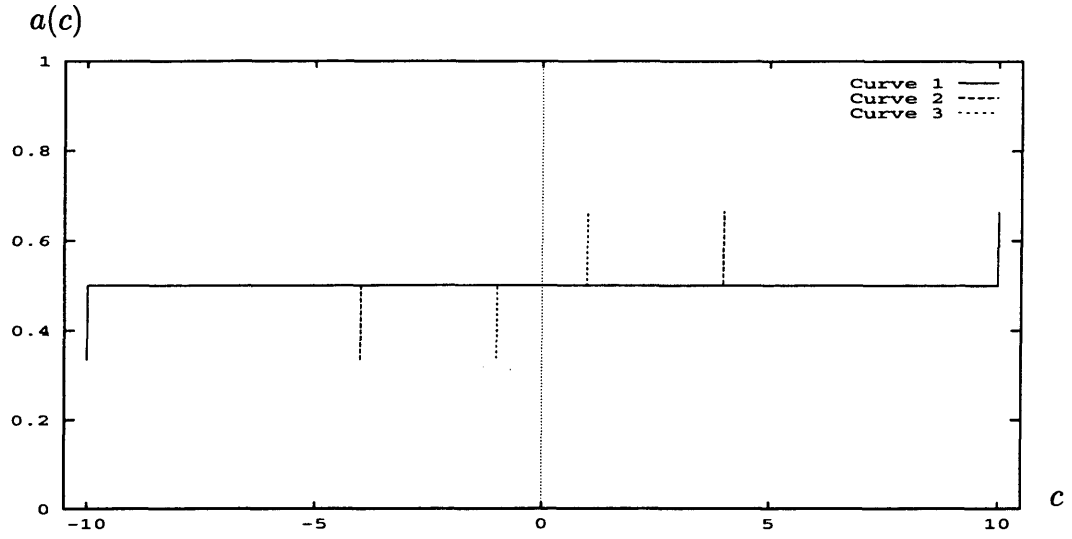

Curve	1	2	3
γ	10	1.6	0.1

Fixed Parameters	α	β	$(\varepsilon_1, \varepsilon_2, \varepsilon_3)$	σ
	10^{-6}	0.1	$(1,1,0)$	$(\frac{\sqrt{2}}{2}, \frac{\sqrt{2}}{2}, 0)$

Figure 2.4: An $a(c)$ plot for the wave equation for various γ.

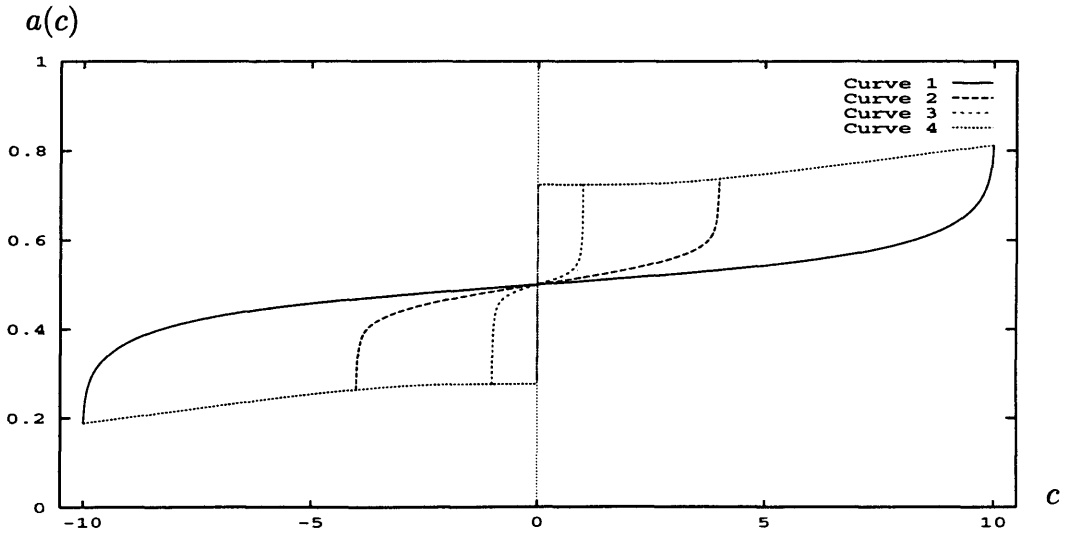

Curve	1	2	3
γ	10	1.6	0.1

Fixed Parameters	α	β	$(\varepsilon_1, \varepsilon_2, \varepsilon_3)$	σ
	0.1	0.1	$(1,0,0)$	$(1,0,0)$

Curve 4	$\gamma = 0$	$\beta = 0$	$\alpha = 0.1$	$(\varepsilon_1, \varepsilon_2, \varepsilon_3) = (1,0,0)$	$\sigma = (1,0,0)$

Figure 2.5: An $a(c)$ plot for the damped wave equation for various γ.

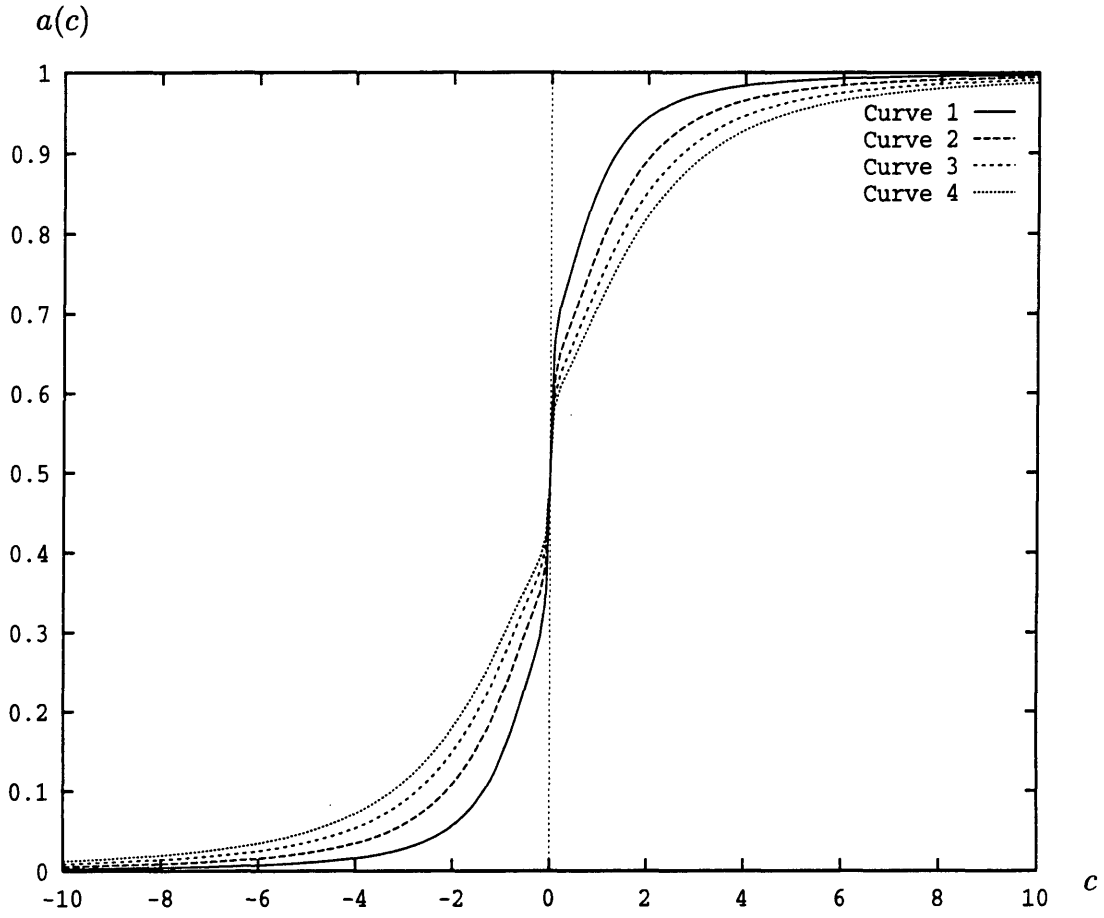

Curve	1	2	3	4
$(\varepsilon_1, \varepsilon_2, \varepsilon_3)$	$(\frac{1}{2}, \frac{1}{2}, 0)$	$(\frac{1}{2}, \frac{3}{2}, 0)$	$(1, 2, 0)$	$(2, 2, 0)$

Fixed	α	β	γ	σ
Parameters	1	0	10^{-3}	$(\frac{\sqrt{2}}{2}, \frac{\sqrt{2}}{2}, 0)$

Figure 2.6: An $a(c)$ plot for the reaction-diffusion equation for various $(\varepsilon_1, \varepsilon_2, \varepsilon_3)$.

and

$$\lim_{|\kappa_c|\to\infty} |\Gamma(\kappa_c,\delta_c)| = \lim_{\kappa_c\to\infty} \frac{1}{\pi}\int_0^\infty \frac{ds}{A^2(s/\kappa_c)+s^2} = \frac{1}{\pi}\int_0^\infty \frac{ds}{1+s^2} = \frac{1}{2}.$$

Now suppose $\beta > 0$. Since $\delta_c \geq 0$, this implies that $|\kappa_c| = |\alpha c| \leq \alpha\sqrt{\gamma/\beta}$. Let $d = \alpha\sqrt{\gamma/\beta}$. Then

$$A(s/\kappa_c) = [1+\delta_c/\kappa_c^2 s^2 + 2\sum_{k=1}^{n} \varepsilon_k(1-\cos((s/\kappa_c)e_k\cdot\sigma)] \geq [1+2\sum_{k=1}^{n} \varepsilon_k(1-\cos((s/\kappa_c)e_k\cdot\sigma)]$$

and

$$\begin{aligned}\lim_{|\kappa_c|\to d} A(s/\kappa_c) &= \lim_{|\kappa_c|\to d}[1+\delta_c/\kappa_c^2 s^2 + 2\sum_{k=1}^{n} \varepsilon_k(1-\cos((s/\kappa_c)e_k\cdot\sigma)] \\ &= [1+2\sum_{k=1}^{n} \varepsilon_k(1-\cos((s/d)e_k\cdot\sigma)]\end{aligned}$$

for $s > 0$. Thus

$$|\Gamma(\kappa_c,\delta_c)| \leq |\Gamma(\kappa_c,0)| \qquad \text{and} \qquad \lim_{|\kappa_c|\to d} |\Gamma(\kappa_c,\delta_c)| = \Gamma(d,0).$$

By Lemma 2.1.4, if $|\kappa_c| \leq d$ then $|\Gamma(\kappa_c,\delta_c)| \leq \Gamma(d,\delta_c)$. This and the inequality above gives us

$$|\Gamma(\kappa_c,\delta_c)| \leq \Gamma(d,\delta_c) \leq \Gamma(d,0).$$

■

Proof of Theorem 2.1.2.

We have that $1 + \delta_c s^2/\kappa_c^2 \leq A(s/\kappa_c)$, which implies

$$\Gamma(\kappa_c) \leq \frac{1}{\pi}\int_0^\infty \frac{ds}{(1+\delta_c s^2/\kappa_c^2)^2 + s^2} = \frac{1}{2\sqrt{1+4\delta_c/\kappa_c^2}}, \tag{2.25}$$

for κ_c small and $\delta_c/\kappa_c^2 \geq 0$. As $\kappa_c \to 0^+$, $\delta_c/\kappa_c^2 \to \infty$ for $\delta_c > 0$. So (2.25) implies that, as $\kappa_c \to 0^+$, $\Gamma(\kappa_c)$ is bounded above by zero when $\delta_c > 0$. Recall that for $\kappa_c > 0$, $\Gamma(\kappa_c) > 0$.

Now suppose $\delta_c = 0$. Then

$$A(s) = 1 + 2\sum_{k=1}^{n} \varepsilon_k[1 - \cos(se_k \cdot \sigma)]$$

and

$$\varrho(0) = \lim_{T\to\infty} \frac{1}{2T}\int_0^T \frac{ds}{A(s)}$$

follows directly from Theorem 4.3 in [10]. ∎

Remark 2.1.8 *i) The quantity*

$$\lim_{T\to\infty} \frac{1}{2T}\int_0^T \frac{ds}{A(s)}$$

always exists and is positive when $\delta_c = 0$.

ii) Since $\delta_c \geq 0$, *when* $\kappa_c \neq 0$, *and* $\beta \geq 0$, $\gamma = 0$ *implies* $\delta_c = \gamma - c^2\beta = 0$. *Thus* $\lim_{\gamma \to 0} \varrho(\delta_c) = \lim_{\delta_c \to 0} \varrho(\delta_c)$.

iii) For $\alpha \neq 0$ *as* $c \to 0$, *there exists a nontrivial interval for the detuning parameter if and only if* $\gamma = 0$. *In other words, we have propagation failure if and only if* $\gamma = 0$.

iv) As $\sum_{k=1}^{n} \varepsilon_k \to 0$, $\varrho(0) \to 1/2$. *This shows that the interval of propagation failure can expand to the interval* $(0, 1)$. *As* $\sum_{k=1}^{n} \varepsilon_k \to \infty$, $\varrho(0) \to 0$.

In our previous discussions, we presented $a(c)$ relations where σ and $(\varepsilon_1, \varepsilon_2, \varepsilon_3)$ are fixed. In Figures 2.7 and 2.8, we see the effects of varying σ, lattice induced anisotropy. In both plots, we see the direct dependence of the $a(c)$ relation on the direction parameter σ. Figure 2.8 shows how the $a(c)$ relation becomes discontinuous and how the interval of propagation failure develops, as $\gamma \to 0+$. We discuss Figures 2.6, 2.7, and 2.8 further in Section 3.

2.1.4 The case $\kappa_c = \delta_c = 0$

In this section, we consider solutions to (2.2) with $\kappa_c = \delta_c = 0$. In this case we are only concerned with values $\varphi(\xi)$ for $\xi \in D$, where $D \subseteq \mathbb{R}$ is the countable set $D = \{\sigma \cdot l | \in \mathbb{Z}^n\}$. This is because with $\kappa_c = 0 = \delta_c$, (2.2) becomes a difference

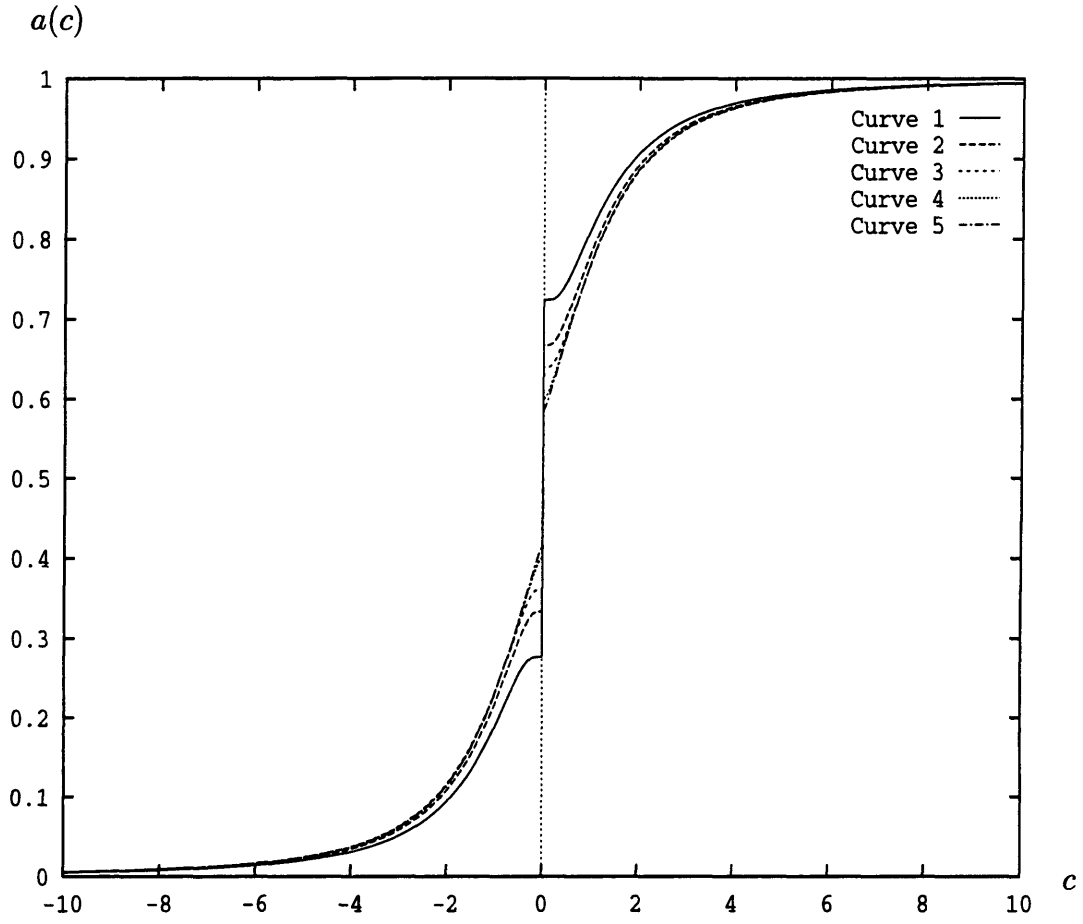

Curve	1	2	3	4	5
σ	$(1,0,0)$	$(\frac{\sqrt{2}}{2},\frac{\sqrt{2}}{2},0)$	$(\frac{\sqrt{3}}{3},\frac{\sqrt{3}}{3},\frac{\sqrt{3}}{3})$	$(\frac{1}{2},\frac{1}{2},\frac{\sqrt{2}}{2})$	$(\frac{\sqrt{2}}{2},\frac{\sqrt{3}}{3},\frac{\sqrt{6}}{6})$

Fixed Parameters	α	β	γ	$(\varepsilon_1,\varepsilon_2,\varepsilon_3)$
	1	0	0	$(1,1,1)$

Figure 2.7: An $a(c)$ plot for the spatially discrete reaction-diffusion equation for various σ.

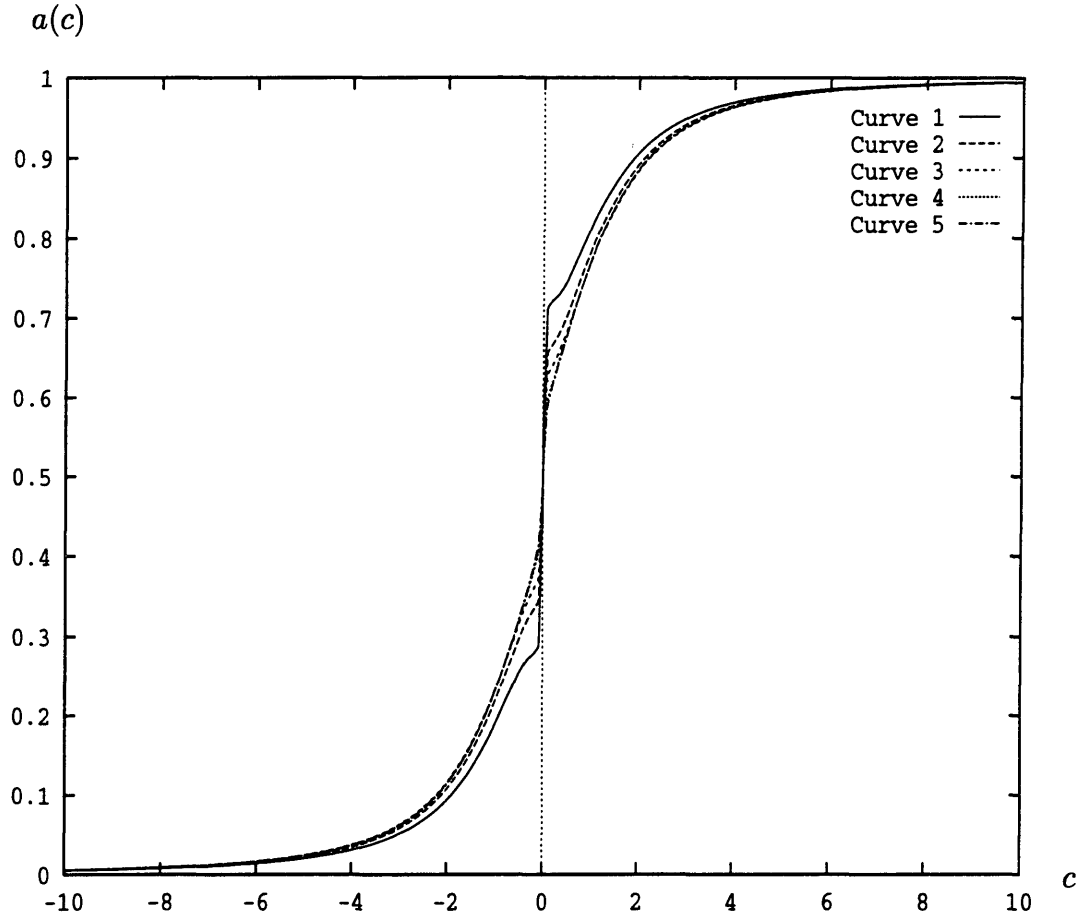

Curve	1	2	3	4	5
σ	$(1,0,0)$	$(\frac{\sqrt{2}}{2},\frac{\sqrt{2}}{2},0)$	$(\frac{\sqrt{3}}{3},\frac{\sqrt{3}}{3},\frac{\sqrt{3}}{3})$	$(\frac{1}{2},\frac{1}{2},\frac{\sqrt{2}}{2})$	$(\frac{\sqrt{2}}{2},\frac{\sqrt{3}}{3},\frac{\sqrt{6}}{6})$

Fixed Parameters	α	β	γ	$(\varepsilon_1,\varepsilon_2,\varepsilon_3)$
	1	0	10^{-4}	$(1,1,1)$

Figure 2.8: An $a(c)$ plot for the reaction-diffusion equation for various σ.

equation. Below is a summary of results, but first some notation.

If for any $j \neq k$, k and $j = 1, ..., n$, σ_j and σ_k are rationally independent, then we call σ rationally independent, and σ is called rationally dependent otherwise. If σ is rationally independent, then D is a dense subset of $\mathbb{R}$, while if σ is rationally dependent, then $D = \{m\nu | m \in \mathbb{Z}\}$ and D is a discrete subset of $\mathbb{R}$. Both forms of D have measure zero. Next we take the limit as $\kappa_c \to 0$ together with the limit $\delta_c \to 0$ of the solution found in the last section. Let $\varphi_*(\xi)$ be defined as the function such that $\varphi(\xi, (\kappa_c)_n, (\delta_c)_n) \to \varphi_*(\xi)$ as the sequences $(\kappa_c)_n \to 0$ and $(\delta_c)_n \to 0$ with $(\delta_c)_n < |(\kappa_c)_n|$ for n greater than some $N \in \mathbb{Z}$. The function $\varphi_*(\xi)$ is defined almost everywhere on $\mathbb{R}$, but can contain jump discontinuities. Let φ_+ equal φ_* everywhere φ_* is defined and equal to the right-hand limit of φ_* elsewhere. Let φ_- equal φ_* everywhere φ_* is defined and equal to the left-hand limit of φ_* elsewhere. Let φ_τ be defined as the linear combination

$$\varphi_\tau(\xi) = \tau\varphi_+(\xi) + (1 - \tau)\varphi_-(\xi).$$

The following is a summary of results for $\kappa_c = 0 = \delta_c$.

Remark 2.1.9 *i) The equation*

$$L_T\varphi_\tau(\xi) - \varphi_\tau(\xi) + h_\tau(\xi) = 0, \tag{2.26}$$

holds for all $\xi \in \mathbb{R}$.

ii) The function φ_τ *is monotone.*

iii) The boundary conditions $\varphi_\tau(-\infty) = 0$ *and* $\varphi_\tau(+\infty) = 1$, *which implies that* φ_τ *satisfies the boundary conditions of (2.2).*

iv) Let $\tau \in [0,1]$. *If* σ *is rationally independent, then the function* φ_τ *is strictly increasing on* $\mathbb{R}$. *If* σ *is rationally dependent, then* $\varphi_\tau(\xi) < \varphi_\tau(\xi + \nu)$ *for all* $\xi \in \mathbb{R}$, *where* ν *is such that* $D = \{m\nu | m \in \mathbb{Z}\}$. *In any case, if we define*

$$\varphi_{\tau_{\xi_0}}(\xi) = \varphi_\tau(\xi - \xi_0), \tag{2.27}$$

then for any $\tau \in [0,1]$ *and* $\xi_0 \in \mathbb{R}$, *the function* $\varphi_{\tau_{\xi_0}}(\cdot)$ *restricted to the set* D *is strictly increasing.*

v) Let $\tau, \xi_0 \in \mathbb{R}$. *Then a bounded function* $\varphi : D \to \mathbb{R}$ *satisfies equation (2.26) for all* $\xi \in D$ *if and only if* $\varphi(\xi) = \varphi_{\tau_{\xi_0}}(\xi)$ *for all* $\xi \in D$.

vi) Assume that σ *is rationally dependent, with* ν *as in* $D = \{j\nu | j \in \mathbb{Z}\}$. *Then for each* $j \in \mathbb{Z}$, *the function* φ_τ *is constant on the interval* $(j\nu, (j+1)\nu)$.

vii) Let σ *be rationally dependent with* ν *as in* $D = \{j\nu | j \in \mathbb{Z}\}$, *let* $\tau \in [0,1]$, *and*

let $\varrho(0)$ be defined as in Theorem 2.1.2. Then

$$\varphi_\tau(\xi) = \begin{cases} \frac{1}{2} + \varrho(0), & \xi \in (0, \nu), \\ \\ \frac{1}{2} - \varrho(0), & \xi \in (-\nu, 0). \end{cases}$$

In addition,

$$\varphi_\tau(0) = \begin{cases} \frac{1}{2} + \varrho(0), & \tau = 1, \\ \\ \frac{1}{2} - \varrho(0), & \tau = 0. \end{cases}$$

viii) Let σ be rationally dependent. From the definition of φ_* and by Remark 2.1.9(vi), $\varphi_*(\xi)$ for $\xi \notin D$ consists of a discrete set of values in $[0, 1]$. These are the values of φ_τ on the constant intervals. Remark 2.1.9(vii) gives us two consecutive values from this set. Using (2.26), we can find all the values of this discrete set.

2.2 Numerical Results

In this section we present our numerical results for equation (2.2) with $n = 3$. We start by defining the numerical method used. After, we present traveling wave solutions across a wide range of the parameters. We also show how the various solution curves are related, i.e. how we can continue from the solution to one set of parameters to the solution with another set of parameters. The solution behavior we present ranges

Traveling Waves	Figure	δ_c	κ_c	α	β	γ	$\varepsilon_1, \varepsilon_2, \varepsilon_3$	σ	c
Reaction-Diffusion	2.11	10^{-5}	0	1	0	10^{-5}	*	$\frac{\sqrt{2}}{2}, \frac{\sqrt{2}}{2}, 0$	0
	2.12	10^{-3}	-0.1	1	0	10^{-3}	*	$\frac{\sqrt{2}}{2}, \frac{\sqrt{2}}{2}, 0$	-0.1
	2.13	10^{-5}	0.01	1	0	10^{-5}	1, 1, 1	*	0.01
	2.14	10^{-5}	0.1	1	0	10^{-5}	1,1,1	*	0.1
	2.15	10^{-5}	*	1	0	10^{-5}	1,0,0	1, 0, 0	*
	2.16	10^{-5}	*	1	0	10^{-5}	1,1,1	$\frac{\sqrt{2}}{2}, \frac{\sqrt{3}}{3}, \frac{\sqrt{6}}{6}$	*
Damped Wave	2.17	10^{-5}	*	0.5	*	*	1, 0, 0	1, 0, 0	*
	2.18	10^{-5}	*	1	*	*	1, 0, 0	1, 0, 0	*
Wave	2.19	10^{-5}	*	0	*	*	1, 0, 0	1, 0, 0	*
	2.20	*	*	0	0.5	*	1, 0, 0	1, 0, 0	*

Table 2.2: The $\varphi(\xi)$ plots. $*$ indicates quantities that vary.

from smooth solutions to solutions with kinks and steps. We finish this section with a survey of the relationship between the numerical and analytical solutions to (2.2).

2.2.1 The Numerical Method

We solve (2.2) with nonlinearity (2.4) on the truncated interval $\xi \in [-T, T]$ and use asymptotic boundary conditions to match the solution on this truncated problem with the boundary conditions (2.3) [7], [19]. We do not use the analytical solution (2.15), or the $a(c)$ relation (2.17) derived from it, in our numerical computations. In (2.2) with (2.4), the wave speed parameter c appears, but the detuning parameter a does not. Thus we only need to provide the wave speed c, not a or the $a(c)$ relation. Our intent is to develop a robust algorithm that we can use to numerically solve equations with

nonlinearities f such that analytical solutions are unknown. Our approach is to use a standard boundary value problem solver and to use continuation techniques to go from one set of parameters to another. The most obvious concerns that appear using this approach are the forward and backward delay terms of $L_T\varphi$ in (2.2). We handle the delay terms by obtaining their values from a previous solution in the continuation sequence. We then perform fixed point iteration, updating the delay terms along the way. Reformulating our traveling wave equation with this relaxation gives us

$$\begin{aligned} &-\kappa_c\varphi'_{m+1}(\xi) - \delta_c\varphi''_{m+1}(\xi) + (1 + 2\sum_{k=1}^{n}\varepsilon_k)\varphi_{m+1}(\xi) \\ &= \sum_{k=1}^{n}\varepsilon_k[\varphi_m(\xi + e_k\cdot\sigma) + \varphi_m(\xi - e_k\cdot\sigma)] + h(\xi), \end{aligned} \tag{2.28}$$

where $\varphi_0(\xi)$ is the solution to (2.2) at a previous choice of parameters. We perform the iteration in (2.28) until the residual generated by substituting φ_m into (2.2) is sufficiently small. We now present results concerning convergence of the method defined by (2.28). Let

$$G(\varphi_m(\xi)) = -\kappa_c\varphi'_m(\xi) - \delta_c\varphi''_m(\xi) + (1 + 2\sum_{k=1}^{n}\varepsilon_k)\varphi_m(\xi)$$

and let

$$F(\varphi_m(\xi)) = \sum_{k=1}^{n}\varepsilon_k[\varphi_m(\xi + e_k\cdot\sigma) + \varphi_m(\xi - e_k\cdot\sigma)].$$

Lemma 2.2.1 *Let φ satisfy $G(\varphi(\xi)) = F(\varphi(\xi))+h(\xi)$ on $\mathbb{R}$ with boundary conditions $\varphi(-\infty) = 0$ and $\varphi(\infty) = 1$. Let $\phi_1(\xi) = 1 - b_1 e^{-c_1\xi}$ for $\xi \geq 0$ and let $\phi_2(\xi) = b_2 e^{c_2\xi}$ for $\xi \leq 0$ with $b_1, c_1, b_2, c_2 > 0$. Let T_- and $T_+ \in \mathbb{R}^+$. Then b_1, c_1, b_2, c_2 may be chosen such that $|\varphi(\xi) - \phi_1(\xi)| \leq b_1 e^{-c_1\xi} \leq b_1 e^{-c_1 T_+}$ for $\xi \geq T_+$ and $|\varphi(\xi) - \phi_2(\xi)| \leq b_2 e^{c_2\xi} \leq b_2 e^{-c_2 T_-}$ for $\xi \leq -T_-$.*

Proof. Let

$$H(\varphi) = \frac{1}{\delta_c}[\delta_c\varphi'' + \kappa_c\varphi' + L_T\varphi - \varphi + h(\xi)].$$

Then for $\xi > 0$,

$$H(\phi_1(\xi)) = H(1-b_1e^{-c_1\xi}) = \frac{1}{\delta_c}[-\delta_c c_1^2 + 2\sum_{k=1}^{n}\varepsilon_k(1-\cosh[c_1(e_k\cdot\sigma)]) + \kappa_c c_1 + 1]b_1 e^{-c_1\xi}.$$

Since we want ϕ_1 to be a subsolution for $\xi \geq T_+$, we set $H(\phi_1(\xi)) \geq 0$ for $\xi \geq T_+$ and obtain the upper bound on c_1 defined by

$$2\sum_{k=1}^{n}\varepsilon_k + 1 \geq \delta_c c_1^2 + -\kappa_c c_1 + 2\sum_{k=1}^{n}\varepsilon_k \cosh[c_1(e_k\cdot\sigma)].$$

Letting $p_1 = \max_{c_1\in\mathbb{R}}[H(1-b_1e^{-c_1\xi}) \geq 0]$ for $\xi \geq T_+$ we see that $c_1 \in (0, p_1]$ for ϕ_1 to be a subsolution. Since we want ϕ_1 to be a subsolution we also need $\phi_1(T_+) \leq \varphi(T_+)$ and $\phi_1(\infty) \leq \varphi(\infty)$. Since both $\phi_1(\infty) = 1$ and $\varphi(\infty) = 1$ the second inequality is satisfied. The inequality $\phi_1(T_+) \leq \varphi(T_+)$ is satisfied when $b_1 \geq (1-\varphi(T_+))e^{c_1 T_+}$ once

c_1 is chosen. Thus for b_1 and c_1 satisfying the above conditions, ϕ_1 is a subsolution for $\xi \geq T_+$. Now let $w_1(\xi) = 1$ for $\xi \geq T_+$. Then $H(w_1) \leq 0$, $w_1(T_+) \geq \varphi(T_+)$, and $w_1(\infty) \geq \varphi(\infty)$. Thus w_1 is a supersolution for $\xi \geq T_+$.

Hence for $\xi \geq T_+$,

$$|\varphi(\xi) - \phi_1(\xi)| \leq |w_1(\xi) - \phi_1(\xi)| = b_1 e^{-c_1 \xi} \leq b_1 e^{-c_1 T_+}.$$

The proof that for $\xi \leq -T_-$,

$$|\varphi(\xi) - \phi_2(\xi)| \leq b_2 e^{c_2 \xi} \leq b_2 e^{-c_2 T_-},$$

is similar. ■

Remark 2.2.1 *When* $\varepsilon_1 = \varepsilon_2 = ... = \varepsilon_n = 0$, *there exist* b_1, c_1, b_2, c_2 *such that for* $\xi \geq T_+$, $|\varphi(\xi) - \phi_1(\xi)| = 0$, *and for* $\xi \leq -T_-$, $|\varphi(\xi) - \phi_2(\xi)| = 0$.

The Lemma 2.2.1 allows us to consider convergence of (2.28) on infinite intervals with the use of asymptotic boundary conditions.

Theorem 2.2.1 *Let* $\delta_c > 0$ *and let* φ *satisfy*

$$G(\varphi(\xi)) = F(\varphi(\xi)) + h(\xi) \tag{2.29}$$

on $\mathbb{R}$ with boundary conditions $\varphi(-\infty) = 0$ and $\varphi(\infty) = 1$. Define the sequence of functions $\{\varphi_m(\xi)\}_{m=0}^{\infty}$ by the iteration

$$G(\varphi_{m+1}(\xi)) = F(\varphi_m(\xi)) + h(\xi) \tag{2.30}$$

in (2.28). Define $\|\cdot\| = \sup_{\xi\in\mathbb{R}}|\cdot|$, $e_m(\xi) = \varphi_m(\xi) - \varphi(\xi)$, and let φ_0 be such that e_0 is continuously differentiable, $\varphi_0(-\infty) = 0$, and $\varphi_0(\infty) = 1$. Then $\lim_{m\to\infty}\|e_m\| = 0$.

Proof. We start off by establishing two inequalities. Let

$$\lambda = (2\sum_{k=1}^{n}\varepsilon_k)/(1 + 2\sum_{k=1}^{n}\varepsilon_k).$$

Then, for $\|e_m\| \neq 0$,

$$\begin{aligned}
\|F(e_m)\| &= \sup_{\xi\in\mathbb{R}}|\sum_{k=1}^{n}\varepsilon_k(e_m(\xi + e_k\cdot\sigma) + e_m(\xi - e_k\cdot\sigma))| \\
&\leq 2\sum_{k=1}^{n}\varepsilon_k\|e_m\| = \lambda(1 + 2\sum_{k=1}^{n}\varepsilon_k)\|e_m\| \\
&\leq \lambda\|-\kappa_c e_m' - \delta_c e_m'' + (1 + 2\sum_{k=1}^{n}\varepsilon_k)e_m\| = \lambda\|G(e_m)\|. \qquad (2.31)
\end{aligned}$$

The last inequality in (2.31) is established by choosing $\xi_0 \in (-\infty, +\infty)$ such that $|e_m(\xi_0)| = \|e_m\|$. Then since $e_m(\infty) = e_m(-\infty) = 0$, $e'_m(\xi_0) = 0$, $-\delta_c e''_m(\xi_0) \geq 0$ when

$$(1 + 2\sum_{k=1}^{n} \varepsilon_k) e_m(\xi_0) > 0,$$

and $-\delta_c e''_m(\xi_0) \leq 0$ when

$$(1 + 2\sum_{k=1}^{n} \varepsilon_k) e_m(\xi_0) < 0,$$

which implies

$$(1 + 2\sum_{k=1}^{n} \varepsilon_k)\|e_m\| \leq |-\kappa_c e'_m(\xi) - \delta_c e''_m(\xi) + (1 + 2\sum_{k=1}^{n} \varepsilon_k) e_m(\xi)|.$$

Applying (2.29) and (2.30) to (2.31), we get the two inequalities

$$\|G(e_m)\| \leq \lambda^m \|G(e_0)\| \quad \text{and} \quad \|F(e_m)\| \leq \lambda^m \|F(e_0)\|. \tag{2.32}$$

Thus $\lim_{m\to\infty} \|G(e_m(\xi))\| = 0$ and $\lim_{m\to\infty} \|F(e_m(\xi))\| = 0$. Using the definition of G, we have

$$e''_m(\xi) + \frac{\kappa_c}{\delta_c} e'_m(\xi) = -\frac{1}{\delta_c} G(e_m(\xi)) + \frac{(1 + 2\sum_{k=1}^{n} \varepsilon_k)}{\delta_c} e_m(\xi). \tag{2.33}$$

Let $C_1 = 1/(1 + 2\sum_{k=1}^{n} \varepsilon_k) > 0$. Since $\lim_{m\to\infty} \|F(e_m(\xi))\| = 0$,

$$\lim_{m\to\infty} |\sum_{k=1}^{n} \varepsilon_k(e_m(\xi + e_k \cdot \sigma) + e_m(\xi - e_k \cdot \sigma))| = 0,$$

and as $m \to \infty$ the local maxima of $e_m(\xi)$ are positive and the local minima are negative. Let ξ_1 be a value of ξ such that $e_m(\xi_1) > 0$ is a local maximum of $e_m(\xi)$. Suppose that there exist an M_1 such that for $m > M_1$, $e_m(\xi_1) > C_1|G(e_m(\xi_1))|$. But if $e_m(\xi_1)$ is a local maximum,

$$e_m''(\xi_1) + \frac{\kappa_c}{\delta_c} e_m'(\xi_1) < 0.$$

This violates equation (2.33) and hence $e_m(\xi_1) \leq C_1 G(e_m(\xi_1))$. Using the same argument for a local minimum, we obtain $|e_m(\xi)| \leq C_1|G(e_m(\xi))|$ whenever $e_m(\xi)$ has a local extrema. This in turn implies that $|e_m(\xi)| \leq C_1\|G(e_m)\|$ and $\|e_m\| \leq C_1\|G(e_m)\|$.

■

Remark 2.2.2 *Recall that when $\delta_c > 0$, the solution φ is continuously differentiable on $\mathbb{R}$. This implies that our initial guess φ_0 should also be at least continuously differentiable on $\mathbb{R}$. In fact, any continuously differentiable function φ_0 such that $\varphi_0(-\infty) = 0$ and $\varphi_0(\infty) = 1$ will work.*

The reformulation (2.28) is an ordinary differential equation, allowing us to use the standard boundary value solver *colmod*, from the family of collocation boundary value solvers which include *colsys* and *colnew* [2], [3], [4], [11], [12]. Our choice of this particular solver is based on several criteria. We want solutions to our system for a wide range of the parameters $\alpha, \beta, \gamma, (\varepsilon_1, \varepsilon_2, \varepsilon_3)$ and wave speed c. We also want a code in which we can perform continuation. Lastly, we want to solve this problem for a family of bistable nonlinearities, which include the cubic $f(\varphi) = \varphi(\varphi - a)(\varphi - 1)$, for example. We have found that, while the continuation feature of *colmod* is quite robust in our application, fixed point iteration is needed if we wish to continue from any solution to any other solution. A complete analysis of the homotopy and convergence properties of our method will appear in future works. The absolute error tolerances for the wave solutions is approximately 10^{-8} except for the curves where δ_c is close to zero. For our numerical method, this is a perturbation limit thus we used the absolute error tolerance of approximately 10^{-6} to limit how small a δ_c ($\approx 10^{-5}$) we could use. The $a(c)$ curves that appear in the previous section are computed using equation (2.19) and the quadrature algorithm *adapt* [59]. The algorithm *adapt* uses three point Gaussian quadrature to estimate the integrals and the seven point Kronrod rule to estimate errors. Absolute and relative errors at each quadrature step are set to 10^{-12} and the estimated error of the tail is set to 10^{-16}. The quadrature steps are of length 10. Since we calculate the $a(c)$ relation using (2.19), the $a(c)$ plots are

generated from the analytically derived traveling wave solution (2.15). Our numerical experiments were performed on a Silicon Graphics Indigo2.

2.2.2 Preliminaries

We now present numerically obtained traveling wave solutions, for a wide range of the parameters, in the form of solution plots which show the range and richness of solutions to (2.2). Recall, for a particular choice of $\delta_c \geq 0$, κ_c, $a \in (0,1)$, and $\varepsilon_1, \varepsilon_2, \varepsilon_3 \geq 0$, we have shown that there exists a traveling wave solution to (2.2) if δ_c and κ_c are not both zero. Table 2.2 lists the choices of the parameters in the plots that appear throughout this section. A $*$ entry indicates that the parameter varies in the particular plot.

Let γ and $(\varepsilon_1, \varepsilon_2, \varepsilon_3)$ be fixed. The κ_c, δ_c parameter maps in Figures 2.9, 2.10 exist for each choice of γ and $(\varepsilon_1, \varepsilon_2, \varepsilon_3)$ with δ_c bounded from above by γ. Each point in the upper half plane of Figures 2.9 and 2.10, excluding $(0,0)$, corresponds to a family of solutions to (2.2) parameterized by α, β, and c. Since $\varphi(-\xi, -\kappa_c) = 1 - \varphi(\xi, \kappa_c)$ (Section 2.2) we focus only on the $\kappa_c, \delta_c \geq 0$ quadrant ($c > 0$). Recall that $\delta_c = \gamma - c^2\beta$ and $\kappa_c = c\alpha$. Thus for each fixed $(\bar{\kappa}_c, \bar{\delta}_c)$, in first quadrant of Figures 2.9 and 2.10, the parameters α and β have the relation $\bar{\kappa}_c^2\beta = \alpha^2(\gamma - \bar{\delta}_c)$, a parabolic curve parameterized by c. In fact all solutions along the parabola for fixed

$\gamma, (\varepsilon_1, \varepsilon_2, \varepsilon_3), \bar{\kappa}_c, \bar{\delta}_c$, have the same a value and thus the α, β map is a map of level sets of the detuning parameter a. The location along a particular parabola is determined by c. As $c \to \infty$, $(\alpha, \beta) \to (0, 0)$ and as $c \to 0+$, $(\alpha, \beta) \to (\infty, \infty)$.

The parameter map κ_c, δ_c also exhibits level sets of a. Figure 2.9 is a contour plot with respect to a for different values of σ. We see that as the magnitudes of κ_c and δ_c increase, the direction σ has a decreasing effect on the value of a. We see that the effect of σ, and in fact of the spatially discrete Laplacian, is greatest when $\delta_c = 0$. In Figure 2.10, we see the effect of varying $(\varepsilon_1, \varepsilon_2, \varepsilon_3)$.

We now provide an outline to help in interpreting the traveling wave solution plots. In Figure 2.11, we have a solution plot where the discrete operator exhibits strong influence on the solution behavior. Recall that the points in the spatial lattice have distance 1 between nearest neighbors. Figure 2.11 is a plot of φ versus $\xi = \eta \cdot \sigma - ct$ where we are "traveling" in the $\sigma = (\sqrt{2}/2, \sqrt{2}/2, 0)$ direction. If we fix η, then these curves are plots, trajectories, of how each point in the lattice travels from one phase to the other. If we fix t, then the curves in Figure 2.11 are a cross section of the lattice and represent a wave traveling through the lattice.

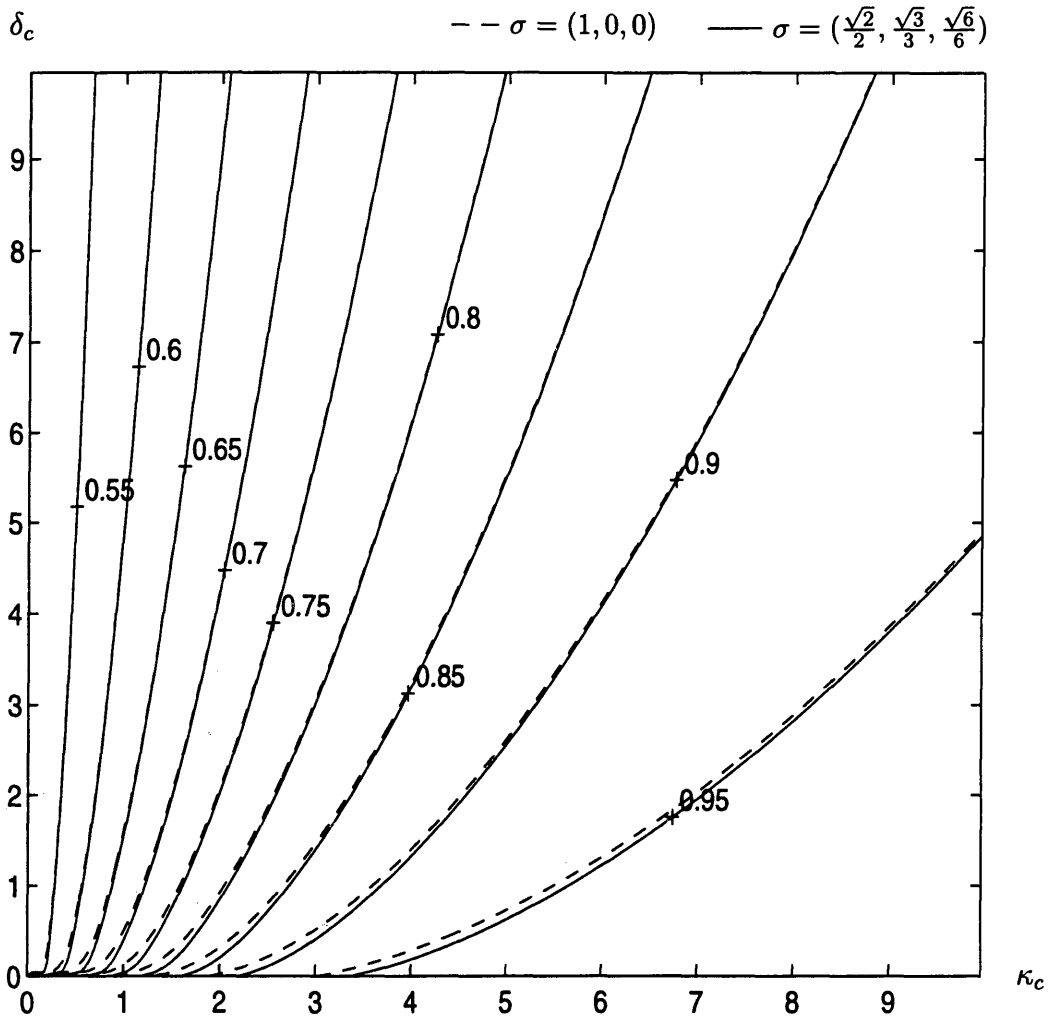

Fixed Parameter	$(\varepsilon_1, \varepsilon_2, \varepsilon_3)$
	$(1,1,1)$

Figure 2.9: Level sets of a with respect to the parameters κ_c and δ_c.

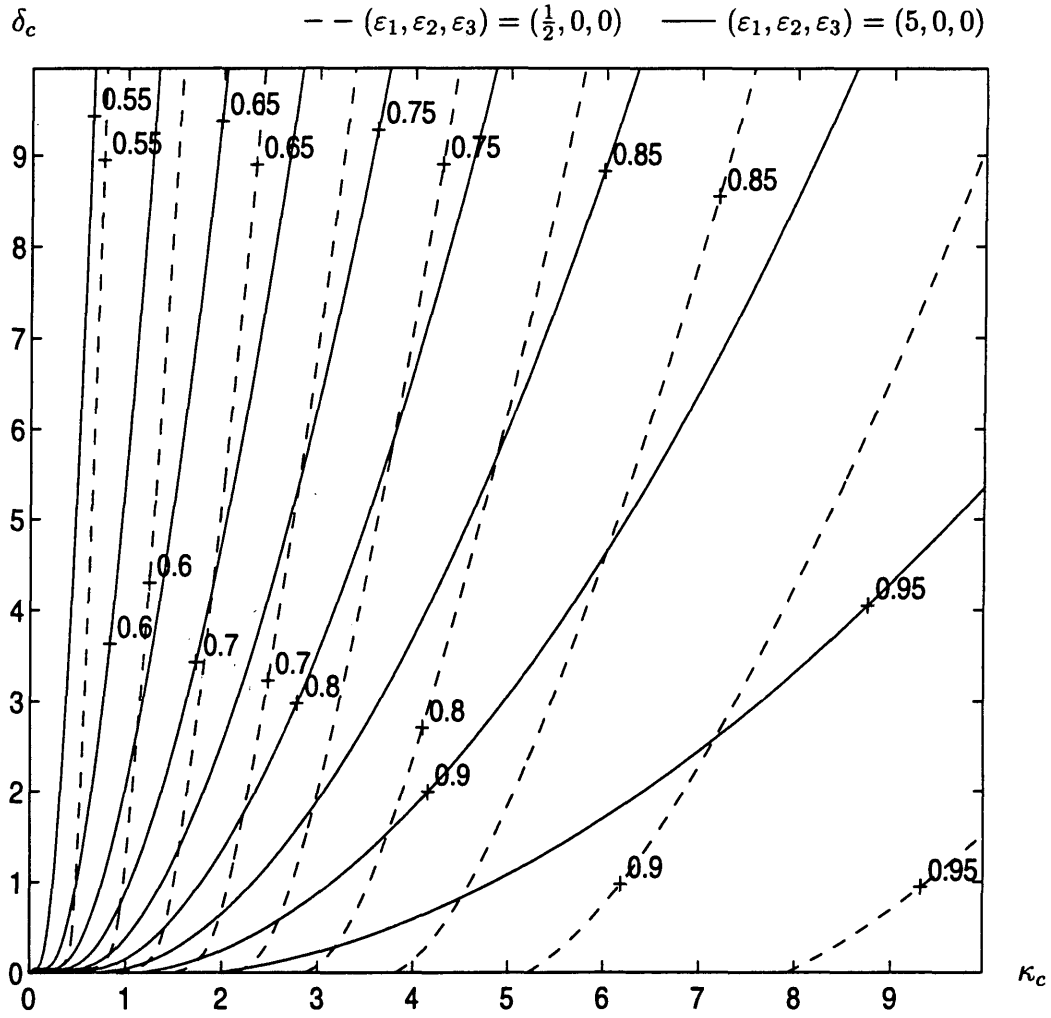

Fixed Parameter	σ
	$(1, 0, 0)$

Figure 2.10: Level sets of a with respect to the parameters κ_c and δ_c.

2.2.3 Impact of the Spatially Discrete Term

We now discuss how the parameters ε_k and σ_k affect the c versus a relation and how they affect the solution wave forms.

Figures 2.11 and 2.12 are sets of solution plots in which we vary ε_k. Figure 2.6 is the corresponding set of $a(c)$ curves where we vary ε_k. The direction vector is $\sigma = (\sqrt{2}/2, \sqrt{2}/2, 0)$ for all three plots. For this choice of σ, the problem becomes equivalent to the two dimensional problem with $\sigma = (\sqrt{2}/2, \sqrt{2}/2)$. With $\sigma_1 = \sigma_2 = \sqrt{2}/2$, changes in the solution curves and the $a(c)$ curves depend directly on the magnitude of $\sum_{k=1}^{3} \varepsilon_k$. If $\sum_{k=1}^{3} \varepsilon_k$ for one curve is greater than $\sum_{k=1}^{3} \varepsilon_k$ for a second curve, with all other parameters fixed, then the first curve will lie inside (closer to a for all $\xi \neq 0$ or closer to $1/2$ for all $c \neq 0$) the second curve.

Figures 2.13 and 2.14 provide a detailed example of lattice induced anisotropy for (2.2). These plots allow us to see what happens as $\kappa_c \to 0, \delta_c \to 0$ for solutions of different direction. Figures 2.13 and 2.14 are sets of solution curves $\varphi(\xi)$ where we vary σ. In Figures 2.13 and 2.14, Curves 1, 2, and 3 have σ's that are rationally dependent. Recall from Remark 2.1.9(vi) that for σ rationally dependent and $\delta_c = 0$, as $c \to 0$, $\varphi_{\tau_{\xi_0}}$ becomes constant on the intervals $(j\nu, (j+1)\nu)$ for all $j \in \mathbb{Z}$, with $\nu = \mathrm{GCD}(\sigma_1, \sigma_2, \sigma_3)$ as in $D = \{j\nu | j \in \mathbb{Z}\}$ and $\varphi = \varphi_{\tau_{\xi_0}}$ on D. In Figures 2.13 and 2.14, Curves 4 and 5 have σs that are as close to rationally independent as computer numbers allow. Recall from Remark 2.1.9(iv) that for σ rationally independent and

$\delta_c = 0$, as $c \to 0$, $\varphi_{\tau_{\xi_0}}$ is strictly increasing.

Figures 2.7 and 2.8 are sets of $a(c)$ curves where we vary σ. In these plots we see how the interval of propagation failure depends on the direction σ of the wave.

2.2.4 Numerical Solutions for the Reaction-Diffusion Equation

We now present and discuss solutions to (2.2) for $\beta = 0$ which implies that $\delta_c = \gamma$. Depending on the magnitudes of γ and $\sum_{k=1}^{3} \varepsilon_k$, (2.2) represents the traveling wave equation for the spatially discrete ($\gamma = 0$, $\sum_{k=1}^{3} \varepsilon_k \neq 0$) to the spatially continuous ($\sum_{k=1}^{3} \varepsilon_k = 0$, $\gamma \neq 0$) reaction-diffusion equations. Since we are using a code to solve a second order ordinary differential equation with γ as the coefficient on the second order term, we treat γ as a perturbation parameter (taking γ as small as possible) when we want to examine the solution behavior for the spatially discrete reaction-diffusion equation.

Looking at $a(c)$ curves for $\beta = 0$, Figures 2.1 and 2.2, we see that for $\delta_c = \gamma_c > 0$ as $\alpha \to 0+$ the $a(c)$ curve goes to $a(c) = 1/2$ and for $\delta_c = \gamma_c = 0$ as $\alpha \to 0+$ the $a(c)$ curve goes to $a(c) = 1/2 \pm \varrho(0)$.

We now consider solution plots where we approach the spatially discrete limit. In Figures 2.15 and 2.16 we vary c and take γ as small as possible ($\approx 10^{-5}$). The feature

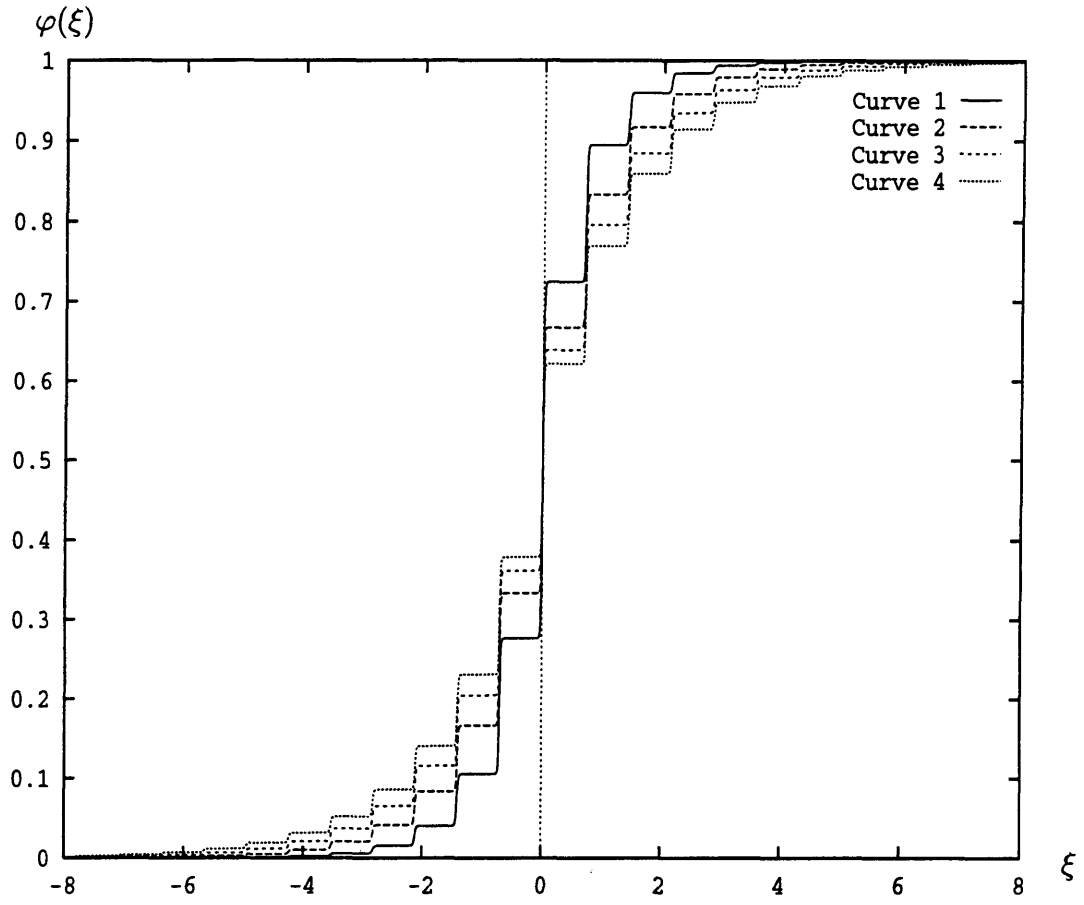

Curve	1	2	3	4
$(\varepsilon_1, \varepsilon_2, \varepsilon_3)$	$(\frac{1}{2}, \frac{1}{2}, 0)$	$(\frac{1}{2}, \frac{3}{2}, 0)$	$(1, 2, 0)$	$(2, 2, 0)$

Fixed	δ_c	κ_c	α	β	γ	σ	c
Parameters	10^{-5}	0	1	0	10^{-5}	$(\frac{\sqrt{2}}{2}, \frac{\sqrt{2}}{2}, 0)$	0

Figure 2.11: A $\varphi(\xi)$ plot approaching the spatially discrete limit for the reaction-diffusion equation.

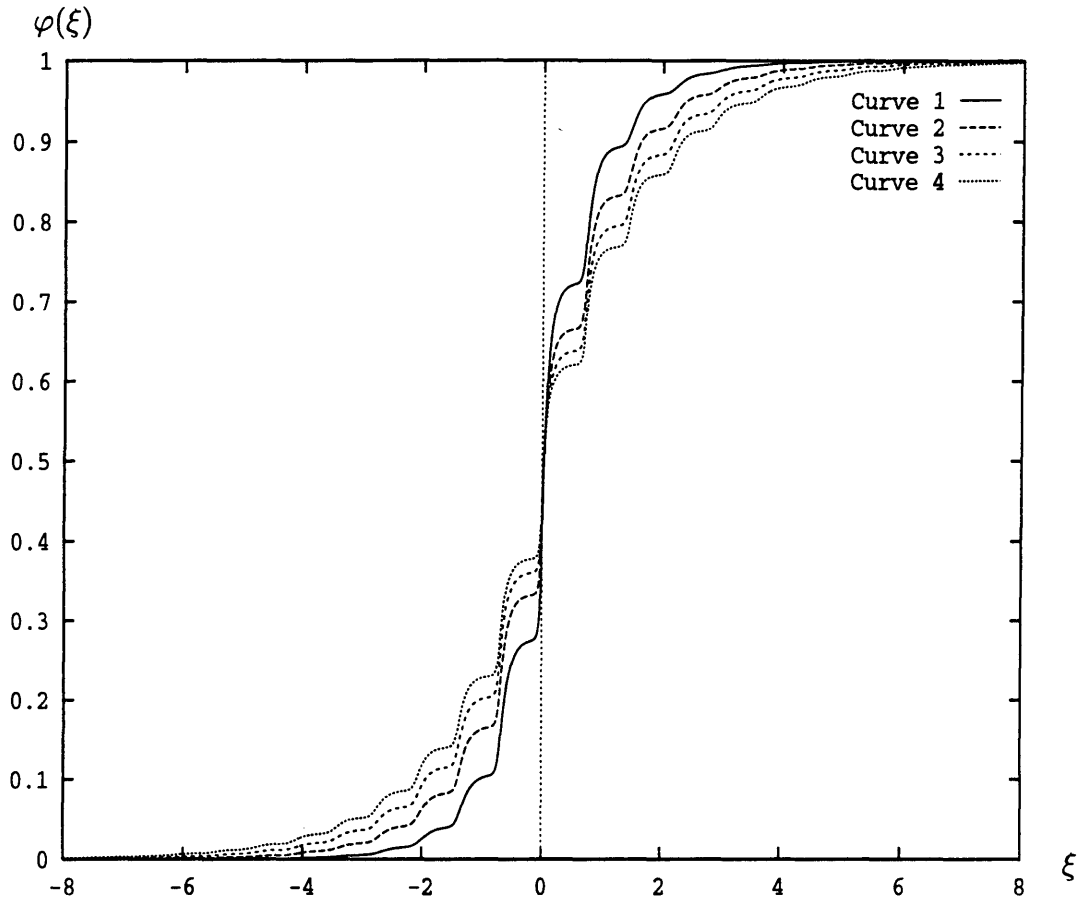

Curve	1	2	3	4
$(\varepsilon_1, \varepsilon_2, \varepsilon_3)$	$(\frac{1}{2}, \frac{1}{2}, 0)$	$(\frac{1}{2}, \frac{3}{2}, 0)$	$(1, 2, 0)$	$(2, 2, 0)$

Fixed	δ_c	κ_c	α	β	γ	σ	c
Parameters	10^{-3}	-0.1	1	0	10^{-3}	$(\frac{\sqrt{2}}{2}, \frac{\sqrt{2}}{2}, 0)$	-0.1

Figure 2.12: A $\varphi(\xi)$ plot for the reaction-diffusion equation.

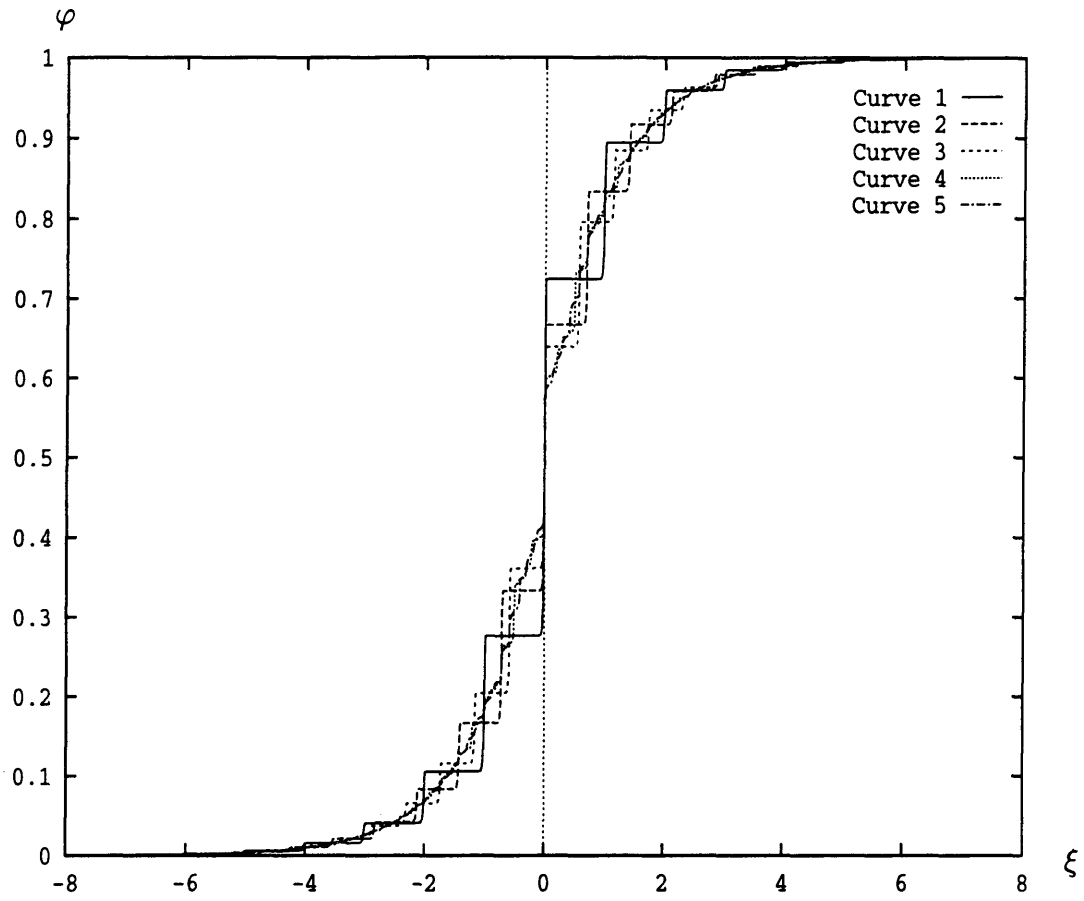

Curve	1	2	3	4	5
σ	$(1,0,0)$	$(\frac{\sqrt{2}}{2},\frac{\sqrt{2}}{2},0)$	$(\frac{\sqrt{3}}{3},\frac{\sqrt{3}}{3},\frac{\sqrt{3}}{3})$	$(\frac{1}{2},\frac{1}{2},\frac{\sqrt{2}}{2})$	$(\frac{\sqrt{2}}{2},\frac{\sqrt{3}}{3},\frac{\sqrt{6}}{6})$

Fixed	δ_c	κ_c	α	β	γ	$(\varepsilon_1,\varepsilon_2,\varepsilon_3)$	c
Parameters	10^{-5}	0.01	1	0	10^{-5}	$(1,1,1)$	0.01

Figure 2.13: A $\varphi(\xi)$ plot approaching the spatially discrete limit for the reaction-diffusion equation.

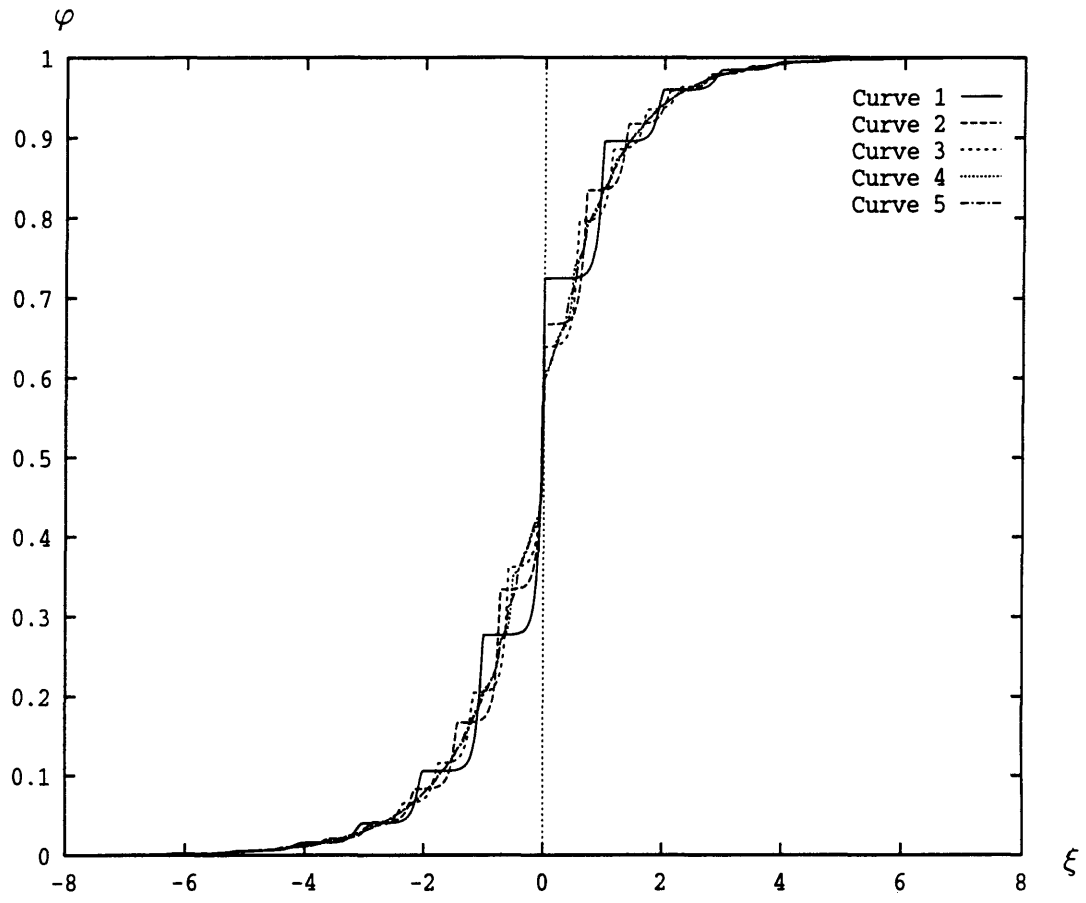

Curve	1	2	3	4	5
σ	$(1,0,0)$	$(\frac{\sqrt{2}}{2},\frac{\sqrt{2}}{2},0)$	$(\frac{\sqrt{3}}{3},\frac{\sqrt{3}}{3},\frac{\sqrt{3}}{3})$	$(\frac{1}{2},\frac{1}{2},\frac{\sqrt{2}}{2})$	$(\frac{\sqrt{2}}{2},\frac{\sqrt{3}}{3},\frac{\sqrt{6}}{6})$

Fixed Parameters	δ_c	κ_c	α	β	γ	$(\varepsilon_1,\varepsilon_2,\varepsilon_3)$	c
	10^{-5}	0.1	1	0	10^{-5}	$(1,1,1)$	0.1

Figure 2.14: A $\varphi(\xi)$ plot for the reaction-diffusion equation.

we wish to illustrate with the plots is the "kink" which forms in the solution curves at $\varphi(0)$. Recall from (2.1.3) that $\delta_c = \gamma = 0$ implies for $\kappa_c \neq 0$ that $\lim_{\xi \to 0+} \varphi'(\xi) \neq \lim_{\xi \to 0-} \varphi'(\xi)$, hence the "kink". In both of these plots, we see that the larger the magnitude of κ_c, the farther a is from 1/2. Also notice that, except for σ, Figures 2.15 and 2.16 have the same set of parameters. These plots show an example of how the solution curves depend on the direction σ.

The first of the $(\varepsilon_1, \varepsilon_2, \varepsilon_3)$ plots, Figure 2.11, and Figures 2.13 and 2.14 are also examples of the solutions to the reaction-diffusion equation as we approach the spatially discrete limit.

2.2.5 Numerical Solutions for the Damped Wave Equation

We now present and discuss solutions to (2.2) for $\alpha, \beta \neq 0$. Figures 2.17 and 2.18 are examples of solutions to the damped wave equation for $\alpha > 0$ and $\beta \to \gamma/c^2$. Here we vary $\gamma = c^2$. These are the same solutions as for the spatially discrete reaction-diffusion equation since $\delta_c = \gamma - c^2\beta \to 0$.

2.2.6 Numerical Solutions for the Wave Equation

We now present and discuss solutions to (2.2) for $\kappa_c = \alpha = 0$ and $\beta > 0$. Figure 2.20 is an example of solutions to the wave equation. The lack of a damping term fixes

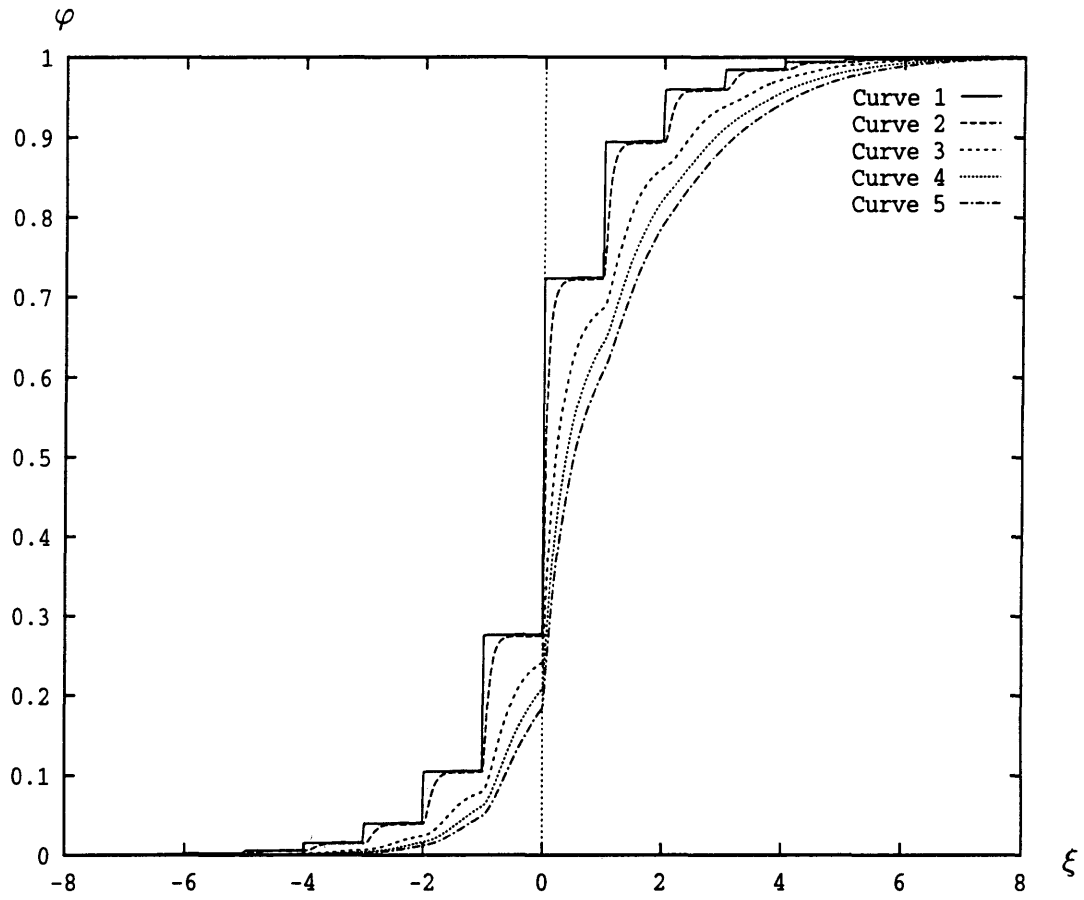

Curve	1	2	3	4	5
$\kappa_c = c$	0	-0.1	-0.5	-0.8	-1

Fixed Parameters	δ_c	α	β	γ	$(\varepsilon_1, \varepsilon_2, \varepsilon_3)$	σ
	10^{-5}	1	0	10^{-5}	$(1,1,1)$	$(1,0,0)$

Figure 2.15: A $\varphi(\xi)$ plot approaching the spatially discrete reaction-diffusion equation.

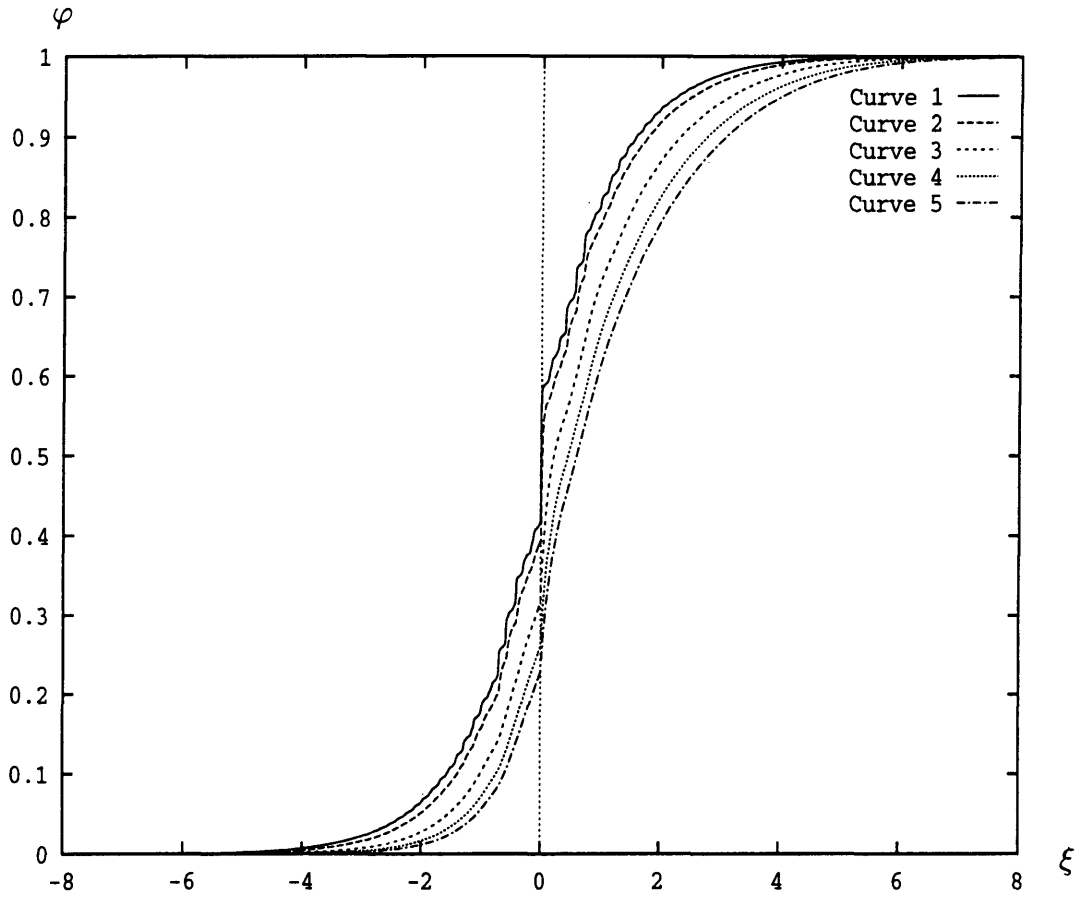

Curve	1	2	3	4	5
$\kappa_c = c$	0	-0.1	-0.5	-0.8	-1

Fixed	δ_c	α	β	γ	$(\varepsilon_1, \varepsilon_2, \varepsilon_3)$	σ
Parameters	10^{-5}	1	0	10^{-5}	$(1,1,1)$	$(\frac{\sqrt{2}}{2}, \frac{\sqrt{3}}{3}, \frac{\sqrt{6}}{6})$

Figure 2.16: A $\varphi(\xi)$ plot approaching the spatially discrete reaction-diffusion equation.

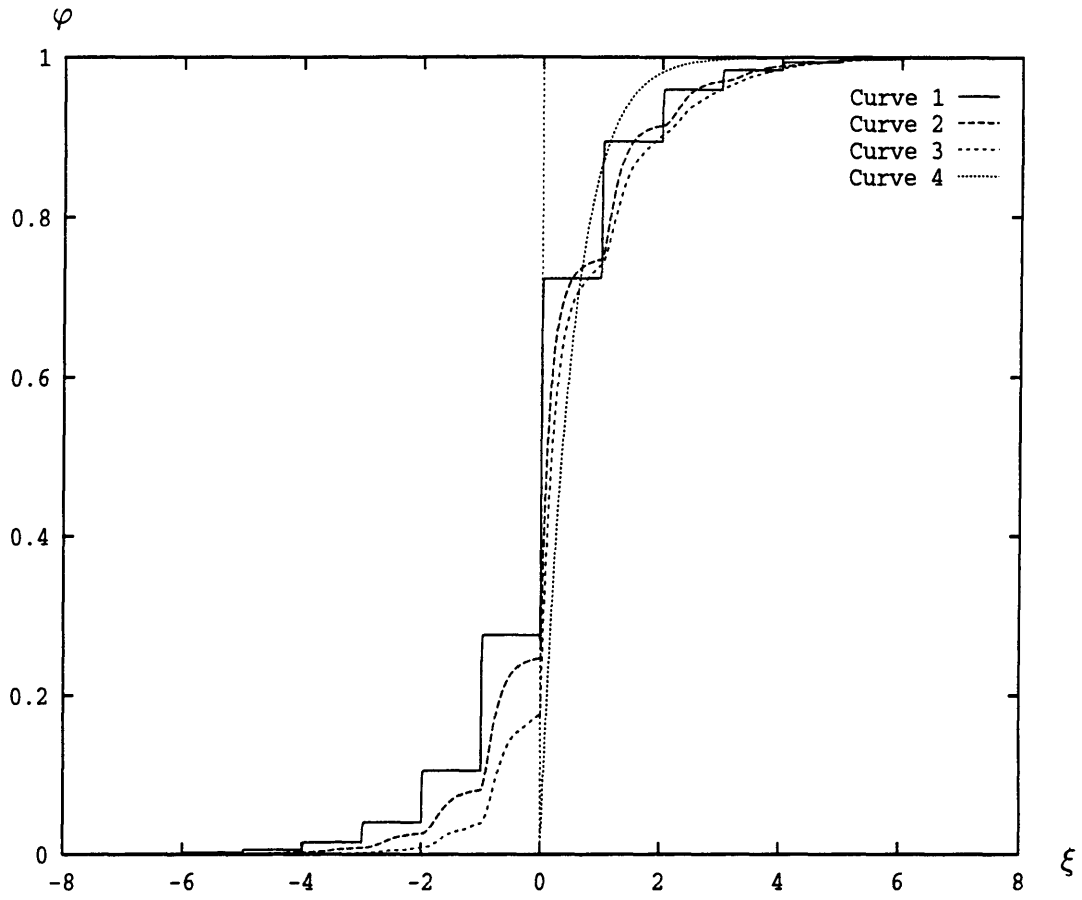

Curve	1	2	3	4
$\gamma = c^2$	0	0.25	0.50	1

Fixed	δ_c	α	$(\varepsilon_1, \varepsilon_2, \varepsilon_3)$	σ
Parameters	10^{-5}	0.5	$(1,0,0)$	$(1,0,0)$

Figure 2.17: A $\varphi(\xi)$ plot of the damped wave equation approaching the spatially discrete reaction-diffusion equation.

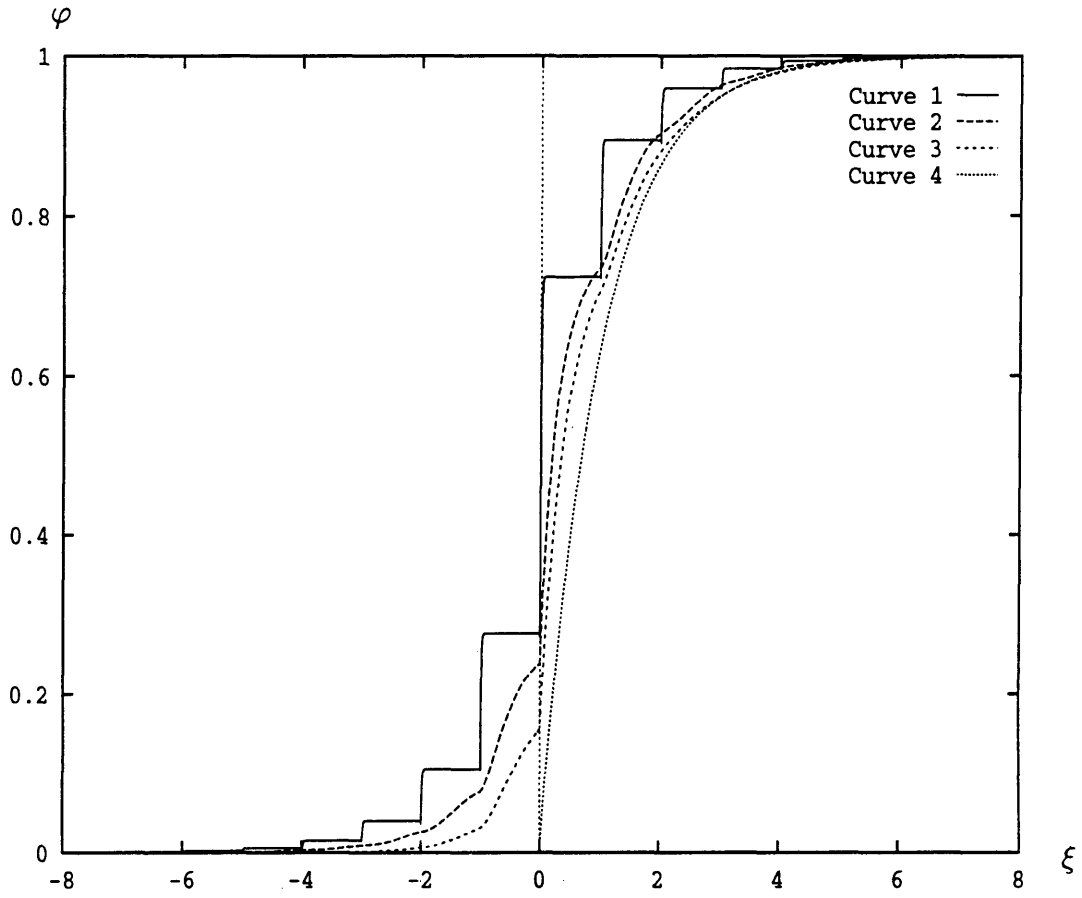

Curve	1	2	3	4
$\gamma = c^2$	0	0.25	0.50	1

Fixed Parameters	δ_c	α	$(\varepsilon_1, \varepsilon_2, \varepsilon_3)$	σ
	10^{-5}	1	$(1,0,0)$	$(1,0,0)$

Figure 2.18: A $\varphi(\xi)$ plot of the damped wave equation approaching the spatially discrete reaction-diffusion equation.

$a = 1/2$ and disallows the possibility of the "kink" effect. Comparing the formation of steps for the wave equation, Figure 2.19, with the formation of steps for the reaction-diffusion or damped wave equation, Figures 2.13, 2.14, 2.17, and 2.18, we see that although all the step solutions are approaching the same solution, $\kappa_c \to 0$ and $\delta_c \to 0$, the formation of kinks depend on how we approach these solutions.

2.3 Chapter Summary

We have presented an investigation of the traveling wave solutions of (2.2) with boundary conditions (2.3) and the piecewise linear nonlinearity (2.4), incorporating the phase condition $\varphi(0) = a$. This investigation consisted of results obtained from an analytically constructed solution and from a numerically calculated solution. The two solution methods used were implemented independently of one another. We derived the relation between the wave speed c and the detuning parameter a from the analytically obtained solution. For $\kappa_c \neq 0, \delta_c \geq 0$, a solution $\varphi(\xi)$ exists, is continuous, and is strictly increasing on the real line, and $\varphi'(\xi)$ is continuous on the real line if and only if $\delta_c > 0$. The piecewise continuous nonlinearity f_1 produces the discontinuity in φ' which we see as the "kinks" in Figures 2.15 and 2.16 (the reaction-diffusion case). For $\sum_{k=1}^{n} \varepsilon_k \neq 0$, there exists a nontrivial interval for a of propagation failure if and only if $\gamma = 0$. The wave speed c is restricted to a proper subinterval of $\mathbb{R}$ for the damped wave equation. This restriction also affects the detuning parameter a.

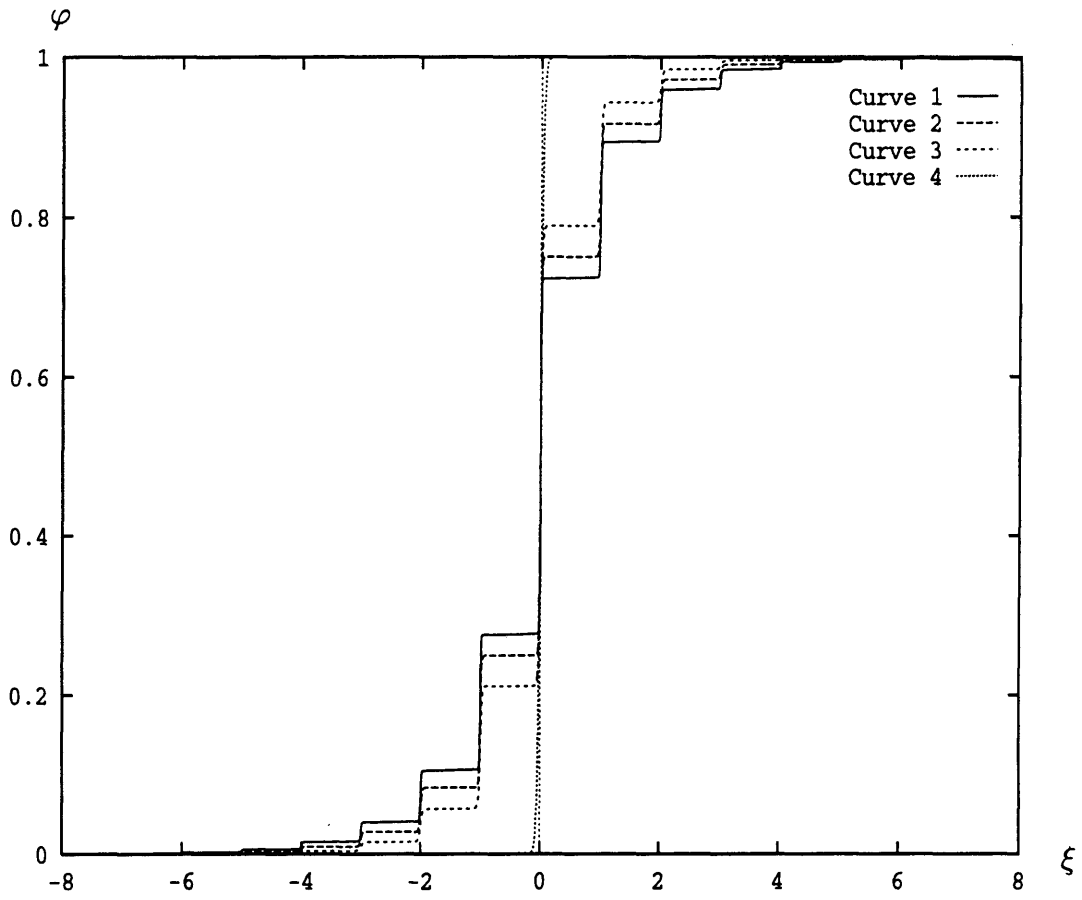

Curve	1	2	3	4
$\gamma = c^2$	0	0.25	0.50	1

Fixed Parameters	δ_c	α	$(\varepsilon_1, \varepsilon_2, \varepsilon_3)$	σ
	10^{-5}	0	$(1,0,0)$	$(1,0,0)$

Figure 2.19: A $\varphi(\xi)$ plot of the damped wave equation approaching the spatially discrete reaction-diffusion equation.

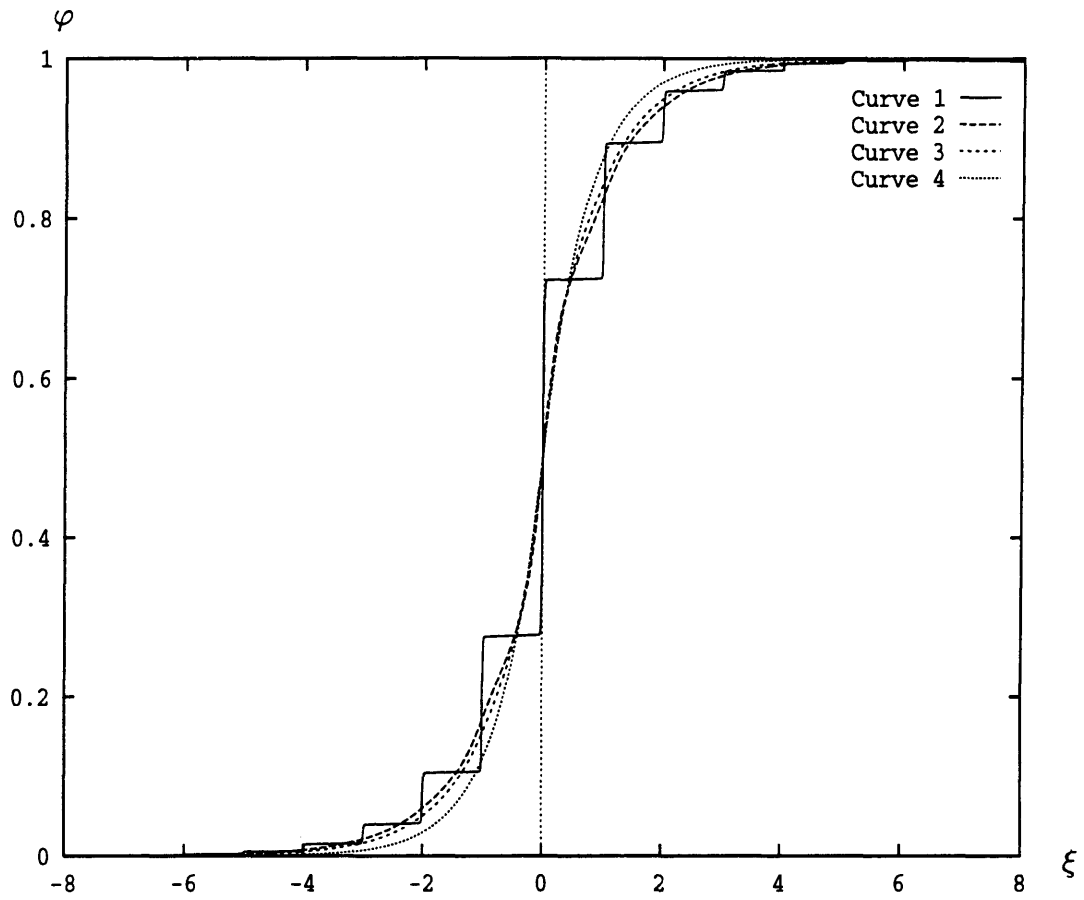

Curve	1	2	3	4
$\gamma = c^2$	0	0.25	0.50	1

Fixed	α	β	$(\varepsilon_1, \varepsilon_2, \varepsilon_3)$	σ
Parameters	0	0.5	$(1,0,0)$	$(1,0,0)$

Figure 2.20: A $\varphi(\xi)$ plot of the damped wave equation approaching the spatially discrete reaction-diffusion equation.

No such restrictions exist for the reaction-diffusion equation. When σ is rationally related, we can construct from the interval of propagation failure the set of discrete φ values that are the zeros of the right-hand side of (2.2). While for the reaction-diffusion and damped wave equations the detuning parameter varies with the wave speed c, $a = 1/2$ for all c for the undamped wave equation. In Chapter 5, we explore solutions (φ, c) of (2.2) for other bistable nonlinearities.

Chapter 3

THE SPATIALLY DISCRETE REACTION DIFFUSION EQUATION WITH VARIABLE DIFFUSION

In this chapter we consider traveling wave solutions to spatially discrete reaction-diffusion equations with diffusion coefficients that vary on a spatially discrete domain of the form

$$\dot{u}(\eta,t) = L_D u(\eta,t) - f(u(\eta,t),a), \tag{3.1}$$

where $u(\eta,t)$ maps $\mathbb{Z} \times \mathbb{R} \to \mathbb{R}$, and "$\cdot$" denotes differentiation with respect to t. We represent variable diffusion over the spatially discrete domain with the operator L_D, a discrete Laplacian operator defined with respect to an integer lattice of the form

$$L_D u(\eta,t) = \alpha(\eta+1)[u(\eta+1,t) - u(\eta,t)] + \alpha(\eta)[u(\eta-1,t) - u(\eta,t)],$$

where $\alpha : \mathbb{Z} \to \mathbb{R}$. This is one choice of several equivalent divergence forms for the operator L_D. Our interest is still in bistable systems, systems where $f(u)$ can be represented by a cubic-like nonlinear function with stable zeros at 0 and 1, and an unstable zero at the detuning parameter $a \in (0,1)$. In this chapter, because we are concentrating on analytical solutions, we use the piecewise linear representation f_1, (1.9). Unlike Chapter 2, only analytical results are presented here. Numerical results for varying diffusion coefficient traveling wave equations appear in Chapter 5.

Due to the dependence of α on η, for a fixed value of the detuning parameter a, the traveling wave ansatz is $u(\eta,t) = \varphi(\eta - c(\eta)t)$, where $\varphi : \mathbb{R} \to \mathbb{R}$ and where the unknown wave speed $c : \mathbb{Z} \to \mathbb{R}$ now varies on the spatial lattice. Substituting the traveling wave ansatz into (3.1), we obtain the spatially discrete equation

$$-c(\eta)\varphi'(\xi) = L_T\varphi(\xi) - f(\varphi(\xi)), \tag{3.2}$$

where $\xi = \eta - c(\eta)t$ and

$$L_T\varphi(\xi) = \alpha(\eta+1)[\varphi(\xi+1) - \varphi(\xi)] + \alpha(\eta)[\varphi(\xi-1) - \varphi(\xi)].$$

In Chapter 2 we were able to use the Fourier transform to solve the traveling wave differential-difference equation (2.2) because the coefficients were constant and did not vary with the lattice. Recall that our traveling wave differential-difference

equation also represents an infinite system of constant coefficient time dependent ordinary differential equations (ODEs). This is true even if the coefficients of the differential-difference equation depend on η, because the infinite system of ODEs is indexed by the lattice. Our method for solving variable diffusion coefficient problems involves redefining the problem in terms of constant coefficient equations. But we would like to work with finite dimensional systems. Thus we consider differential-difference equations periodic diffusion coefficients of period P because they can be represented by a system of dimension P of constant coefficient, constant wave speed ordinary differential and differential-difference equations.

In Section 3.1 we first complete the definition of the problem, including boundary conditions and a phase condition. Next we derive a solution to the periodic version of (3.2) when $c(\eta)$ is not equal to zero for all $\eta \in \mathbb{Z}$, by solving the equivalent constant coefficient system, in Section 3.2. Since the general periodic case is rather cumbersome algebraically, in Section 3.3, we demonstrate the periodic coefficient result for an equation of the form (3.2) with period $P = 2$, along with its $a(c(\eta))$ relation. In addition, we show that $\varphi(\xi)$, for period two diffusion, is strictly increasing in time. Section 3.4 consists of a summary of this chapter.

3.1 Background

As in Chapter 2, we impose the boundary conditions

$$\varphi(-\infty) = 0, \quad \varphi(\infty) = 1 \tag{3.3}$$

and the phase condition $\varphi(0) = a$ to (3.2). Recall also that

$$f(\varphi(\xi)) = \varphi(\xi) - h(\varphi(\xi) - a) = \varphi(\xi) - h(\xi) \qquad \text{for} \quad \xi \neq 0, \tag{3.4}$$

and $\lim_{\xi \to 0-} \varphi'(\xi) \neq \lim_{\xi \to 0+} \varphi'(\xi)$.

3.1.1 Periodic Diffusion Coefficient

Consider a diffusion coefficient function that is periodic in $\eta \in \mathbb{Z}$ of period $P = N_l + N_r + 1$, with $N_l, N_r \in \mathbb{Z}^+ \cup \{0\}$ defined for $n \in \mathbb{Z}$ as

$$\alpha(\eta) = \begin{cases} \alpha_{-N_l}, & \eta = Pn - N_l, \\ \alpha_{-N_l+1}, & \eta = Pn - N_l + 1, \\ \alpha_{-N_l+2}, & \eta = Pn - N_l + 2, \\ \vdots & \\ \alpha_0, & \eta = Pn, \\ \vdots & \\ \alpha_{N_l}, & \eta = Pn + N_r, \end{cases} \tag{3.5}$$

where $\alpha_{-N_l}, \alpha_{-N_l+1}, \alpha_{-N_l+2}, ..., \alpha_{N_r} \in \mathbb{R}^+$. Let $\xi = Pn - ct$, $n \in \mathbb{Z}$ and define

$$\begin{array}{rclcrcl}
c_{-N_l} & = & c(-N_l), & & \varphi_{-N_l}(\xi) & = & \varphi(\xi - N_l), \\
c_{-N_l+1} & = & c(-N_l+1), & & \varphi_{-N_l+1}(\xi) & = & \varphi(\xi - N_l + 1), \\
c_{-N_l+2} & = & c(-N_l+2), & & \varphi_{-N_l+2}(\xi) & = & \varphi(\xi - N_l + 2), \\
 & \vdots & & & & \vdots & \\
c_0 & = & c(0), & & \varphi_0(\xi) & = & \varphi(\xi). \\
 & \vdots & & & & \vdots & \\
c_{N_r} & = & c(N_r), & & \varphi_{N_r}(\xi) & = & \varphi(\xi + N_r).
\end{array} \tag{3.6}$$

Thus $\varphi = \varphi_k$ when $\eta = Pn + k$, for any $k \in \{N_l, .., N_r\}$, and equation (3.2) can be represented by the following system of equations. When $\eta = Pn - N_l$,

$$\begin{aligned}
-c_{-N_l}\varphi'_{-N_l}(\xi) &= \alpha(\eta+1)[\varphi_{-N_l+1}(\xi) - \varphi_{-N_l}(\xi)] \\
&\quad + \alpha(\eta)[\varphi_{N_r}(\xi - P) - \varphi_{-N_l}(\xi)] - f(\varphi_{-N_l}(\xi)) \\
&= \alpha_{-N_l+1}[\varphi_{-N_l+1}(\xi) - \varphi_{-N_l}(\xi)] \\
&\quad + \alpha_{-N_l}[\varphi_{N_r}(\xi - P) - \varphi_{-N_l}(\xi)] - f(\varphi_{-N_l}(\xi)),
\end{aligned}$$

when $\eta = Pn + j$, $j = -N_l + 1, ..., N_r - 1$,

$$-c_j\varphi'_j(\xi) = \alpha(\eta+1)[\varphi_{j+1}(\xi) - \varphi_j(\xi)] + \alpha(\eta)[\varphi_{j-1}(\xi) - \varphi_j(\xi)] - f(\varphi_j(\xi))$$

$$= \alpha_{j+1}[\varphi_{j+1}(\xi) - \varphi_j(\xi)] + \alpha_j[\varphi_{j-1}(\xi) - \varphi_j(\xi)] - f(\varphi_j(\xi)),$$

and when $\eta = Pn + N_r$,

$$\begin{aligned} -c_{N_r}\varphi'_{N_r}(\xi) &= \alpha(\eta+1)[\varphi_{-N_l}(\xi+P) - \varphi_{N_r}(\xi)] \\ &\quad +\alpha(\eta)[\varphi_{N_r-1}(\xi) - \varphi_{N_r}(\xi)] - f(\varphi_{N_r}(\xi)) \\ &= \alpha_{-N_l}[\varphi_{-N_l}(\xi+P) - \varphi_{N_r}(\xi)] \\ &\quad +\alpha_{N_r}[\varphi_{N_r-1}(\xi) - \varphi_{N_r}(\xi)] - f(\varphi_{N_r}(\xi)). \end{aligned} \tag{3.7}$$

The phase condition $\varphi(0) = a$ implies $\varphi_k(-k) = a$ and the nonlinearity $f(\varphi(\xi)) = \varphi(\xi) - h(\xi)$ implies $f(\varphi_k(\xi)) = \varphi_k(\xi) - h(\xi + k)$, for $k = N_l, ..., N_r$. Since $\varphi_k = \varphi$, $\varphi_k(\xi) \to 0$ as $\xi \to -\infty$ and $\varphi_k(\xi) \to 1$ as $\xi \to \infty$, for $k = N_l, ..., N_r$.

3.2 An Analytic Solution

We now derive the solution of the traveling wave equation (3.2) with periodic diffusion coefficient $\alpha(\eta)$, the boundary conditions (3.3), and the piecewise linear function f_1 (1.9). We begin our derivation with the construction of solutions, $\varphi_k(\xi)$, $k = -N_l, ..., N_r$, for (3.2) with diffusion coefficient (3.5). The construction consists of defining functions $\phi_k(\xi) = e^{-\varepsilon\xi}\varphi_k(\xi)$ for $k = -N_l, ..., N_r$ and transforming the system (3.7). To the $\phi_k(\xi)$ versions of the equations, we apply the Fourier transform, the

reason for using f_1, and after some manipulation, we derive a formula for each $\varphi_k(\xi)$, $k = -N_l, ..., N_r$. We begin our derivation of a solution with a preliminary lemma.

Lemma 3.2.1 *Let φ_k, $k = N_l, ..., N_r$ be the solution elements of (3.2). Then there exists an $\varepsilon_0 > 0$ such that, for some $K > 0$,*

$$|\varphi_k(\xi)| \leq Ke^{\varepsilon_0 \xi} \quad \text{for} \quad \xi \leq 0. \tag{3.8}$$

Proof. Lemma 2.1.1 implies that for each φ_k, $k = N_l, ..., N_r$ there exists an $\varepsilon_{k0} > 0$ such that, for some $K_k > 0$, $\quad |\varphi_k(\xi)| \leq K_k e^{\varepsilon_{k0}\xi} \quad$ for $\quad \xi \leq 0$. Let

$$K = \max_{k=N_l,...,N_r} K_k \qquad \text{and} \qquad \varepsilon_0 = \min_{k=N_l,...,N_r} \varepsilon_{k0}.$$

■

Let $\phi_k(\xi) = e^{-\varepsilon\xi}\varphi_k(\xi)$ for $k = N_l, ..., N_r$ with $\varepsilon > 0$, ε small. By Lemma 3.2.1, if φ_k, $k = N_l, ..., N_r$, is a solution element to (3.2), then, as $\xi \to -\infty$,

$$\phi_k(\xi) = e^{-\varepsilon\xi}\varphi_k(\xi) \leq |e^{-\varepsilon\xi}||\varphi_k(\xi)| \leq |Ke^{(\varepsilon_0-\varepsilon)\xi}| \to 0 \quad \text{for} \quad 0 < \varepsilon < \varepsilon_0.$$

Also as $\xi \to \infty$,

$$\phi_k(\xi) = e^{-\varepsilon\xi}\varphi_k(\xi) \to 0$$

since $\varphi_k(+\infty) = 1$ and $\varepsilon_k > 0$. This implies that $\phi_k(-\infty) = 0$ and $\phi_k(+\infty) = 0$.

Substituting $\varphi_k(\xi) = e^{\varepsilon\xi}\phi_k(\xi)$, $k = -N_l, ..., N_r$, into (3.7), we obtain

$$\begin{aligned} -c_{-N_l}e^{\varepsilon\xi}[\varepsilon\phi_{-N_l}(\xi) &+ \phi'_{-N_l}(\xi)] = \alpha_{-N_l+1}e^{\varepsilon\xi}[\phi_{-N_l+1}(\xi) - \phi_{-N_l}(\xi)] \\ &+ \alpha_{-N_l}e^{\varepsilon\xi}[e^{-P\varepsilon}\phi_{N_r}(\xi - P) - \phi_{-N_l}(\xi)] - e^{\varepsilon\xi}\phi_{-N_l}(\xi) + h(\xi - N_l), \end{aligned}$$

$$\begin{aligned} -c_j e^{\varepsilon\xi}[\varepsilon\phi_j(\xi) + \phi'_j(\xi)] &= \alpha_{j+1}e^{\varepsilon\xi}[\phi_{j+1}(\xi) - \phi_j(\xi)] \\ &+ \alpha_j e^{\varepsilon\xi}[\phi_{j-1}(\xi) - \phi_j(\xi))] - e^{\varepsilon\xi}\phi_j(\xi) + h(\xi + j), \end{aligned}$$

$$\begin{aligned} -c_{N_r}e^{\varepsilon\xi}[\varepsilon\phi_{N_r}(\xi) + \phi'_{N_r}(\xi)] &= \alpha_{-N_l}e^{\varepsilon\xi}[e^{P\varepsilon}\phi_{-N_l}(\xi + P) - \phi_{N_r}(\xi)] \\ &+ \alpha_{N_r}e^{\varepsilon\xi}[\phi_{N_r-1}(\xi) - \phi_{N_r}(\xi)] - e^{\varepsilon\xi}\phi_{N_r}(\xi) + h(\xi + N_r), \end{aligned}$$

which simplifies to

$$\begin{aligned} - \; & c_{-N_l}\phi'_{-N_l}(\xi) = \alpha_{-N_l+1}[\phi_{-N_l+1}(\xi) - \phi_{-N_l}(\xi)] \\ & +\alpha_{-N_l}[e^{-P\varepsilon}\phi_{N_r}(\xi - P) - \phi_{-N_l}(\xi)] - (1 - c_{-N_l}\varepsilon)\phi_{-N_l}(\xi) + e^{-\varepsilon\xi}h(\xi - N_l), \end{aligned}$$

$$- \quad c_j\phi_j'(\xi) = \alpha_{j+1}[\phi_{j+1}(\xi) - \phi_j(\xi)] + \alpha_j[\phi_{j-1}(\xi) - \phi_j(\xi)]$$
$$-(1 - c_j\varepsilon)\phi_j(\xi) + e^{-\varepsilon\xi}h(\xi + j),$$

$$- \quad c_{N_r}\phi_{N_r}'(\xi) = \alpha_{-N_l}[e^{P\varepsilon}\phi_{-N_l}(\xi + P) - \phi_{N_r}(\xi)] + \alpha_{N_r}[\phi_{N_r-1}(\xi) - \phi_{N_r}(\xi)]$$
$$-(1 - c_{N_r}\varepsilon)\phi_{N_r}(\xi) + e^{-\varepsilon\xi}h(\xi + N_r), \tag{3.9}$$

with $j = -N_l + 1, ..., N_r - 1$. Now let's apply the Fourier transforms

$$\hat{\phi}_k(s) = \int_{-\infty}^{\infty} e^{-is\xi}\phi_k(\xi)d\xi, \qquad k = -N_l, ..., N_r$$

where $\varepsilon > 0$ is sufficiently small, to both sides of (3.9). Then

$$\begin{aligned}
\hat{\phi}_{-N_l}(s) &= \int_{-\infty}^{\infty} e^{-is\xi}\phi_{-N_l}(\xi)d\xi = -\frac{i}{s}\int_{-\infty}^{\infty} e^{-is\xi}\phi_{-N_l}'(\xi)d\xi \\
&= \frac{i}{sc_{-N_l}}\int_{-\infty}^{\infty}[\alpha_{-N_l+1}e^{-is\xi}\phi_{-N_l+1}(\xi) - \alpha_{-N_l+1}e^{-is\xi}\phi_{-N_l}(\xi) \\
&\quad +\alpha_{-N_l}e^{-is\xi}e^{-P\varepsilon}\phi_{N_r}(\xi - P) - \alpha_{-N_l}e^{-is\xi}\phi_{-N_l}(\xi) \\
&\qquad -(1 - c_{-N_l}\varepsilon)e^{-is\xi}\phi_{-N_l}(\xi) + e^{-(is+\varepsilon)\xi}h(\xi - N_l)]d\xi,
\end{aligned}$$

$$\begin{aligned}
\hat{\phi}_j(s) &= \frac{i}{sc_j}\int_{-\infty}^{\infty}[\alpha_{j+1}e^{-is\xi}\phi_{j+1}(\xi) - \alpha_{j+1}e^{-is\xi}\phi_j(\xi) + \alpha_j e^{-is\xi}\phi_{j-1}(\xi) \\
&\qquad -\alpha_j e^{-is\xi}\phi_j(\xi) - (1 - c_j\varepsilon)e^{-is\xi}\phi_j(\xi) + e^{-(is+\varepsilon)\xi}h(\xi + j)]d\xi,
\end{aligned}$$

$$\begin{aligned}\hat{\phi}_{N_r}(s) &= \frac{i}{sc_{N_r}}\int_{-\infty}^{\infty}[\alpha_{-N_l}e^{-is\xi}e^{P\varepsilon}\phi_{-N_l}(\xi+P)-\alpha_{-N_l}e^{-is\xi}\phi_{N_r}(\xi)\\ &\quad +\alpha_{N_r}e^{-is\xi}\phi_{N_r-1}(\xi)-\alpha_{N_r}e^{-is\xi}\phi_{N_r}(\xi)\\ &\quad -(1-c_{N_r}\varepsilon)e^{-is\xi}\phi_{N_r}(\xi)+e^{-(is+\varepsilon)\xi}h(\xi+N_r)]d\xi, \qquad (3.10)\end{aligned}$$

or

$$-\alpha_{-N_l}e^{-P(is+\varepsilon)}\hat{\phi}_{N_r}(s)+(-c_{-N_l}(is+\varepsilon)+\alpha_{-N_l+1}+\alpha_{-N_l}+1)\hat{\phi}_{-N_l}(s)$$

$$-\alpha_{-N_l+1}\hat{\phi}_{-N_l+1}(s)=\frac{e^{-(is+\varepsilon)N_l}}{is+\varepsilon},$$

$$-\alpha_j\hat{\phi}_{j-1}(s)+(-c_j(is+\varepsilon)+\alpha_{j+1}+\alpha_j+1)\hat{\phi}_j(s)-\alpha_{j+1}\hat{\phi}_{j+1}(s)=\frac{e^{(is+\varepsilon)j}}{is+\varepsilon},$$

$$-\alpha_{N_r}\hat{\phi}_{N_r-1}(s)+(-c_{N_r}(is+\varepsilon)+\alpha_{-N_l}+\alpha_{N_r}+1)\hat{\phi}_{N_r}(s) \qquad (3.11)$$

$$-\alpha_{-N_l}e^{P(is+\varepsilon)}\hat{\phi}_{-N_l}(s) = \frac{e^{(is+\varepsilon)N_r}}{is+\varepsilon}.$$

Let $A_k=(-c_k(is+\varepsilon)+\alpha_{k+1}+\alpha_k+1)$ where $\alpha_{N_r+1}=\alpha_{-N_l}$, let

$$\underline{\hat{\phi}}(s) = [\hat{\phi}_{-N_l}(s),\hat{\phi}_{-N_l+1}(s),...,\hat{\phi}_{N_r}(s)]^T$$

and let

$$\underline{v} = \left[\frac{e^{-(is+\varepsilon)N_l}}{is+\varepsilon}, \frac{e^{(is+\varepsilon)(-N_l+1)}}{is+\varepsilon}, ..., \frac{e^{(is+\varepsilon)N_r}}{is+\varepsilon}\right]^T. \tag{3.12}$$

Then for the matrix

$$\mathbf{M} = \begin{bmatrix} A_{-N_l} & -\alpha_{-N_l+1} & 0 & \cdots & -\alpha_{-N_l}e^{-P(is+\varepsilon)} \\ -\alpha_{-N_l+1} & A_{-N_l+1} & -\alpha_{-N_l+2} & & 0 \\ 0 & -\alpha_{-N_l+2} & A_{-N_l+2} & & \\ \vdots & & & \ddots & \\ & & -\alpha_{N_r-1} & A_{N_r-1} & -\alpha_{N_r} \\ -\alpha_{-N_l}e^{P(is+\varepsilon)} & \cdots & 0 & -\alpha_{N_r} & A_{N_r} \end{bmatrix},$$

the system (3.11) can be written as

$$\mathbf{M}\underline{\hat{\phi}} = \underline{v}.$$

Definition 3.2.1 *An $n \times n$ matrix, $A = (a_{ij})$, that maps $\mathbb{C}^n$ into $\mathbb{C}^n$ is* irreducible *if for any two indices $1 \leq i, j \leq n$, there is a sequence of nonzero elements of A of the form $\{a_{i,i_1}, a_{i_1,i_2}, ..., a_{i_m,j}\}$, [49].*

Lemma 3.2.2 *The matrix* **M** *is irreducible.*

Proof. For $N_l \leq i, j \leq N_r$ the sequence $\alpha_{i,i+1}, \alpha_{i+1,i+2}, ..., \alpha_{j-1,j}$ satisfies the condition of Definition 3.2.1. ■

Definition 3.2.2 *An $n \times n$ complex matrix $A = (a_{ij})$ is* diagonally dominant *if*

$$\sum_{j=1, j\neq i}^{n} |a_{ij}| \leq |a_{ii}|, \qquad i = 1, ..., n. \tag{3.13}$$

We call the matrix A irreducibly diagonally dominant *if A is irreducible, diagonally dominant, and strict inequality holds in (3.13) for at least one i, [49].*

Lemma 3.2.3 *If a matrix A is irreducibly diagonally dominant then A is invertible.*

Proof. Theorem 2.3.8 in [49]. ■

Remark 3.2.1 **M** *is irreducibly diagonally dominant and hence invertible.*

We obtain $\varphi_k(\xi)$ by taking the inverse Fourier transform

$$\varphi_k(\xi) = e^{\varepsilon\xi}\phi_k(\xi) = \frac{1}{2\pi}\int_{-\infty}^{\infty} e^{(is+\varepsilon)\xi}\hat{\phi}_k(s)ds,$$

which is absolutely convergent. Although in theory this appears simple enough, we present the case for $P = 2$, to demonstrate important features of the solutions of spatially discrete reaction-diffusion equation with periodic diffusion.

3.3 Example: Alternating Diffusion Coefficient

The simplest case of a spatially discrete reaction-diffusion equation with a periodic diffusion coefficient that we can study is when the diffusion coefficient is of period $P = 1$. On the spatially discrete domain, this is equivalent to the constant coefficient problem we solved in Chapter 2 (when $\delta_c = 0$ and $n = 1$). The next simplest case is when we have period $P = 2$, which we now present.

Lets consider a steplike diffusion coefficient function of period $P = 2$ defined as

$$\alpha(\eta) = \begin{cases} \alpha_e & \eta \text{ even}, \\ \alpha_o & \eta \text{ odd}, \end{cases} \tag{3.14}$$

with $\alpha_e, \alpha_o \in \mathbb{R}^+$. Let $\xi = 2i - ct$, $i \in \mathbb{R}$ and define

$$\begin{aligned} \varphi_e(\xi) &= \varphi(\xi), \\ \varphi_o(\xi) &= \varphi(\xi + 1) \end{aligned} \tag{3.15}$$

and $c_e = c(\eta)$, η even, $c_o = c(\eta)$, η odd. Thus $\varphi = \varphi_e$ when η is even and $\varphi = \varphi_o$

when η is odd. Then

$$\begin{aligned} -c_e\varphi_e'(\xi) &= \alpha(\eta+1)(\varphi_o(\xi)-\varphi_e(\xi))+\alpha(\eta)(\varphi_o(\xi-2)-\varphi_e(\xi))-f(\varphi_e(\xi)) \\ &= \alpha_o(\varphi_o(\xi)-\varphi_e(\xi))+\alpha_e(\varphi_o(\xi-2)-\varphi_e(\xi))-f(\varphi_e(\xi)), \end{aligned} \tag{3.16}$$

when η is even, and

$$\begin{aligned} -c_o\varphi_o'(\xi) &= \alpha(\eta+1)(\varphi_e(\xi+2)-\varphi_o(\xi))+\alpha(\eta)(\varphi_e(\xi)-\varphi_o(\xi))-f(\varphi_o(\xi)) \\ &= \alpha_e(\varphi_e(\xi+2)-\varphi_o(\xi))+\alpha_o(\varphi_e(\xi)-\varphi_o(\xi))-f(\varphi_o(\xi)), \end{aligned} \tag{3.17}$$

when η is odd. The phase condition $\varphi(0) = a$ implies $\varphi_e(0) = a$ and $\varphi_o(-1) = a$. The nonlinearities $f(\varphi_e) = \varphi_e - h(\xi)$, $f(\varphi_o) = \varphi_o - h(\xi+1)$.

3.3.1 An Analytic Solution

We now derive the solution of the traveling wave equation (3.2) by deriving the solution for the pair of traveling wave equations (3.16) and (3.17) with the boundary conditions (3.3) and the piecewise linear function f_1, (1.9). From our derived solution, we obtain a relationship between the detuning parameter, a, and the wave speed, c. Also, from this solution and the $a(c)$ relation, we present results concerning propagation failure.

This section begins with the construction of solutions, $\varphi_e(\xi)$ and $\varphi_o(\xi)$, for (3.2). The construction consists of defining functions $\phi_e(\xi) = e^{-\varepsilon\xi}\varphi_e(\xi)$ and $\phi_o(\xi) = e^{-\varepsilon\xi}\varphi_o(\xi)$ and transforming (3.2). To the $\phi_e(\xi)$,$\phi_o(\xi)$ versions of the equations, we apply the Fourier transform, and after some manipulation, we derive a formula for $\varphi_e(\xi)$ and $\varphi_o(\xi)$.

Using the derivation from the general period derivation, we obtain

$$(-c_e(is+\varepsilon)+\alpha_o+\alpha_e+1)\hat{\phi}_e(s)-(\alpha_o+\alpha_e e^{-2(is+\varepsilon)})\hat{\phi}_o(s)=\frac{1}{is+\varepsilon},$$

$$(-c_o(is+\varepsilon)+\alpha_o+\alpha_e+1)\hat{\phi}_o(s)-(\alpha_o+\alpha_e e^{2(is+\varepsilon)})\hat{\phi}_e(s)=\frac{e^{is+\varepsilon}}{is+\varepsilon}, \qquad (3.18)$$

or

$$\begin{bmatrix} A_e & -\alpha_o-\alpha_e e^{-2(is+\varepsilon)} \\ -\alpha_o-\alpha_e e^{2(is+\varepsilon)} & A_o \end{bmatrix}\begin{bmatrix} \hat{\phi}_e \\ \hat{\phi}_o \end{bmatrix}=\begin{bmatrix} \frac{1}{is+\varepsilon} \\ \frac{e^{is+\varepsilon}}{is+\varepsilon} \end{bmatrix},$$

with $A_e = -c_e(is+\varepsilon)+\alpha_o+\alpha_e+1$ and $A_o = -c_o(is+\varepsilon)+\alpha_o+\alpha_e+1$. This is a special case of the matrix **M**. Solving, we obtain

$$\hat{\phi}_e(s)=\frac{P(s-i\varepsilon)}{(is+\varepsilon)R(s-i\varepsilon)}, \qquad \hat{\phi}_o(s)=\frac{Q(s-i\varepsilon)}{(is+\varepsilon)R(s-i\varepsilon)}, \qquad (3.19)$$

where

$$\begin{aligned} P(q) &= -ic_o q + \alpha_o e^{iq} + \alpha_e e^{-iq} + \alpha_o + \alpha_e + 1, \\ Q(q) &= e^{iq}[-ic_e q + \alpha_e e^{iq} + \alpha_o e^{-iq} + \alpha_o + \alpha_e + 1], \\ R(q) &= -i(c_e + c_o)q(\alpha_o + \alpha_e + 1) + 2\alpha_o + 2\alpha_e + 1 + 2\alpha_o\alpha_e(1 - \cos 2q) - c_e c_o q^2. \end{aligned} \tag{3.20}$$

The following lemma is a simple extension of Lemma 4.4 in [10] and is based on the characteristic equation of the system.

Lemma 3.3.1 *For $c \neq 0$, the function R in (3.20) possesses a simple root $q = -iz_0$ with $z_0 > 0$. Moreover, there exists an $\epsilon_0 > 0$ such that if $q \in \mathbb{C}$ is any other root of R satisfying Im $q \leq 0$, then in fact* Im $q < -z_0 - \epsilon_0$.

We now use the Fourier inversion theorem which gives

$$\varphi_e(\xi) = e^{\varepsilon\xi}\phi_e(\xi) = \frac{1}{2\pi}\int_{-\infty}^{+\infty} e^{(is+\varepsilon)\xi}\hat{\phi}_e(s)ds,$$

$$\varphi_o(\xi) = e^{\varepsilon\xi}\phi_o(\xi) = \frac{1}{2\pi}\int_{-\infty}^{+\infty} e^{(is+\varepsilon)\xi}\hat{\phi}_o(s)ds,$$

which are absolutely convergent. This implies

$$\varphi_e(\xi) = \frac{1}{2\pi}\int_{-\infty}^{+\infty} \frac{e^{(is+\varepsilon)\xi}P(s-i\varepsilon)}{(is+\varepsilon)R(s-i\varepsilon)}ds = \frac{1}{2\pi i}\int_{-i\varepsilon-\infty}^{-i\varepsilon+\infty} \frac{e^{is\xi}P(s)}{sR(s)}ds,$$

$$\varphi_o(\xi) = \frac{1}{2\pi}\int_{-\infty}^{+\infty} \frac{e^{(is+\varepsilon)\xi}Q(s-i\varepsilon)}{(is+\varepsilon)R(s-i\varepsilon)}ds = \frac{1}{2\pi i}\int_{-i\varepsilon-\infty}^{-i\varepsilon+\infty} \frac{e^{is\xi}Q(s)}{sR(s)}ds.$$

Because of the simple pole at $s = 0$, we break up the integrals into

$$\varphi_e(\xi) = \frac{1}{2\pi i}\left(\int_{C_\varepsilon} + \int_{S_\varepsilon}\right) \frac{e^{is\xi}P(s)}{sR(s)}ds,$$

$$\varphi_o(\xi) = \frac{1}{2\pi i}\left(\int_{C_\varepsilon} + \int_{S_\varepsilon}\right) \frac{e^{is\xi}Q(s)}{sR(s)}ds, \tag{3.21}$$

where C_ε is $(-\infty, -\varepsilon]$ and $[+\varepsilon, +\infty)$ on the real axis, and S_ε is the half-circle at the origin. First consider the C_ε integrals. We have

$$\begin{aligned}
\frac{1}{2\pi i}\int_{C_\varepsilon} \frac{e^{is\xi}P(s)}{sR(s)}ds &= \frac{1}{2\pi i}\left(\int_{-\infty}^{-\varepsilon} + \int_{+\varepsilon}^{+\infty}\right) \frac{e^{is\xi}P(s)}{sR(s)}ds \\
&= \frac{1}{2\pi i}\int_{+\varepsilon}^{+\infty} \left[\frac{e^{is\xi}P(s)}{sR(s)} - \frac{e^{-is\xi}P(-s)}{sR(-s)}\right] ds \\
&= \frac{1}{2\pi i}\int_{+\varepsilon}^{+\infty} \frac{e^{is\xi}P(s)R(-s) - e^{-is\xi}P(-s)R(s)}{sR(s)R(-s)}ds
\end{aligned}$$

$$= \frac{1}{\pi}\int_{+\varepsilon}^{+\infty} \frac{(sc_oB(s)+(\alpha_o+\alpha_e+1)A(s))\sin(s\xi)}{s(A^2(s)+B^2(s))}ds$$

$$+\frac{1}{\pi}\int_{+\varepsilon}^{+\infty} \frac{(-sc_oA(s)+(\alpha_o+\alpha_e+1)B(s))\cos(s\xi)}{s(A^2(s)+B^2(s))}ds$$

$$+\frac{1}{\pi}\int_{+\varepsilon}^{+\infty} \frac{A(s)(\alpha_o\sin s(\xi+1)+\alpha_e\sin s(\xi-1))}{s(A^2(s)+B^2(s))}ds$$

$$+\frac{1}{\pi}\int_{+\varepsilon}^{+\infty} \frac{B(s)(\alpha_o\cos s(\xi+1)+\alpha_e\cos s(\xi-1))}{s(A^2(s)+B^2(s))}ds,$$

and

$$\frac{1}{2\pi i}\int_{C_\varepsilon}\frac{e^{is\xi}Q(s)}{sR(s)}ds = \frac{1}{2\pi i}\left(\int_{-\infty}^{-\varepsilon}+\int_{+\varepsilon}^{+\infty}\right)\frac{e^{is\xi}Q(s)}{sR(s)}ds$$

$$= \frac{1}{\pi}\int_{+\varepsilon}^{+\infty} \frac{(sc_eB(s)+(\alpha_o+\alpha_e+1)A(s))\sin(s(\xi+1))}{s(A^2(s)+B^2(s))}ds$$

$$+\frac{1}{\pi}\int_{+\varepsilon}^{+\infty} \frac{(-sc_eA(s)+(\alpha_o+\alpha_e+1)B(s))\cos(s(\xi+1))}{s(A^2(s)+B^2(s))}ds$$

$$+\frac{1}{\pi}\int_{+\varepsilon}^{+\infty} \frac{A(s)(\alpha_e\sin s(\xi+2)+\alpha_o\sin(s\xi))}{s(A^2(s)+B^2(s))}ds$$

$$+\frac{1}{\pi}\int_{+\varepsilon}^{+\infty}\frac{B(s)(\alpha_e\cos s(\xi+2)+\alpha_o\cos(s\xi))}{s(A^2(s)+B^2(s))}ds,$$

where

$$\begin{aligned} A(s) &= 1-c_ec_os^2+2\alpha_e\alpha_o(1-\cos(2s))+2(\alpha_e+\alpha_o), \\ B(s) &= (c_e+c_o)s(\alpha_e+\alpha_o+1). \end{aligned} \tag{3.22}$$

For $s\in I\!R$, $A(s)=\mathrm{Re}[R(s)]$ and $B(s)=-\mathrm{Im}[R(s)]$.

For the S_ε integrals, we have

$$\begin{aligned} \frac{1}{2\pi i}\int_{S_\varepsilon}\frac{e^{is\xi}P(s)}{sR(s)}ds &= \frac{1}{2\pi i}2\pi i\frac{1}{2}\mathrm{Res}\left(\frac{e^{is\xi}P(s)}{sR(s)},0\right)=\frac{1}{2}, \\ \frac{1}{2\pi i}\int_{S_\varepsilon}\frac{e^{is\xi}Q(s)}{sR(s)}ds &= \frac{1}{2}. \end{aligned} \tag{3.23}$$

Combining the integral results (3.22) and (3.23) in (3.21), and letting $\varepsilon\to 0$, we obtain an explicit formula for $\varphi(\xi)$. From (3.21), we have the following formula for the solution of (3.2) with (3.14) for $c_e, c_o\neq 0$:

$$\varphi_e(\xi)=\frac{1}{2}+\frac{1}{\pi}\int_0^\infty\frac{(sc_oB(s)+(\alpha_o+\alpha_e+1)A(s))\sin(s\xi)}{s(A^2(s)+B^2(s))}ds$$

$$+ \frac{1}{\pi}\int_0^\infty \frac{(-sc_oA(s)+(\alpha_o+\alpha_e+1)B(s))\cos(s\xi)}{s(A^2(s)+B^2(s))}ds$$

$$+ \frac{1}{\pi}\int_0^\infty \frac{A(s)(\alpha_o\sin s(\xi+1)+\alpha_e\sin s(\xi-1))}{s(A^2(s)+B^2(s))}ds$$

$$+ \frac{1}{\pi}\int_0^\infty \frac{B(s)(\alpha_o\cos s(\xi+1)+\alpha_e\cos s(\xi-1))}{s(A^2(s)+B^2(s))}ds,$$

and

$$\varphi_o(\xi) = \frac{1}{2} + \frac{1}{\pi}\int_0^\infty \frac{(sc_eB(s)+(\alpha_o+\alpha_e+1)A(s))\sin(s(\xi+1))}{s(A^2(s)+B^2(s))}ds$$

$$+ \frac{1}{\pi}\int_0^\infty \frac{(-sc_eA(s)+(\alpha_o+\alpha_e+1)B(s))\cos(s(\xi+1))}{s(A^2(s)+B^2(s))}ds$$

$$+ \frac{1}{\pi}\int_0^\infty \frac{A(s)(\alpha_e\sin s(\xi+2)+\alpha_o\sin(s\xi))}{s(A^2(s)+B^2(s))}ds$$

$$+ \frac{1}{\pi}\int_0^\infty \frac{B(s)(\alpha_e\cos s(\xi+2)+\alpha_o\cos(s\xi))}{s(A^2(s)+B^2(s))}ds. \tag{3.24}$$

Remark 3.3.1 *Let φ_e and φ_o be considered as functions of c_e and c_o, i.e. $\varphi_e(\xi, c_e, c_o)$ and $\varphi_o(\xi, c_e, c_o)$.*

i)Observing that

$$1-\varphi_e(-\xi-1,-c_o,-c_e)$$

$$=\frac{1}{2}-\frac{1}{\pi}\int_0^\infty \frac{(sc_eB(s)+(\alpha_o+\alpha_e+1)A(s))\sin(s(-\xi-1))}{s(A^2(s)+B^2(s))}ds$$

$$-\frac{1}{\pi}\int_0^\infty \frac{(sc_eA(s)-(\alpha_o+\alpha_e+1)B(s))\cos(s(\xi+1))}{s(A^2(s)+B^2(s))}ds$$

$$-\frac{1}{\pi}\int_0^\infty \frac{A(s)(\alpha_o\sin s(-\xi)+\alpha_e\sin s(-\xi-2))}{s(A^2(s)+B^2(s))}ds$$

$$-\frac{1}{\pi}\int_0^\infty \frac{-B(s)(\alpha_o\cos s(\xi)+\alpha_e\cos s(\xi+2))}{s(A^2(s)+B^2(s))}ds$$

$$=\varphi_o(\xi,c_e,c_o),$$

and

$$1-\varphi_o(-\xi-1,-c_o,-c_e)$$

$$=\frac{1}{2}-\frac{1}{\pi}\int_0^\infty \frac{(sc_oB(s)+(\alpha_o+\alpha_e+1)A(s))\sin(s(-\xi))}{s(A^2(s)+B^2(s))}ds$$

$$-\frac{1}{\pi}\int_0^\infty \frac{(sc_oA(s)-(\alpha_o+\alpha_e+1)B(s))\cos(s\xi)}{s(A^2(s)+B^2(s))}ds$$

$$-\frac{1}{\pi}\int_0^\infty \frac{A(s)(\alpha_e \sin s(-\xi+1)+\alpha_o \sin(s(-\xi-1)))}{s(A^2(s)+B^2(s))}ds$$

$$-\frac{1}{\pi}\int_0^\infty \frac{-B(s)(\alpha_e \cos s(\xi+1)+\alpha_o \cos(s(\xi-1)))}{s(A^2(s)+B^2(s))}ds$$

$$= \varphi_e(\xi, c_e, c_o),$$

we see that, for $\varphi(\xi)=\varphi(\xi,c)$, *we have the symmetry property*

$1-\varphi_e(-\xi-1,-c_o,-c_e)=\varphi_o(\xi,c_e,c_o)$, *and* $1-\varphi_o(-\xi-1,-c_o,-c_e)=\varphi_e(\xi,c_e,c_o)$.

ii) Recalling that

$$\varphi_e(\xi)=\frac{1}{2\pi i}\int_{-i\varepsilon-\infty}^{-i\varepsilon+\infty}\frac{e^{is\xi}P(s)}{sR(s)}ds, \qquad \varphi_o(\xi)=\frac{1}{2\pi i}\int_{-i\varepsilon-\infty}^{-i\varepsilon+\infty}\frac{e^{is\xi}Q(s)}{sR(s)}ds,$$

we can see that as $\xi\to-\infty$, $\varphi_e(\xi)\to 0$ *and* $\varphi_o(\xi)\to 0$. *Our symmetry property then gives us that* $\varphi_e(+\infty)=1$ *and* $\varphi_o(+\infty)=1$. *This confirms our choice of boundary conditions.*

Remark 3.3.2 *i) As discussed before,* $\varphi(\xi)=a$ *for only one value of* ξ. *Let* $\xi=0$.

This then gives us the following relation between a and (c_e, c_o)*:*

$$\varphi(0) = a = \varphi_e(0) = \frac{1}{2} + \frac{1}{\pi}\int_0^\infty \frac{(-sc_oA(s) + (\alpha_o + \alpha_e + 1)B(s))}{s(A^2(s) + B^2(s))}ds$$

$$+ \frac{1}{\pi}\int_0^\infty \frac{A(s)(\alpha_o - \alpha_e)\sin s}{s(A^2(s) + B^2(s))}ds$$

$$+ \frac{1}{\pi}\int_0^\infty \frac{B(s)(\alpha_o + \alpha_e)\cos s}{s(A^2(s) + B^2(s))}ds \tag{3.25}$$

and

$$\varphi(0) = a = \varphi_o(-1) = \frac{1}{2} + \frac{1}{\pi}\int_0^\infty \frac{(-sc_eA(s) + (\alpha_o + \alpha_e + 1)B(s))}{s(A^2(s) + B^2(s))}ds$$

$$+ \frac{1}{\pi}\int_0^\infty \frac{A(s)(\alpha_e - \alpha_o)\sin s}{s(A^2(s) + B^2(s))}ds$$

$$+ \frac{1}{\pi}\int_0^\infty \frac{B(s)(\alpha_o + \alpha_e)\cos s}{s(A^2(s) + B^2(s))}ds, \tag{3.26}$$

when $c_e \neq 0$ *and* $c_o \neq 0$*. Adding and subtracting (3.25) and (3.26) we obtain, for* $c_e, c_o \neq 0$*,*

$$a = \frac{1}{2} + \frac{1}{\pi}\int_0^\infty \frac{-\frac{s}{2}(c_e + c_o)A(s) + [(\alpha_o + \alpha_e)(1 + \cos(s)) + 1]B(s)}{s(A^2(s) + B^2(s))}ds, \tag{3.27}$$

subject to the condition that

$$\int_0^\infty \frac{(s(c_e - c_o) + 2(\alpha_o - \alpha_e)\sin s)A(s)}{s(A^2(s) + B^2(s))} ds = 0. \tag{3.28}$$

ii) When $c_e = c_o = 0$,

$$\varphi(0) = a = \frac{1}{2}$$

and

$$\int_0^\infty \frac{A(s)(\alpha_o - \alpha_e)\sin s}{s(A^2(s) + B^2(s))} ds = 0.$$

The condition (3.28) insures that the detuning parameter a is a constant value and does not vary with η.

Now that we have derived a solution $\varphi(\xi)$ we need to justify the assumption that the solution to (3.16) and (3.17), with (3.14), (1.9), and (3.3) is either monotone increasing or monotone decreasing in time. This is equivalent to stating that each point in the spatial lattice has a unique nonintersecting trajectory from one phase to the other.

Lemma 3.3.2 *Let* $\eta \in \mathbb{Z}$. *The solution* φ, *(3.24), of (3.2) with (3.14), (1.9), and (3.3), is strictly increasing in time for* $c_e, c_o < 0$. *The solution* φ *is strictly decreasing in time for* $c_e, c_o > 0$.

Proof. Let $c(\eta) > 0$. Then $-c(\eta)t$ is monotone decreasing in t. Let $c(\eta) < 0$. Then $-c(\eta)t$ is monotone increasing in t. The results now follow the proofs of Corollary 4.5 and Theorem 4.6 in [10]. ∎

We now address exactly what is meant by a solution to (3.2) with (3.14). To solve (3.2), it is sufficient to regard both $f_1(\varphi)$, (1.9), and $h(\xi)$ as set valued functions, with f and h singleton sets for $\varphi \neq a$ and $\xi \neq 0$, and $f(a) = [a-1, a]$ and $h(0) = [0, 1]$. This amounts to filling in the jump discontinuities in the graphs of f and h. By a solution to (2.2), we mean that $\varphi \in C(\mathbb{R})$ and the differential inclusion

$$-c\varphi'(\xi) \in L_T\varphi(\xi) - \varphi(\xi) + h(\xi)$$

holds for $\xi \in \mathbb{R}$. Since we are solving on a discrete spatial domain, we need to discuss what we mean by continuity with respect to ξ. If we fix η, then both φ_e and φ_o are continuous over time and either φ_e or φ_o (depending on whether η is even or odd) describes the continuous time trajectories of φ at η. If we fix t, then the domain and ranges of φ_e, φ_o, and φ are countably infinite discrete sets of points. The domain of φ is the union of the domains of φ_e and φ_o, and the range of φ is the union of the ranges of φ_e and φ_o. The domains of φ_e and φ_o are disjoint.

Lemma 3.3.3 *For $c \neq 0$, the derivative $\varphi'(\xi)$ of (2.15) is discontinuous in time. In*

addition, for fixed η,

$$\lim_{\xi \to 0-} \varphi'(\xi) - \lim_{\xi \to 0+} \varphi'(\xi) = \frac{1}{c}.$$

Proof. Any difficulty in smoothness occurs in φ at $\xi = 0$ for (3.2) with (3.14) and (1.9). Taking the difference of (3.2) with (1.9) as ξ approaches zero from the left and from the right, for fixed η we obtain

$$\lim_{\xi \to 0-} -c\varphi'(\xi) - \lim_{\xi \to 0+} -c\varphi'(\xi) = -1 \tag{3.29}$$

since φ is continuous in t. ∎

3.3.2 The $a(c)$ Relation

We now analyze the relationship between the wave speed c and the detuning parameter a. We are particularly interested in the phenomenon of propagation failure, the existence of a nontrivial interval for a such that the wave speed is zero.

For $c(\eta) \neq 0$, set

$$\begin{aligned} \Gamma(c_e, c_o) &= \varphi(0) - \frac{1}{2} = a - \frac{1}{2} \\ &= \frac{1}{\pi} \int_0^\infty \frac{-s\frac{1}{2}(c_e + c_o)A(s) + [(\alpha_o + \alpha_e)(1 + \cos(s)) + 1]B(s)}{s(A^2(s) + B^2(s))} ds, \end{aligned} \tag{3.30}$$

where

$$\begin{aligned} A(s) &= 1 - c_e c_o s^2 + 2\alpha_e\alpha_o(1-\cos(2s)) + 2(\alpha_e+\alpha_o), \\ B(s) &= (c_e+c_o)s(\alpha_e+\alpha_o+1). \end{aligned} \tag{3.31}$$

Throughout this subsection, c_e and c_o are subject to the constraint

$$\int_0^\infty \frac{(s(c_e-c_o)+2(\alpha_o-\alpha_e)\sin s)A(s)}{s(A^2(s)+B^2(s))}ds = 0. \tag{3.32}$$

Remark 3.3.3 *When $c_e = c_o = 0$, $\varphi(0) = a = 1/2$. This along with constraint (3.32), implies that c_e and c_o are of the same sign.*

Let $c = (c_e + c_o)/2$. With the simple change of variable $s \to s/c$, Γ can be written as

$$\Gamma(c_e, c_o) = \frac{1}{\pi}\int_0^\infty \frac{-sA(s/c)+[(\alpha_o+\alpha_e)(1+\cos(s/c))+1]B(s/c)}{s(A^2(s/c)+B^2(s/c))}ds, \tag{3.33}$$

for $c_e \neq 0$ and $c_o \neq 0$.

Remark 3.3.4 $\Gamma(c_e, c_o)$ *with $c_e, c_o \neq 0$ is nonzero.*

Let $c_{min} = \min(|c_e|, |c_o|)$ and $c_{max} = \max(|c_e|, |c_o|)$.

Theorem 3.3.1 *Let $\varphi(\xi)$ be a solution to (3.2) with (3.14), (1.9), and (3.3), so that $\Gamma(c_e, c_o)$ is defined by (3.30) with $c_e, c_o \neq 0$. Then*

$$\lim_{c_{max}\to\infty} |\Gamma(c_e, c_o)| \leq \lim_{c_{min}\to\infty} |\Gamma(c_e, c_o)| = \frac{1}{2}. \tag{3.34}$$

Proof. Let $c_e \neq 0$ and $c_o \neq 0$. Then

$$\begin{aligned}
&\lim_{c_{min}\to\infty} |\Gamma(c_e, c_o)| \\
&= \lim_{c_{min}\to\infty} \frac{1}{\pi}\int_0^\infty \frac{-sA(s/c) + [(\alpha_o+\alpha_e)(1+\cos(s/c))+1]B(s/c)}{s(A^2(s/c)+B^2(s/c))}ds \\
&= \frac{1}{\pi}\int_0^\infty \frac{s^2+2d+1}{s^4+2(d+1)s^2+2d+1}ds \\
&= \frac{1}{\pi}\int_0^\infty \frac{1}{s^2+1}ds \quad = \quad \frac{1}{2},
\end{aligned} \tag{3.35}$$

where $d = 2(\alpha_e+\alpha_o)(\alpha_e+\alpha_o+1)$.

The quantity c_{max} is equal to either c_e, c_o, or both c_e and c_o. Suppose $c_{max} = c_e$

and we hold c_o fixed (this is equivalent to $c_{max} = c_o$, c_e fixed). Then

$$\begin{aligned}
&\lim_{c_{max}\to\infty} \quad |\Gamma(c_e, c_o)| \\
&= \quad \lim_{c_{max}\to\infty} \frac{1}{\pi}\int_0^\infty \frac{-sA(s/c) + [(\alpha_o + \alpha_e)(1+\cos(s/c)) + 1]B(s/c)}{s(A^2(s/c) + B^2(s/c))} ds \\
&= \quad \frac{1}{\pi}\int_0^\infty \frac{2d+1}{(2d+4)s^2 + 2d + 1} ds \\
&< \quad \frac{1}{\pi}\int_0^\infty \frac{1}{s^2+1} ds \quad = \quad \frac{1}{2},
\end{aligned}$$

where $d = 2(\alpha_e + \alpha_o)(\alpha_e + \alpha_o + 1)$. If $c_{max} = c_e = c_o$, then (3.35) applies. ■

3.3.3 Application: Laminar Material

Suppose that we have a laminar material composed of periodically alternating layers, of integer thickness, with every other layer possessing the same diffusion coefficient. Let all other properties of the laminates be the same. Let $\overline{n}$ be the normal direction to the interfaces of the layers and let θ be the angle between the traveling wave direction vector σ and the normal vector $\overline{n}$. Then if $\cos\theta$ is a rational number, this problem is equivalent to the one dimensional periodic coefficient traveling wave problem.

3.4 Chapter Summary

In this chapter, we provided a solution method for spatially discrete reaction-diffusion equations with "linearized" nonlinearity f_1 and periodic variable diffusion. This was accomplished by treating variable diffusion differential-difference equations as a mixed system of constant coefficient ordinary differential and differential-difference equations which is solved using Fourier integral transforms. The period two diffusion coefficient case is provided to demonstrate the details of the solution method, in particular, the inverse transform. If we consider these solutions as time trajectories for the points in the lattice, then the trajectories are strictly monotone. The period two diffusion coefficient case also gives us a chance to investigate the $a(c)$ relation for a nonconstant wave speed c. The discontinuity in the nonlinearity f_1 causes φ' to be discontinuous which appears as "kinks" in the solution curves.

Chapter 4

A NUMERICAL METHOD FOR THE COMPUTATION OF TRAVELING WAVE SOLUTIONS OF NONLINEAR DIFFERENTIAL-DIFFERENCE EQUATIONS

In previous chapters, we used a linearized nonlinearity f (f_1 from equation (1.9)) to represent the the bistable nonlinearity. This allowed us to produce both analytical (using integral transforms) and numerical solutions (using fixed point methods). In this chapter we concentrate on a numerical method which allows us to solve differential-difference equations with any bistable nonlinearity that possesses a continuous derivative.

In Section 4.1 we introduce the class of equations we solve, we introduce the numerical method (a modified Newton's method) we use to solve this class of equations, and we introduce the main theorem of this chapter, a convergence result for our modified Newton's method. The proof of this theorem relies on detailed func-

tional analysis of the class of equations we are solving. Section 4.2 consists of the background, definitions, concepts, and results that we use in the proof of the main theorem and relies heavily on the work of J. Mallet-Paret in [46] and [47]. This section includes analysis based on Fredholm operator theory and asymptotic hyperbolicity. Once these preliminary results are stated we proceed to Section 4.3 and the proof of our convergence theorem. We conclude with a summary and remarks about the class of equations that can be solved with this method.

Although we are solving nonlinear differential-difference equations, the numerical method that we present relies on several results on linear differential operators with an exponential dichotomy and on several results on linear differential-difference operators that enjoy behavior similar to an exponential dichotomy. Our method also relies on the fact that our nonlinear differential-difference equation can be treated as a (sometimes large) perturbation of a nonlinear differential equation. While we present the method for a specific subclass of the class of equations that exhibit a heteroclinic orbit dependent on one parameter (c), this method appears to be applicable to a general class of parameterized differential-difference equations that connect two points (either in a heteroclinic or homoclinic orbit).

4.1 A Variant of Newton's Method

We present a numerical method for solving the nonlinear autonomous equation

$$-diag(c)\varphi'(\xi) - diag(\gamma)\varphi''(\xi) = F(\varphi(\xi), \rho) + G(\varphi(\xi + r_1), \varphi(\xi + r_2), ..., \varphi(\xi + r_N), \rho), \tag{4.1}$$

where $\varphi = (\varphi^{(1)}, \varphi^{(2)}, ..., \varphi^{(n)})$ with $\rho \in [0,1] \equiv U$, $\xi \in I\!R$, $c(\rho) : I\!R \to I\!R^n$, and the constant vector γ of dimension n consists of elements in $I\!R^+ \cup \{0\}$. The notation $diag(c)$ and $diag(\gamma)$ represent $n \times n$ diagonal matrices whose i, i^{th} elements are the i^{th} element of c and γ, respectively. We use equation (2.1) as an example to help illustrate the assumptions that are made on (4.1). Let $\varphi_{r_i^l}(\xi) = \varphi^{(l)}(\xi + r_i)$, let $\overline{\varphi}^{(l)} = (\varphi_{r_1^l}, \varphi_{r_2^l}, ..., \varphi_{r_N^l})$, and let $\overline{\varphi} = (\overline{\varphi}^{(1)}, \overline{\varphi}^{(2)}, ..., \overline{\varphi}^{(n)})$, for $l = 1, ..., n$, $i = 1, ..., N$.

The following is a list of five conditions for F and G:

(c1) $F : I\!R^n \times U \to I\!R^n$ is C^1 in $I\!R^n$ and U, and $G : I\!R^{nN} \times U \to I\!R^n$ is C^1 in $I\!R^{nN}$ and U.

(c2) $D_\varphi F : I\!R^n \times U \to I\!R^n$ is locally Lipschitz in φ and $D_{\overline{\varphi}} G : I\!R^{n \times N} \times U \to I\!R^{n \times N}$ is locally Lipschitz in $\overline{\varphi}$.

(c3) For $j = 1, ..., N$ and $l = 1, ..., n$,

$$\frac{\partial G(\overline{\varphi}, \rho)}{\partial \varphi_{r_j^l}} > 0. \tag{4.2}$$

For (2.1), this means that the $\varepsilon_k > 0$.

(c4) The r_i^l, $i = 1, ..., N$, $l = 1, ..., n$, are the forward and backward shifts. As a matter of notation, let $r_j^l \neq r_k^l$ for $1 \leq j < k \leq N$ and $r_i^l \neq 0$ for $i = 1, ..., N$. The r_i^1 correspond to the $e_k \cdot \sigma$ in (2.1) where the shifts occur in plus and minus pairs.

(c5) Let $\varphi_-, \varphi_+ \in I\!R^n$ such that $\varphi_-^{(l)} < \varphi_+^{(l)}$, and let $\Gamma : I\!R^n \times U \to I\!R^n$ be defined as

$$\Gamma(\varphi, \rho) = F(\varphi, \rho) + G(\varphi, \varphi, \varphi, ..., \varphi, \rho).$$

For some $a(\rho)$ such that $a^{(l)}(\rho) \in [\varphi_-^{(l)}, \varphi_+^{(l)}]$,

$$\begin{aligned}
\Gamma^{(l)}(\varphi, \rho) &< 0, \qquad \varphi^{(l)} \in (-\infty, \varphi_-^{(l)}) \cup (a^{(l)}, \varphi_+^{(l)}), \\
\Gamma^{(l)}(\varphi, \rho) &< 0, \qquad \varphi^{(l)} \in (\varphi_-^{(l)}, a^{(l)}) \cup (\varphi_+^{(l)}, \infty), \\
\Gamma(\varphi_-, \rho) &= \Gamma(a, \rho) = \Gamma(\varphi_+, \rho) = \mathbf{0},
\end{aligned} \tag{4.3}$$

with

$$D_{\varphi^{(l)}}\Gamma(\varphi_-,\rho) < 0 \quad \text{if} \quad a^{(l)} \neq \varphi_-^{(l)}, \qquad D_{\varphi^{(l)}}\Gamma(\varphi_+,\rho) < 0 \quad \text{if} \quad a^{(l)} \neq \varphi_+^{(l)},$$

$$D_{\varphi^{(l)}}\Gamma(a,\rho) > 0 \quad \text{if} \quad a^{(l)} \in (\varphi_-^{(l)}, \varphi_+^{(l)}). \tag{4.4}$$

For equation (2.1), $\varphi_-^{(1)} = 0$ and $\varphi_+^{(1)} = 1$. Assumptions (4.3) and (4.4) imply a bistable nature to (4.1) along with the fact that we have exactly the three equilibrium solutions $\varphi = \varphi_-, a, \varphi_+$ when $a^{(l)} \in (\varphi_-^{(l)}, \varphi_+^{(l)})$. Assumptions (4.3) and (4.4) also imply that $\varphi = \varphi_+$ is stable for positive increasing ξ and that $\varphi = \varphi_-$ is stable for negative decreasing ξ. The operators F and G of all the equations that we are currently studying can be expressed in the form

$$F(\varphi(\xi),\rho) + G(\varphi(\xi+r_1),\varphi(\xi+r_2),...,\varphi(\xi+r_N),\rho)$$
$$= \sum_{i=1}^{N} \alpha_i[\varphi(\xi+r_i) - \varphi(\xi)] - f(\varphi(\xi),\rho)$$

where $f(\varphi(\xi),\rho)$ is one of our bistable nonlinearities, f_1, f_2, or f_3. We are interested in solutions of (4.1), (φ, c), that connect φ_- and φ_+. In other words, for each $\rho \in (0,1)$, we want to find $\mathcal{G}(\varphi, c, \rho) = \mathbf{0}$ for

$$\mathcal{G}(\varphi,c,\rho)(\xi) = -diag(c)\varphi'(\xi) - diag(\gamma)\varphi''(\xi) - F(\varphi(\xi),\rho) - G(\overline{\varphi}(\xi),\rho), \tag{4.5}$$

with boundary conditions

$$\varphi(-\infty) = \varphi_- \qquad \text{and} \qquad \varphi(\infty) = \varphi_+. \tag{4.6}$$

As we have done previously, we define the phase condition $\varphi(0) = a(\rho)$ to select a unique translate. An advantage gained from (4.3) and (4.4) is that we do not need to consider solutions which join φ_- and $a(\rho)$, and $a(\rho)$ and φ_+.

Let

$$\mathcal{F}(\varphi, c, \rho)(\xi) = -diag(c)\varphi'(\xi) - diag(\gamma)\varphi''(\xi) - F(\varphi(\xi), \rho). \tag{4.7}$$

Since F and G do not depend on c and since F and G are in C^1, $\mathcal{F}$ and $\mathcal{G}$ are also C^1 Frechet-differentiable. Taking the derivative of $\mathcal{F}$ with respect to the first two variables we obtain

$$\begin{aligned} &D_{1,2}\mathcal{F}(\varphi, c, \rho)(\psi, b, \rho)(\xi) \qquad (4.8)\\ &\qquad = -diag(c)\psi'(\xi) - diag(\gamma)\psi''(\xi) - D_1F(\varphi, \rho)\psi(\xi) - b\varphi'(\xi). \end{aligned}$$

Notice that $D_{1,2}\mathcal{F}(\varphi, c, \rho)$ is a linear nonautonomous (the diagonal matrix $D_\varphi F(\varphi, \rho)$ depends on ξ) operator.

Definition 4.1.1 *Using operator (4.8), we define the modified Newton's method*

$$D_{1,2}\mathcal{F}(\varphi_n, c_n, \rho)(\varphi_{n+1}, c_{n+1}, \rho) = D_{1,2}\mathcal{F}(\varphi_n, c_n, \rho)(\varphi_n, c_n, \rho) - \mathcal{G}(\varphi_n, c_n, \rho). \quad (4.9)$$

Unless otherwise stated, ρ is fixed throughout this chapter. In Sections 4.2 and 4.3 we construct a proof that shows the modified Newton's method in (4.9) converges for (φ_0, c_0) in an open neighborhood about the solution of (4.1). Let

$$L^\infty \equiv L^\infty(\mathbb{R}),$$

let

$$L_n^\infty = \{(f^{(1)}, f^{(2)}, ..., f^{(n)}) | f^{(l)} \in L^\infty, l = 1, ..., n\},$$

let

$$W^{1,\infty} = \{f \in L^\infty | f \text{ is absolutely continuous and } f' \in L^\infty\},$$

let

$$W_l^{1,\infty} = \{f \in W^{1,\infty} | f(0) = a^{(l)}(\rho)\}, l = 1, ..., n,$$

and let

$$W_0^{1,\infty} = \{(f^{(1)}, f^{(2)}, ..., f^{(n)}) | f^{(l)} \in W_l^{1,\infty}, l = 1, ..., n\}.$$

Definition 4.1.2 *The pair* (φ, c) *is a* point of attraction *of the iteration defined in (4.9) if there is an open neighborhood,* S*, of* (φ, c) *such that* $S \subset W_0^{1,\infty} \times \mathbb{R}^n$ *and, for any* $(\varphi_0, c_0) \in S$*, the iterates defined by (4.9) all lie in* $W_0^{1,\infty} \times \mathbb{R}^n$ *and converge to* (φ, c)*.*

We now present the main result in this chapter.

Theorem 4.1.1 *(Convergence of Modified Newton's Method) Let* (φ, c) *be a pair of functions such that* $\mathcal{G}(\varphi, c) = \mathbf{0}$*, with* $\mathcal{G}(\varphi, c)$ *as defined in (4.5) and boundary conditions (4.6). Also assume that the operators* F *and* G *of* $\mathcal{G}(\varphi, c)$ *satisfy conditions c1 through c5. Then* (φ, c) *is a point of attraction for the modified Newton iteration (4.9).*

4.2 Preliminary Results

The following results on asymptotic hyperbolicity and Fredholm theory follow directly from the work of W.-J. Beyn [7], K.J. Palmer [50], and J. Mallet-Paret [46], [47]. Unless specified otherwise, $c \neq \mathbf{0}$ throughout this section.

4.2.1 Definitions

In this subsection, we define what we mean when we call an operator *hyperbolic*, *asymptotically autonomous*, or *asymptotically hyperbolic.*

For $c \neq \mathbf{0}$, let $\Lambda_c : W_0^{1,\infty} \to L_n^\infty$ be a nonautonomous bounded linear operator of the form

$$(\Lambda_c\psi)(\xi) = -diag(c)\psi'(\xi) - diag(\gamma)\psi''(\xi) - A_0(\xi)\psi(\xi) - \sum_{j=1}^{N} A_j(\xi)\psi(\xi + r_j), \quad (4.10)$$

where the matrices A_j, $j = 1, ..., N$, are diagonal.

Definition 4.2.1 *Suppose that the A_i $(i = 0, ..., N)$ in (4.10) can be written in the form*

$$A_i(\xi) = A_{i\pm} + B_{i\pm}(\xi)$$

where $A_{i\pm}$, $i = 0, ..., N$, are constant coefficient operators, of dimension $n \times n$, such that

$$A_{i+} = \lim_{\xi\to\infty} A_i(\xi), \qquad A_{i-} = \lim_{\xi\to-\infty} A_i(\xi), \qquad i = 0, ..., N.$$

Then the operator (4.10) is called asymptotically autonomous.

If Λ_c is asymptotically autonomous then

$$\Lambda_c = \Lambda_c^{\pm} - M_{\pm},$$

where $\Lambda_c^{\pm} : W_0^{1,\infty} \to L_n^{\infty}$ is the autonomous bounded linear operator

$$(\Lambda_c^{\pm}\psi)(\xi) = -diag(c)\psi'(\xi) - diag(\gamma)\psi''(\xi) - A_{0,\pm}\psi(\xi) - \sum_{i=1}^{N} A_{i\pm}\psi(\xi + r_i) \qquad (4.11)$$

and $M_{\pm} : W_0^{1,\infty} \to L_n^{\infty}$ such that

$$(M_{\pm}\psi)(\xi) = B_{0\pm}(\xi)\psi(\xi) + \sum_{i=1}^{N} B_{i\pm}(\xi)\psi(\xi + r_i). \qquad (4.12)$$

where

$$\lim_{\xi\to\infty} \|M_+\| = 0, \qquad \lim_{\xi\to-\infty} \|M_-\| = 0.$$

A particular case of (4.10) is $\Lambda_c^0 : W_0^{1,\infty} \to L_n^{\infty}$, the autonomous bounded linear operator

$$(\Lambda_c^0\psi)(\xi) = -diag(c)\psi'(\xi) - diag(\gamma)\psi''(\xi) - A_{0,0}\psi(\xi) - \sum_{i=1}^{N} A_{i,0}\psi(\xi + r_i) \qquad (4.13)$$

where $A_{i,0}$, $i = 0, ..., N$, are constant coefficient operators. Consider solutions to

$\Lambda_c^0\psi = 0$ of the form $\psi = e^{\mu\xi}v$, $v \in \mathbb{R}^n$, $v \neq 0$. Then for each root $s = \mu$ of the characteristic equation $\det \Delta_c^0(s) = 0$, where

$$\Delta_c^0(s) = -s\ diag(c) - s^2\ diag(\gamma) - A_{0,0} - \sum_{j=1}^{N} A_{j,0}e^{sr_j}, \tag{4.14}$$

there corresponds a set of eigensolutions to $\Lambda_c^0\psi = 0$.

Definition 4.2.2 *The constant coefficient operator Λ_c^0 (4.13) is called* hyperbolic *if its characteristic equation (4.14) has no roots on the imaginary axis; i.e, if $\det \Delta_c^0(i\eta) \neq 0$ for $\eta \in \mathbb{R}$, then (4.13) is called* hyperbolic.

We define hyperbolicity solely based on the characteristic equation $\det \Delta_c^0(s) = 0$ and not on the dynamics of the operator or of the solution. Having a constant coefficient operator be hyperbolic is an essential element to having an exponential dichotomy. We desire to imply that an asymptotically autonomous operator whose asymptotic limit is an hyperbolic operator that has an exponential dichotomy also exhibits an exponential dichotomy.

Definition 4.2.3 *If (4.10) is asymptotically autonomous and (4.11) is hyperbolic, then we call (4.10)* asymptotically hyperbolic.

An asymptotically hyperbolic operator allows us to set up a linear Fredholm theory for the operator. Let

$$\mathcal{R}_c = \mathcal{R}(\Lambda_c) = \{\psi \in L_n^\infty | \psi = \Lambda_c \phi \text{ for some } \phi \in W_0^{1,\infty}\},$$

the range Λ_c (4.10), and let

$$\mathcal{K}_c = \mathcal{K}(\Lambda_c) = \{\phi \in W_0^{1,\infty} | \Lambda_c \phi = \mathbf{0}\},$$

the kernel of Λ_c (4.10). The operator Λ_c is a Fredholm operator if

1) the kernel $\mathcal{K}_c \subseteq W_0^{1,\infty}$ is finite dimensional,

2) the range $\mathcal{R}_c \subseteq L_n^\infty$ is closed, and

3) $\mathcal{R}_c$ has finite codimension in L_n^∞.

4.2.2 Results

The following results depend on Λ_c being a Fredholm operator which includes knowing specific information about the kernel and range of Λ_c.

Theorem 4.2.1 *Let Λ_c be defined as in (4.10) and assume Λ_c is asymptotically hyperbolic. Then Λ_c is a Fredholm operator.*

Proof. The result follows from Theorem A in [46] and from Lemma 4.2 in [50]. ■

The formal adjoint operator Λ_c^* of Λ_c is defined

$$(\Lambda_c^*\psi)(\xi) = diag(c)\psi'(\xi) - diag(\gamma)\psi''(\xi) - A_0^*(\xi)\psi(\xi) - \sum_{j=1}^{N} A_j^*(\xi - r_j)\psi(\xi - r_j),$$

where A_i^* is the conjugate transpose of A_i, $i = 1, ..., N$. Let $\mathcal{R}_c^*$ be the range of adjoint of Λ_c and $\mathcal{K}_c^*$ be the kernel of the adjoint of Λ_c. Then we have from Theorem A in [46] that

$$\mathcal{R}_c = \left\{ h \in L_n^\infty | \int_{-\infty}^{\infty} \overline{y(\xi)} h(\xi) d\xi = 0 \quad \text{for} \quad \text{all} \quad y \in \mathcal{K}_c^* \right\}.$$

We now present two hypotheses which are used in the lemma below.

(H1) Let Λ_c be defined as in (4.10) and assume that, for $k = 1, ..., n$, there exist quantities

$$\alpha_{j,k}, \beta_{j,k} \in I\!R, \quad 0 \leq j \leq N, \quad \text{with} \quad \alpha_{j,k} > 0, \quad 1 \leq j \leq N,$$

such that

$$\alpha_{j,k} \leq a_{k,k}^{(j)}(\xi) \leq \beta_{j,k} \quad \forall \xi \in I\!R, \quad \forall \quad k \in \{1, 2, ..., n\},$$

$$\text{and} \quad \forall \quad j \in \{1, 2, ..., N\},$$

where $a_{k,k}^{(j)}(\xi)$ is the k,k^{th} element of $A_j(\xi)$ and

$$\alpha_{0,k} \leq a_{k,\cdot}^{(0)}(\xi) \leq \beta_{0,k} \quad \forall \xi \in I\!R, \quad \forall \quad k \in \{1, 2, ..., n\},$$

where $a_{k,\cdot}^{(0)}(\xi)$ is any element of the k^{th} row of $A_0(\xi)$. In addition, for $k = 1, ..., n$, assume

$$\sum_{l=1}^{n} a_{k,l} < 0,$$

where $a_{k,l}$ is the k,l^{th} element of $A_{\pm} = \sum_{i=0}^{N} A_{i\pm}$.

(H2) Let Λ_c be defined as in (4.10) and assume that, for $k = 1, ..., n$, there exist quantities

$$\alpha_{j,k}, \beta_{j,k} \in I\!R, \quad 0 \leq j \leq N, \quad \text{with} \quad \alpha_{j,k} \geq 0, \quad 1 \leq j \leq N,$$

such that

$$-\alpha_{j,k} \geq a_{k,k}^{(j)}(\xi) \geq \beta_{j,k} \quad \forall \xi \in \quad I\!R, \qquad \forall \quad k \in \{1, 2, ..., n\},$$

$$\text{and} \qquad \forall \quad j \in \{1, 2, ..., N\},$$

where $a_{k,k}^{(j)}(\xi)$ is the k, k^{th} element of $A_j(\xi)$ and

$$\alpha_{0,k} \leq a_{k,\cdot}^{(0)}(\xi) \leq \beta_{0,k} \quad \forall \xi \in I\!R, \quad \forall \quad k \in \{1, 2, ..., n\},$$

where $a_{k,\cdot}^{(0)}(\xi)$ is any element of the k^{th} row of $A_0(\xi)$. In addition, for $k = 1, ..., n$, assume

$$\sum_{l=1}^{n} a_{k,l}^{(0)} < 0.$$

Lemma 4.2.1 *Let Λ_c be defined as in (4.10) and assume Λ_c is asymptotically autonomous. Also assume that there exists a solution to $\Lambda_c(\psi) = 0$ which is nonnegative and bounded. If Λ_c satisfies either (H1) or (H2), then*

1) Λ_c is asymptotically hyperbolic, (is a Fredholm operator)

2) there exists an element $p = (p_1, p_2, ..., p_n)$ in the kernel of Λ_c, such that $p_i > 0$, $i = 1, ..., n$,

3) there exists an element $p^* = (p_1^*, p_2^*, ..., p_n^*)$ in the kernel of the adjoint such that each element $p_i^*(\xi) > 0$ for all $\xi \in I\!R$, $i = 1, ..., n$, and

4) the range of Λ_c contains no elements, $h(\xi)$, such that $h_i(\xi) < 0$ or $h_i(\xi) > 0$, for all $\xi \in I\!R$ and $i = 1, ..., n$.

Proof. In this proof, we combine the results of Mallet-Paret, [46], [47], for first order differential-difference operators of the form

$$(\Lambda_{H1}\psi)(\xi) = -diag(c)\psi'(\xi) - A_0(\xi)\psi(\xi) - \sum_{j=1}^{N} A_j(\xi)\psi(\xi + r_j),$$

and the results of Fife and McLeod [26] and Beyn [7] for reaction-diffusion equations whose linearized form can be represented by operators of the form

$$(\Lambda_{H2}\psi)(\xi) = -diag(c)\psi'(\xi) - diag(\gamma)\psi'' - B_0(\xi)\psi(\xi).$$

Consider hypothesis (H1). Then the operator Λ_c can be treated as a perturbation of the operator Λ_{H1}. For the conditions set forth in the lemma and in (H1), Theorem 4.1 in [47] implies conclusions 1), 2), and 3).

Now consider hypothesis (H2). Then the operator Λ_c can be treated as a perturbation of the operator Λ_{H2}. Results 1), 2), and 3) follow from the fact that this operator has an exponential dichotomy.

As for result 4), with either (H1) or (H2), by result 3) there exists an element, p^*, in $\mathcal{R}_c^*$ such that $p_i^*(\xi) > 0$ for all $\xi \in I\!R$. Since

$$\mathcal{R}_c = \left\{ h \in L_n^\infty \mid \int_{-\infty}^{\infty} y(\xi)h(\xi)d\xi = 0 \quad \text{for} \quad \text{every} \quad y \in \mathcal{K}_c^* \right\},$$

any $h(\xi) \in \mathcal{R}_c$ must satisfy

$$\int_{-\infty}^{\infty} p^*(\xi) h(\xi) d\xi = 0.$$

Hence $h(\xi) \in \mathcal{R}_c$ cannot be have $h_i(\xi) < 0$ for all $\xi \in I\!R$ and $i = 1, ..., n$, or $h_i > 0$ for all $\xi \in I\!R$ and $i = 1, ..., n$. ∎

4.3 Proof of Theorem 4.1.1

We now present the proof of Theorem 4.1.1. First we establish that $D_{1,2}\mathcal{F}(\phi, b)$ is invertible in a neighborhood of the solution (φ, c). Then we rewrite the Newton iteration (4.9) as

$$(\varphi_{n+1}, c_{n+1}) = H(\varphi_n, c_n)$$

where

$$H(\phi, b) = (\phi, b) - [D_{1,2}\mathcal{F}(\phi, b)]^{-1}\mathcal{G}(\phi, b), \tag{4.15}$$

which is well-defined. We next show that H (4.15) is Frechet differentiable in the neighborhood in which it is well-defined. Last, we show that the Newton iteration converges to the solution in our neighborhood, that the solution is a point of attraction. This includes showing that the spectral radius of $D_{1,2}H$ is less than 1.

Let ρ be fixed. Let $(\varphi, c) \in W_0^{1,\infty} \times I\!R^n$ be such that $\mathcal{G}(\varphi, c) = \mathbf{0}$. And let F and G satisfy conditions c1 through c5 throughout this section.

Lemma 4.3.1 *There exists a ball of radius δ defined as*

$$S_{\varphi,c,\delta} = \{(\varphi_*, c_*) \in W_0^{1,\infty} \times I\!R^n \mid \|(\varphi, c) - (\varphi_*, c_*)\| \leq \delta \quad \text{for} \quad \delta > 0\} \subset W_0^{1,\infty} \times I\!R^n$$

such that $D_{1,2}\mathcal{F}(\varphi_*, c_*)$ is invertible for all $(\varphi_*, c_*) \in S_{\varphi,c,\delta}$.

Proof. It follows from the work of Beyn [7] that $D_{1,2}\mathcal{F}(\varphi, c)$ is an isomorphism from $W_0^{1,\infty} \times I\!R^n$ onto L_n^∞, and hence is invertible. Set $v = \|[D_{1,2}\mathcal{F}(\varphi, c)]^{-1}\|$ and let $0 < \epsilon < 1/(2v)$. Since $D_{1,2}\mathcal{F}(\varphi, c)$ is continuous at (φ, c), we can choose a $\delta > 0$ such that when $(\varphi_*, c_*) \in S_{\varphi,c,\delta}$,

$$\|D_{1,2}\mathcal{F}(\varphi, c) - D_{1,2}\mathcal{F}(\varphi_*, c_*)\| < \epsilon.$$

Let I be the identity operator from $W_0^{1,\infty} \times I\!R^n$ to $W_0^{1,\infty} \times I\!R^n$. Since

$$\begin{aligned} &\|I - [D_{1,2}\mathcal{F}(\varphi, c)]^{-1} D_{1,2}\mathcal{F}(\varphi_*, c_*)\| \\ &\quad = \|[D_{1,2}\mathcal{F}(\varphi, c)]^{-1}(D_{1,2}\mathcal{F}(\varphi, c) - D_{1,2}\mathcal{F}(\varphi_*, c_*))\| \leq \epsilon v \leq \frac{1}{2} < 1, \end{aligned}$$

Neumann's Lemma implies that $[D_{1,2}\mathcal{F}(\varphi, c)]^{-1} D_{1,2}\mathcal{F}(\varphi_*, c_*)$,

and hence $D_{1,2}\mathcal{F}(\varphi_*, c_*)$, is invertible. Also

$$\|[D_{1,2}\mathcal{F}(\varphi_*, c_*)]^{-1}\| \;=\; \|[I - (I - [D_{1,2}\mathcal{F}(\varphi, c)]^{-1} D_{1,2}\mathcal{F}(\varphi_*, c_*))]^{-1}[D_{1,2}\mathcal{F}(\varphi, c)]^{-1}\|$$

$$\leq \upsilon \sum_{i=1}^{\infty} (\upsilon\epsilon)^i = \frac{\upsilon}{1-\upsilon\epsilon}$$

for all $(\varphi_*, c_*) \in S_{\varphi,c,\delta}$. ∎

Remark 4.3.1 *Thus the operator* $H : S_{\varphi,c,\delta} \to W_0^{1,\infty} \times I\!R^n$ *defined as*

$$H(\varphi_*, c_*) = (\varphi_*, c_*) - [D_{1,2}\mathcal{F}(\varphi_*, c_*)]^{-1}\mathcal{G}(\varphi_*, c_*) \tag{4.16}$$

is well defined.

Lemma 4.3.2 *The operator* H *(4.16) is Frechet-differentiable and the derivative with respect to* φ *and* c *is*

$$D_{1,2}H(\varphi, c) = I - [D_{1,2}\mathcal{F}(\varphi, c)]^{-1} D_{1,2}\mathcal{G}(\varphi, c).$$

Proof. Since $\mathcal{G}$ is Frechet-differentiable at (φ, c),

$$\|\mathcal{G}(\varphi_*, c_*) - \mathcal{G}(\varphi, c) - D_{1,2}\mathcal{G}(\varphi, c)[(\varphi_*, c_*) - (\varphi, c)]\| \leq \epsilon \|(\varphi_*, c_*) - (\varphi, c)\|$$

for all $(\varphi_*, c_*) \in S_{\varphi,c,\delta}$. Using the fact that $(\varphi, c) = H(\varphi, c)$, we obtain

$$\|H(\varphi_*, c_*) - H(\varphi, c) - [I - [D_{1,2}\mathcal{F}(\varphi, c)]^{-1} D_{1,2}\mathcal{G}(\varphi, c)][(\varphi_*, c_*) - (\varphi, c)]\|$$

$$= \|[D_{1,2}\mathcal{F}(\varphi,c)]^{-1}D_{1,2}\mathcal{G}(\varphi,c)[(\varphi_*,c_*)-(\varphi,c)]-[D_{1,2}\mathcal{F}(\varphi_*,c_*)]^{-1}\mathcal{G}(\varphi_*,c_*)\|$$

$$\leq \|-[D_{1,2}\mathcal{F}(\varphi_*,c_*)]^{-1}[\mathcal{G}(\varphi_*,c_*)-\mathcal{G}(\varphi,c)-D_{1,2}\mathcal{G}(\varphi,c)((\varphi_*,c_*)-(\varphi,c))]\|$$

$$+\|[D_{1,2}\mathcal{F}(\varphi_*,c_*)]^{-1}[\mathcal{F}(\varphi,c)-\mathcal{F}(\varphi_*,c_*)][D_{1,2}\mathcal{F}(\varphi,c)]^{-1}$$

$$D_{1,2}\mathcal{G}(\varphi,c)((\varphi_*,c_*)-(\varphi,c))\|$$

$$\leq (2\upsilon\epsilon+2\upsilon^2\epsilon\|D_{1,2}\mathcal{G}(\varphi,c)\|)\|(\varphi_*,c_*)-(\varphi,c)\|, \tag{4.17}$$

for all $(\varphi_*,c_*)\in S_{\varphi,c,\delta}$. This implies H is Frechet-differentiable and the derivative of (4.16) about the solution (φ,c) is

$$D_{1,2}H(\varphi,c)=I-[D_{1,2}\mathcal{F}(\varphi,c)]^{-1}D_{1,2}\mathcal{G}(\varphi,c) \tag{4.18}$$

where

$$D_{1,2}\mathcal{G}(\varphi,c)(\psi,b)(\xi)=D_{1,2}\mathcal{F}(\varphi,c)(\psi,b)(\xi)-\sum_{i=1}^{N}[D_{\varphi_{r_i}}G(\overline{\varphi})]\psi(\xi+r_i).$$

The operator $D_{\varphi_{r_i}}G(\overline{\varphi})$ is a diagonal matrix with $\partial G(\overline{\varphi},\rho)/\partial\varphi_{r_i^l}$ as the l,l^{th} entry. Hence $D_{\varphi_{r_i}}G(\overline{\varphi})$ is a linear, possibly nonautonomous, operator. ■

Lemma 4.3.3 *Let $\hat{\sigma}$ be the spectral radius of $D_{1,2}H(\varphi,c)$. Then $\hat{\sigma}<1$.*

Proof. Writing the eigenproblem for $D_{1,2}H(\varphi, c)$ we obtain the equation

$$[D_{1,2}\mathcal{F}(\varphi, c)]^{-1}\sum_{i=1}^{N}[D_{\varphi_{r_i}}G(\overline{\varphi})]\phi(\xi + r_i) - \lambda I(\phi, b) = (0, 0)$$

where λ is the eigenvalue, and (ϕ, b) are the eigenfunctions. Rewriting this relation we obtain

$$-D_{1,2}\mathcal{F}(\varphi, c)(\phi, b) + \frac{1}{\lambda}\sum_{i=1}^{N}[D_{\varphi_{r_i}}G(\overline{\varphi})]\phi(\xi + r_i) = 0,$$

$$\begin{aligned}\Rightarrow \quad & \lambda[diag(c)\phi'(\xi) + diag(\gamma)\phi''(\xi) + D_{\varphi}F(\varphi)\phi(\xi)] \\ & + \sum_{i=1}^{N}[D_{\varphi_{r_i}}G(\overline{\varphi})]\phi(\xi + r_i) + \lambda b\varphi'(\xi) = 0,\end{aligned}$$

$$\begin{aligned}\Rightarrow \quad & \lambda[diag(c)\phi'(\xi) + diag(\gamma)\phi''(\xi) + D_{\varphi}F(\varphi)\phi(\xi)] \\ & + \sum_{i=1}^{N}[D_{\varphi_{r_i}}G(\overline{\varphi})]\phi(\xi + r_i) = -\lambda b\varphi'(\xi).\end{aligned} \tag{4.19}$$

The right-hand side of (4.19), contains the derivative of the solution to (4.1), $\varphi'(\xi)$, which we know from Lemma 4.2.1 with (H1), is strictly positive.

We now analyze the left-hand side of (4.19) using the results presented in the

previous section. Let $J_\lambda(\phi, b)$ be

$$J_\lambda(\phi, b) = \lambda[diag(c)\phi'(\xi) + diag(\gamma)\phi''(\xi) + D_\varphi F(\varphi)\phi(\xi)] + \sum_{i=1}^{N}[D_{\varphi_{r_i}} G(\overline{\varphi})]\phi(\xi + r_i).$$

Let $A_0(\xi) = \lambda D_\varphi F(\varphi)$ and $A_j(\xi) = D_{\varphi_{r_j}} G(\overline{\varphi})$, $j = 1, ..., N$. Then J_λ, the left-side of (4.19) can be written as Λ_c as defined in (4.10).

We now show that $\Lambda_c = J_\lambda$ satisfies (H1) and the assumptions of Lemma 4.2.1 for $\lambda \geq \lambda_1$ where $\lambda_1 \in (0, 1)$. By (4.2), $0 < \alpha_{j,k} \leq a_{k,k}^{(j)}(\xi) \leq \beta_{j,k}$ for all $\xi \in I\!R$, for all $k = 1, ..., n$, $j = 1, ..., n$, where $a_{k,k}^{(j)}$ is the k, k^{th} element of the diagonal matrix A_j. From the conditions on $\Gamma(\varphi, \rho)$ (4.3), (4.4), along with the boundary conditions (4.6) we have that there exists a $0 < \lambda_1 < 1$ such that for $\lambda > \lambda_1$, $\sum_{l=1}^{n} a_{k,l} < 0$ for $k = 1, ..., n$ where $a_{k,l}$ is the k, l^{th} element of $\sum_{i=0}^{N} A_{i\pm}$ and that J_λ is asymptotically autonomous. Let λ_1 be the smallest such λ_1. Hence by Lemma 4.2.1, for $\lambda \geq 1$, the range of J_λ contains no strictly positive nor negative sets of elements. Now notice that the right-hand side of (4.19), a constant times the derivative of the solution φ, is a set of strictly positive or negative elements. Thus (4.19) has no nontrivial solution ψ for $b \neq \mathbf{0}$ and $\lambda \geq \lambda_1$.

Next we consider $\lambda < 0$,

$$|\lambda|[c\phi'(\xi) + \gamma\phi''(\xi) + D_\varphi F(\varphi)\phi(\xi)] - \sum_{i=1}^{N}[D_{\varphi_{r_i}} G(\overline{\varphi})]\phi(\xi + r_i),$$

and Lemma 4.2.1 with (H2). For $\lambda < 0$, the conditions of Lemma 4.2.1 with (H2) are met for the same reasons the conditions of Lemma 4.2.1 with (H1) are met for $\lambda \geq \lambda_1$. Thus the right-hand side of (4.19) is not in the range of J_λ, the left-hand side, when $\lambda < 0$. Hence $\lambda \geq \lambda_1$, for $0 < \lambda_1 < 1$, and $\lambda < 0$ are not in the spectral radius of (4.18).

In Section 4 of [47], Mallet-Paret shows that when $\lambda > \lambda_1$, the real eigenvalues of (4.19) lie in both the intervals $(-\infty, 0)$ and $(0, \infty)$, and as we saw above, when $\lambda > \lambda_1$, λ is not in the spectrum of (4.18). He also showed that for $0 < \lambda < \lambda_1$, the real eigenvalues of the determinant of the characteristic equation of (4.19) all lie in either $(-\infty, 0)$ or $(0, \infty)$. Suppose $0 < \lambda < \lambda_1$, and consider the formal adjoint of the left-hand side of (4.19). This adjoint operator has a kernel, $\mathcal{K}_c^*$, of dimension zero. Since the operator represented by the left-hand side of (4.19) is a Fredholm operator, the codimension of the range of (4.19) equals the dimension of $\mathcal{K}_c^*$ which is zero. Hence the right-hand side of (4.19) is in the range of the left-hand side. Thus $0 < \lambda < \lambda_1$ is in the spectrum of (4.18). ∎

Remark 4.3.2 *1) We would like to point out that if* $diag(\gamma) = \mathbf{0}$ *in our differential-difference equation (4.1), then we would not even be able to show that the spectral radius of (4.18) is bounded. This indicates that this Newton's method would not converge for* $diag(\gamma) = 0$ *and implies why the limit* $diag(\gamma) \to \mathbf{0}$ *is difficult to*

approach with this numerical method. The reason for this is that we "breakup" the spatially discrete diffusion operator with our relaxation. Thus the convergence is dependent on the continuous diffusion operator, $diag(\gamma)\varphi''$.

2) The value λ_1 can be thought of as the contraction factor for our method.

3) The value λ_1 is both direction and dimension dependent.

Lemma 4.3.4 *For $D_{1,2}H : W_0^{1,\infty} \to W_0^{1,\infty}$ the limit*

$$\lim_{m\to\infty} \|[D_{1,2}H]^m\|^{1/m} = \hat{\sigma}$$

exists, where $\hat{\sigma}$ is the spectral radius.

Proof. The result is a statement of Theorem 10.13 in Rudin [53]. ∎

Lemma 4.3.5 *The solution (φ, c) is a point of attraction of (4.9).*

Proof. By Lemma 4.3.4, for any $\epsilon > 0$ there exists an integer $N_{\hat{\sigma}}$ such that for all $m \geq N_{\hat{\sigma}}$

$$\|[D_{1,2}H(\varphi, c)]^m\|^{1/m} \leq \hat{\sigma} + \epsilon,$$

which implies

$$\|[D_{1,2}H(\varphi, c)]^m\| \leq (\hat{\sigma} + \epsilon)^m.$$

Let $H^p(\psi, b) = H[H(H\{...[H(\psi, b)]...\})]$, the operator H applied p times. Observe that $H^p : W_0^{1,\infty} \to W_0^{1,\infty}$ and that $H^p(\varphi, c) = (\varphi, c)$. Choose $\epsilon > 0$ such that $\hat{\sigma}+\epsilon < 1$, choose $p_1 \in \mathbb{Z}^+$ such that $(\hat{\sigma} + \epsilon)^{p_1} + \epsilon < 1$, and let $p > \max(N_{\hat{\sigma}}, p_1)$. Since H is Frechet-differentiable at (φ, c), H^p is also. Thus there exists a $\delta > 0$ such that, for all $(\varphi_*, c_*) \in S_{\varphi,c,\delta}$,

$$\|H^p(\varphi_*, c_*) - H^p(\varphi, c) - D_{1,2}H^p(\varphi, c)((\varphi_*, c_*) - (\varphi, c))\| \leq \epsilon\|(\varphi_*, c_*) - (\varphi, c)\|.$$

The Frechet derivative of H^p,

$$D_{1,2}H^p(\varphi, c) = [D_{1,2}H(\varphi, c)]^p,$$

through application of the chain rule. Thus,

$$\begin{aligned} \|H^p(\varphi_*, c_*) - (\varphi, c)\| &\leq \|H^p(\varphi_*, c_*) - H^p(\varphi, c) - D_{1,2}H^p(\varphi, c)((\varphi_*, c_*) - (\varphi, c))\| \\ &\quad + \|[D_{1,2}H(\varphi, c)]^p\|\|(\varphi_*, c_*) - (\varphi, c)\| \\ &\leq [(\hat{\sigma} + \epsilon)^p + \epsilon]\|(\varphi_*, c_*) - (\varphi, c)\| \end{aligned}$$

for all $(\varphi_*, c_*) \in S_{\varphi,c,\delta}$.

Therefore, if $(\varphi_0, c_0) \in S_{\varphi,c,\delta}$,

$$\|(\varphi_p, c_p) - (\varphi, c)\| = \|H^p(\varphi_0, c_0) - (\varphi, c)\| \leq [(\hat{\sigma} + \epsilon)^p + \epsilon]\|(\varphi_0, c_0) - (\varphi, c)\|,$$

which implies that $(\varphi_p, c_p) \in S_{\varphi,c,\delta}$. By an induction argument,

$$\|(\varphi_{n\cdot p}, c_{n\cdot p}) - (\varphi, c)\| \leq [(\hat{\sigma} + \epsilon)^p + \epsilon]^n\|(\varphi_0, c_0) - (\varphi, c)\| \tag{4.20}$$

and $(\varphi_{n\cdot p}, c_{n\cdot p}) \in S_{\varphi,c,\delta}$ for all $n \in \mathbb{Z}^+ \cup 0$. Since $(\hat{\sigma} + \epsilon)^p + \epsilon < 1$, (4.20) implies that

$$\lim_{n\to\infty}(\varphi_{n\cdot p}, c_{n\cdot p}) = (\varphi, c).$$

Since H is a bounded operator, and since (4.20) holds for all $p > \max(N_{\hat{\sigma}}, p_1)$,

$$\lim_{n\to\infty}(\varphi_n, c_n) = (\varphi, c).$$

■

This concludes the proof of Theorem 4.1.1.

Remark 4.3.3 *In Section 4.1, we assumed that F and G were C^1. In proving Theorem 4.1.1, we only need that $\mathcal{G}$, $D_{1,2}\mathcal{G}(\varphi_*, c_*)$, and $D_{1,2}\mathcal{F}(\varphi_*, c_*)$ are continuous in a neighborhood of the solution (φ, c). Thus we only need $(\varphi_*, c_*) \in S_{\varphi,c,\delta}$, $D_{\varphi_*}F$, and*

$D_{\varphi_{r_{i^*}}}G$ to be continuous. If we define $f_1(a) = 0$ and $D_\varphi f_1(a) = d_1$, then (4.1) with the piecewise linear nonlinearity f_1, appears to be included in the class of equations that can be solved with this numerical method. But recall that for this problem, with nonlinearity f_1, $\varphi''(\xi)$ is discontinuous at a and the spectral radius argument holds for continuous operators. It is not clear at this time if the proof can be made to hold for nonlinearities such as f_1.

4.4 Chapter Summary

We presented a numerical method for general nonlinear systems of bistable traveling wave differential-difference equations. The key to this method is treating the forward and backward delay terms as "known" information, and then solving the problem with iteration. The iterative method used is Newton's since we wished to work with the linear variation of the nonlinear equation being solved. Convergence of this iterative method was proved through the use of linear Fredholm operator theory which is a way to formulate the exponential-dichotomy-like behavior that the systems exhibit.

The primary limitation of our iterative technique is that the second derivative term φ'' is needed so that the difference operator can be "split". This limitation, among others, indicates the need to develop a differential-difference solver where the difference term need not be dealt with through relaxation.

Chapter 5

NUMERICAL EXAMPLES

This chapter focuses on several numerical examples which exhibit behavior that we are only beginning to investigate analytically. One of the primary difficulties in developing analytical results, including solutions, to differential-difference models is the unknown nature of the phenomena they contain. Numerically obtained results have the potential to point out the path to follow in our analytical investigations. The algorithms presented in Chapters 2 and 4 provide us with the numerical tools for investigating a large class of both linear and nonlinear traveling wave differential-difference equations.

In the first example, Example 1, we revisit the reaction-diffusion, wave, and damped wave differential-difference equations of Chapter 2. In addition to the non-

linearity f_1, we also consider the bistable nonlinearities

$$f_2(\varphi) = d_1\varphi(\varphi - a)(\varphi - 1),$$

$$f_3(\varphi) = d_1(a - \varphi + 0.1\log\left[\frac{\varphi(a-1)}{a(\varphi-1)}\right]).$$

We discover that the phenomena of propagation failure and step-like solution profiles occur for all three nonlinearities and are not artifacts of the piecewise continuous nonlinearity f_1. In the second example we present solution and $a(c)$ relations for the variable diffusion reaction-diffusion differential-difference equation of period two. Included in this presentation is an example of period two bifurcation of the constant coefficient equation. The third example is consists of solving differential-difference equations with inhomogeneous equilibria. A feature of this example is wave propagation for a symmetric nonlinearity.

5.1 Example 1: Nonlinear Reaction-Diffusion, Wave, and Damped Wave Differential-Difference Equations

In this example, we consider the traveling wave equation (2.1), which is of the form

$$-\kappa_c\varphi'(\xi) - \delta_c\varphi''(\xi) = L_D\varphi(\xi) - f(\varphi(\xi), a), \tag{5.1}$$

where

$$L_D\varphi(\xi) = \sum_{k=1}^{n} \varepsilon_k[\varphi(\xi - \sigma_k) - 2\varphi(\xi) + \varphi(\xi + \sigma_k)],$$

with $\sum_{k=1}^{n} \sigma_k^2 = 1$ and $\sigma_k \neq 0$, $k = 1, ...n$.

Comparing Equation (5.1) with the general differential-difference form (4.1) from Chapter 4, the operator $F(\varphi, \rho) = -2\sum_{k=1}^{n} \varepsilon_k \varphi(\xi) - f(\varphi(\xi), a)$, the operator $G(\overline{\varphi}, \rho) = \sum_{k=1}^{n} \varepsilon_k[\varphi(\xi - \sigma_k) + \varphi(\xi + \sigma_k)]$ and is linear, and $a(\rho) = \rho = a$. The condition that $F \in C^1$ requires that we use a C^1 nonlinearity f when solving with the Newton's method of Chapter 4. We have experimented with using this method to solve (5.1) with f_1 with limited success. There are five conditions imposed on F and G in Chapter 4 for convergence of the Newton's method. Equation (5.1) satisfies conditions (1) through (4) with condition (5) satisfied by (5.1) with nonlinearities f_2 and f_3.

Since in Chapter 2 we presented several numerical experiments for this problem with nonlinearity f_1, we concentrate here on the comparison of these results with results obtained with the cubic nonlinearity f_2 and the logarithmic nonlinearity f_3. The numerical solutions with the nonlinearities f_1, f_2, and f_3, presented in this section, are obtained using the Newton's method of Chapter 4.

5.1.1 Step-Like Wave Profiles

We begin our presentation with Figures 5.1 and 5.2. The problems solved to produce the solution curves in these two figures are identical except for the scaling of the nonlinearities. In Figure 5.1 a), we plot the three nonlinearities f_1, f_2, and f_3, all of which have maximum and minimum values that are approximately the same (the same order of magnitude). In addition, f_2 and f_3 have approximately the same slope at a. Figure 5.1 b) shows the solution curves, $\varphi(\xi)$, for (5.1) for each of the three nonlinearities with $a = 1/2$.

Remark 5.1.1 *In the equation at the bottom of Figure 5.1 we claim that* $c = 0$. *In actuality, because of numerical error,* $c \approx 10^{-7}$.

Remark 5.1.2 *In the solution plot of for Equation (5.1), Figure 5.1 b), the step phenomenon appears reguardless of which nonlinearity is used. This implies that the step-like solution profile is not generated by the jump discontinuity in the nonlinearity* f_1, *but is generated by the nonlocal nature of the spatially discrete diffusion term.*

In Figure 5.2 a), we have the same relationships between f_1, f_2, and f_3 as in Figure 5.1 a), only now the magnitude is about a factor of 12 smaller.

Remark 5.1.3 *In the solution plot of Figure 5.2, plot b), we see that the solution curves for* f_2 *and* f_3 *no longer have a step like behavior. Comparing Figures 5.1*

a)

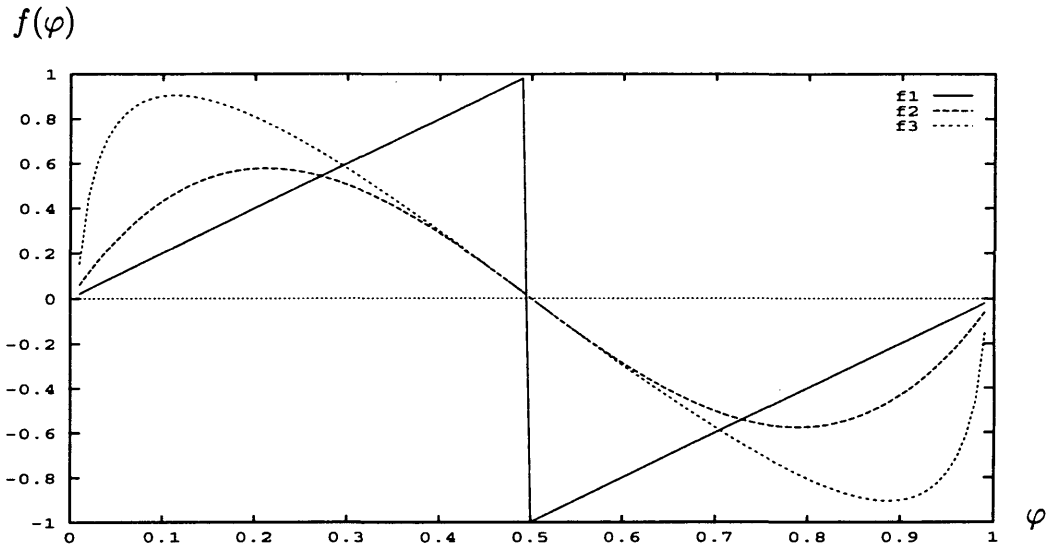

$$f_1(\varphi, 0.5) = 2\begin{cases} \varphi, & \varphi < 0.5 \\ \varphi - 1, & \varphi > 0.5 \end{cases} \qquad f_2(\varphi, 0.5) = 12\varphi(\varphi - 0.5)(\varphi - 1)$$

$$f_3(\varphi, 0.0) = 4[0.5 - \varphi + 0.1 \log\left(\tfrac{\varphi}{1-\varphi}\right)]$$

b)

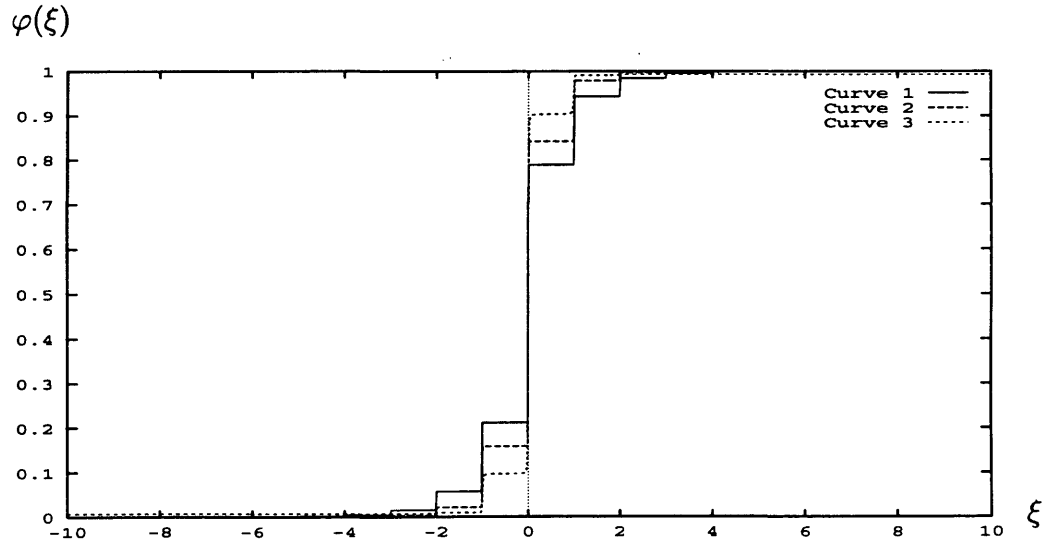

$$10^{-5}\varphi''(\xi) = [\varphi(\xi + 1) - 2\varphi(\xi) + \varphi(\xi - 1)] - f(\varphi(\xi), 0.5)$$

Figure 5.1: Example 1: Step-like solution profiles and nonlinearity plots for nonlinearities f_1, f_2, and f_3.

and 5.2 gives us our first indication that the slope of the nonlinearity at the detuning parameter a effects the solution profile.

5.1.2 The Cubic Nonlinearity

In Figure 5.3 we solve (5.1) with the cubic nonlinearity f_2. A set of solution curves, for various values of the detuning parameter a, is plotted in plot a) and the $a(c)$ curve for this problem is plotted in plot b).

Remark 5.1.4 *i) We present only solution curves for $a \geq 0.5$ in Figure 5.3 because of the symmetry these solutions possess with the solutions for $a \leq 0.5$.*

ii) In Chapter 2, for the nonlinearity f_1, we saw $a(c)$ plots which admitted a non-trivial interval of a in which $c = 0$ (Figures 2.2, 2.4, 2.5, and 2.7). We also learned that this propagation failure only occurs when $\gamma = 0$, but we saw that for γ small, $a(c)$ curves possess an interval of a (approximately the same interval as for propagation failure) for which c is small (compare Figures 2.7 and 2.8). In the $a(c)$ plot, Figure 5.3 b), we once again see this behavior, where for $\gamma = 10^{-4}$, there exists an interval of a for which $|c| < 10^{-3}$. This suggests that we may also have propagation failure for $\gamma = 0$ when solving with the cubic nonlinearity f_2. This also suggests that propagation failure is due to the discrete diffusion term, not the discontinuity in the nonlinearity f_1.

a)

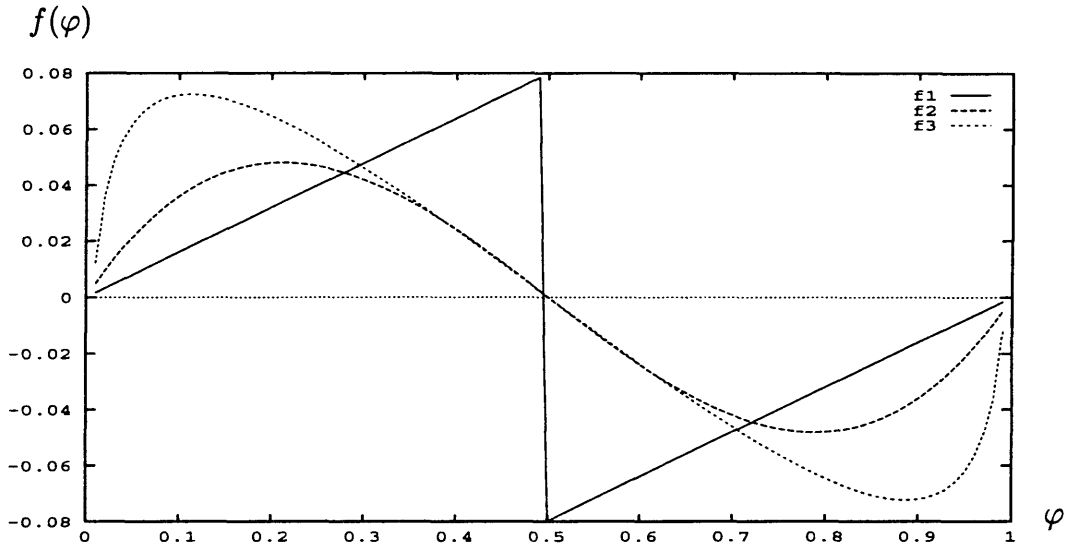

$$f_1(\varphi, 0.5) = 0.16 \begin{cases} \varphi, & \varphi < 0.5 \\ \varphi - 1, & \varphi > 0.5 \end{cases} \qquad f_2(\varphi, 0.5) = \varphi(\varphi - 0.5)(\varphi - 1)$$

$$f_3(\varphi, 0.5) = 0.4[0.5 - \varphi + 0.1 \log\left(\tfrac{\varphi}{1-\varphi}\right)]$$

b)

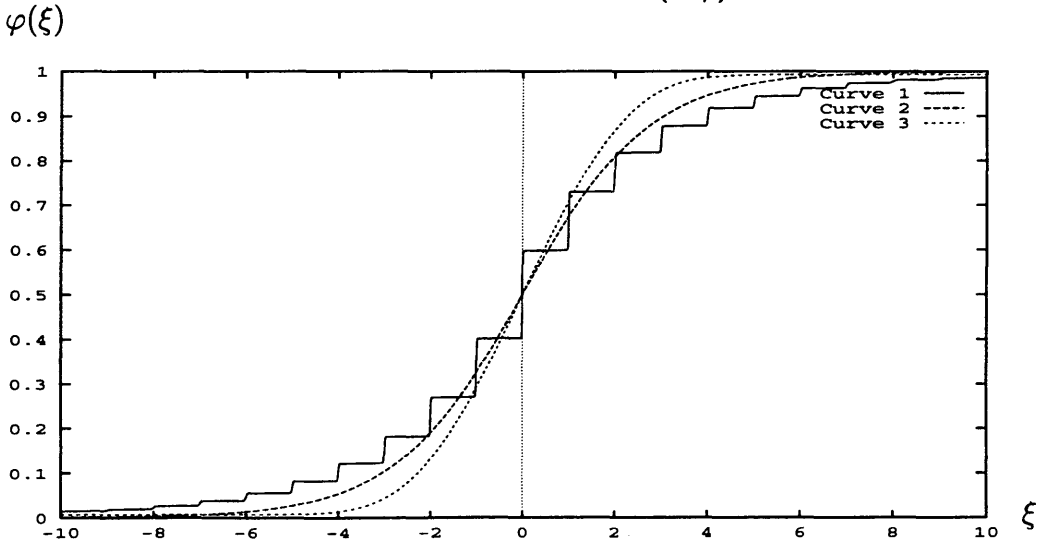

$$10^{-5}\varphi''(\xi) = [\varphi(\xi + 1) - 2\varphi(\xi) + \varphi(\xi - 1)] - f(\varphi(\xi), 0.5)$$

Figure 5.2: Example 1: A plot of nonlinearities and a plot of solutions.

Referring to both the solution $\varphi(\xi)$ plot and the $a(c)$ plot in Figure 5.3, we point out three main types of solution profiles that can be classified by $|a - 1/2|$. The first type (solutions C6 and C7 in Figure 5.3) are solutions that have a hyperbolic tangent shape. The values of a are the farthest from $1/2$ for this type.

Remark 5.1.5 *As $|a - 1/2|$ increases towards $1/2$, the magnitude of the wave speed $|c|$ becomes large. This first type of solution profile, the large wave speed case, is typically what is studied when traveling wave solutions are considered.*

The third type of profile (solutions C1, C2, and C3) consists of solutions whose profile exhibit step-like behavior. Away from the wave front (the internal layer), the tails of these solutions decay asymptotically. The values of a for this type define an interval about $1/2$.

Remark 5.1.6 *i) The interval for a for which c is small corresponds to the solutions that are step-like.*

ii) Existing work on propagation failure considers solutions of this type.

The second type of solution profile (solutions C4 and C5) consists of "transition" solutions, solutions that contain a mix of elements from the first and third types of solution profiles. The distance from $1/2$, $|a - 1/2|$, for the values of a for this type of solution profile is greater than $|a - 1/2|$ for the values of a of the third type and is less than $|a - 1/2|$ for the values of a of the first type.

Remark 5.1.7 *The second type of solution profiles is least often considered when traveling wave solutions are sought.*

We will have more to say about solution profiles of the second type in Example 2 below.

5.1.3 The Logarithmic Nonlinearity

Continuing with our first example, in Figure 5.4 we solve (5.1) with the same parameter values as for the cubic case above, Figure 5.3, only now we use the logarithmic nonlinearity f_3.

Remark 5.1.8 *The $a(c)$ plot (bottom plot) of Figure 5.4, has an interval of a values for which c is small, a region that may imply propagation failure as in the cubic case. These values of a correspond to the step-like solution profiles, Figure 5.4 a).*

Remark 5.1.9 *The main difference between the solutions which appear in Figure 5.4 and the solutions which appear in Figure 5.3 is that the stable equilibria of (5.1) with nonlinearity f_3 depend on the value of the unstable equilibrium a while the stable equilibria, 0 and 1, for (5.1) with nonlinearity f_2 do not depend on a.*

a)

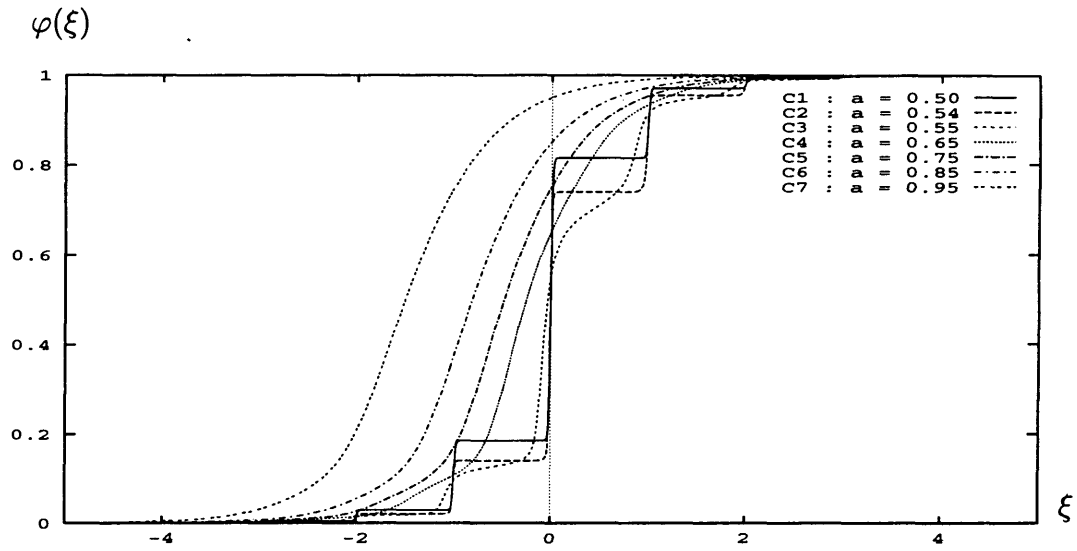

$$-c\varphi'(\xi) - 10^{-4}\varphi''(\xi) = [\varphi(\xi+1) - 2\varphi(\xi) + \varphi(\xi-1)] - 10\varphi(\varphi - a)(\varphi - 1)$$

b)

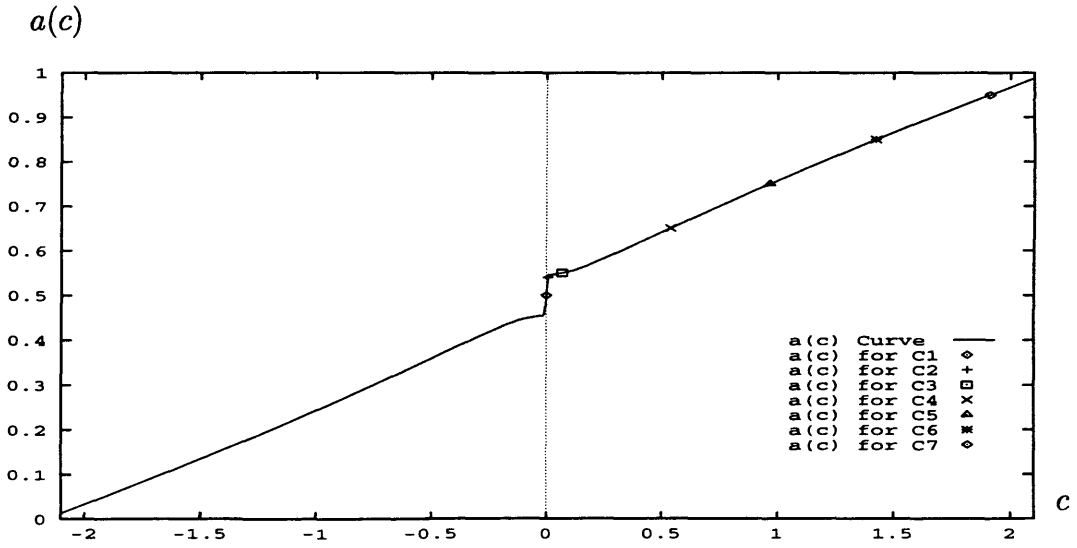

Figure 5.3: Example 1: The spatially discrete/continuous reaction-diffusion equation with the cubic nonlinearity and various values of the detuning parameter a.

a)

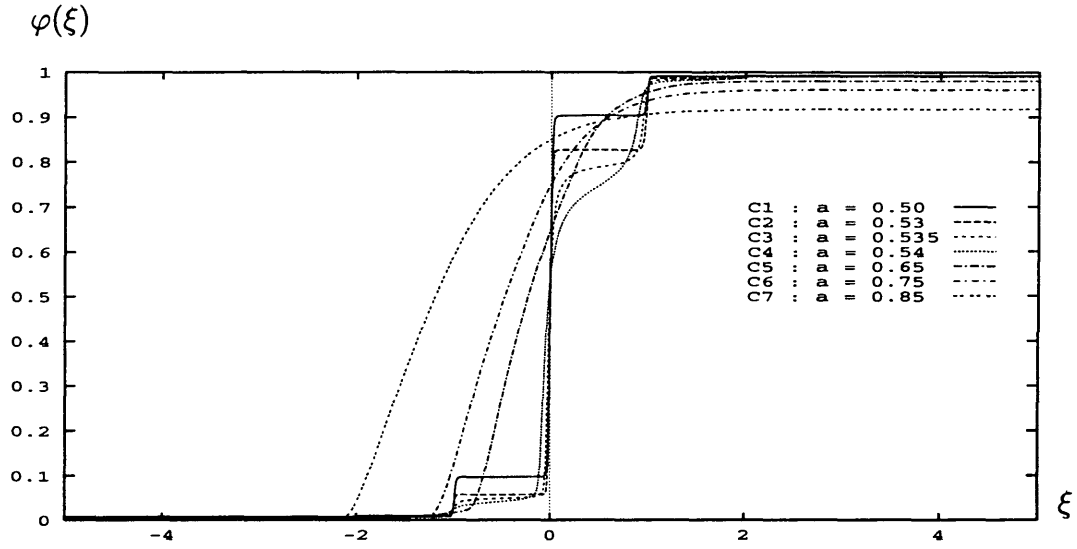

$$-c\varphi'(\xi) - 10^{-4}\varphi''(\xi) = [\varphi(\xi+1) - 2\varphi(\xi) + \varphi(\xi-1)] - 4(a - \varphi + 0.1\log\left[\tfrac{(a-1)\varphi}{a(\varphi-1)}\right])$$

b)

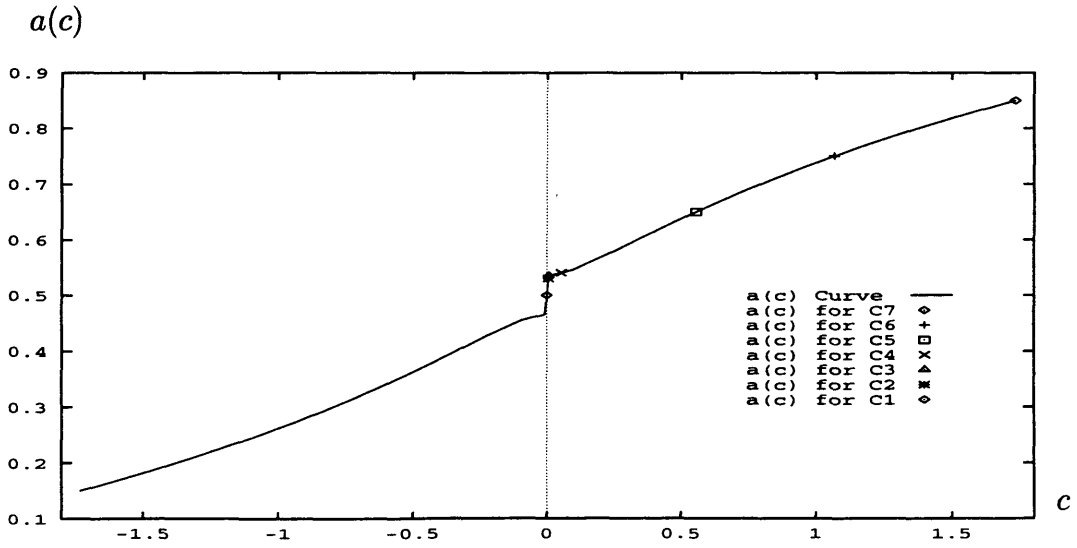

Figure 5.4: Example 1: The spatially discrete/continuous reaction-diffusion equation with the logarithmic nonlinearity and various values of the detuning parameter a.

5.2 Example 2: Variable Diffusion and Wave Speed of Period Two

Our next example returns to the variable diffusion equation of Chapter 3, the equation

$$\begin{aligned} & -\ c(\eta)\varphi'(\xi) - \gamma\varphi''(\xi) \\ & \qquad = \alpha(\eta+1)[\varphi(\xi+1) - \varphi(\xi)] + \alpha(\eta)[\varphi(\xi-1) - \varphi(\xi)] - f(\varphi(\xi), a), \end{aligned} \tag{5.2}$$

where $\alpha(\eta)$ is of period two in $\eta \in \mathbb{Z}$. Although (3.2) in Chapter 3 does not include the term $\gamma\varphi''(\xi)$, we include it in Equation (5.2) so that we may apply our numerical solvers. We want to find the solution pair $(\varphi(\xi, a), c(\eta, a))$ to (5.2) with boundary conditions $\varphi(-\infty, \cdot) = 0$ and $\varphi(\infty, \cdot) = 1$.

Typically the period two diffusion coefficient problem will consist of two solution curves, $\varphi = (\varphi_1, \varphi_2)$, each with its own corresponding wave speed. This indicates that we have two possible trajectories that points in the lattice follow from one phase to the other. Since α is period two on the lattice, every other lattice point follows the same trajectory in time.

5.2.1 Constant Diffusion, Variable Wave Speed, and Period Two Bifurcation

When deriving and solving the constant coefficient traveling wave equation (2.2) in Chapter 2, and solving Example 1 above, we used the traveling wave ansatz $u(\eta, t) =$

$\varphi(\eta - ct)$ where the unknown wave speed c was constant, or equivalently, on a spatial lattice, had period one. We then proved that for the nonlinearity f_1, the function $c(a)$ is monotone, exhibits propagation failure, as well as many other analytical properties. Most of these results have been verified numerically for all three nonlinearities, f_1, f_2, and f_3. Suppose instead we consider the constant coefficient problem, but we allow $c(\eta, a)$ to vary periodically on the spatial lattice. If we consider the case where c has period two, this is equivalent to considering the period two diffusion coefficient problem with $\alpha(\eta)$ constant.

We begin with Figure 5.5, where we have plotted the $a(c)$ curve for the period two wave speed case (the curves labeled c2), along with the $a(c)$ curve (the curve labeled c1) for the case where c is assumed constant. The two $a(c)$ curves (c1 and c2) coincide except for two regions, one for $c > 0$ and one for $c < 0$.

Remark 5.2.1 *The regions where the $a(c)$ curves do not coincide are bounded by four bifurcation points, two for each region. These are the points where the $a(c)$ curves split. Letting $\varphi = (\varphi_1, \varphi_2)$ and $c = (c_1, c_2)$, these points indicate the values of a for which the fixed point of (5.2), (φ, c), bifurcates. We will refer to these regions where the $a(c)$ curves c1 and c2 are distinct as the bifurcation regions or the regions of period two bifurcation.*

If we look at solutions of the period two wave speed problem, outside the bifurcation regions, Figures 5.6 and 5.9, where the wave speed maintains a single value,

we see that there is one solution curve per c, a pair. Note the solution curves for $a = 0.78$ (Figure 5.6) and $a = 0.63$ (Figure 5.9), a values that lie just outside a region of bifurcation.

As we decrease a from $a = 0.78$ into the region of bifurcation, (φ, c) goes through a period two bifurcation and we begin to obtain a pair of distinct solution trajectories and wave speeds for each a (Figure 5.7, $a = 0.77$ and $a = 0.73$), one solution and wave speed similar to the solution and wave speed for $a = 0.78$ (Curve 2) and the other solution (Curve 1) and wave speed moving towards the solution and wave speed for $a = 0.63$.

Continuing to decrease a, once the solution represented by Curve 1 has reached a neighborhood of the solution for $a = 0.63$, Curve 2 begins to approach this solution as well (Figure 5.8, $a = 0.70$ and $a = 0.65$).

As a decreases further towards $a = 0.63$, (φ, c) goes through another period two bifurcation, and we once again have only one solution trajectory and one wave speed (Figure 5.9).

In the previous example (Example 1) we point out that we could classify the solution curves into three types. The first type, the hyperbolic tangent type, relates to solutions for $|a|$ greater than the values of a that correspond with the bifurcation regions. The third type, the step-like type, corresponds to solutions for $|a|$ less than the values of a that correspond with the bifurcation regions. And the second type,

the "transition" solutions, are the solutions which correspond to the region of period two bifurcation in Figure 5.5.

When c is assumed to be constant, we saw that the solutions of "transition" type possessed a mix of features from both the first and third types. When we consider wave speeds c of period two, we see that solutions of "transition" type are a pair of solutions, each containing properties of the first and third types.

5.2.2 Period Two Diffusion Coefficient

Again consider equation (5.2) where the diffusion coefficient varies with period two on the spatial lattice. For comparison purposes, all the variables in this example, except for the diffusion coefficient $\alpha(\eta)$, are the same as in Subsection 5.2.1.

In this example we are solving the period two equation

$$\begin{aligned} -c(\eta)\varphi'(\xi) - 10^{-3}\varphi''(\xi) \quad &= \\ \alpha(\eta+1)[\varphi(\xi+1)-\varphi(\xi)] \quad &+ \quad \alpha(\eta)[\varphi(\xi-1)-\varphi(\xi)] - 15\varphi(\xi)(\varphi(\xi)-a)(\varphi(\xi)-1). \end{aligned}$$

In Figure 5.10 we present the $a(c)$ curve associated with this problem with the diffusion coefficient varying from 1.3 to 1.9 in a period two fashion.

Remark 5.2.2 *There are at least three new phenomena, new to us at least, that the $a(c)$ curves possess.*

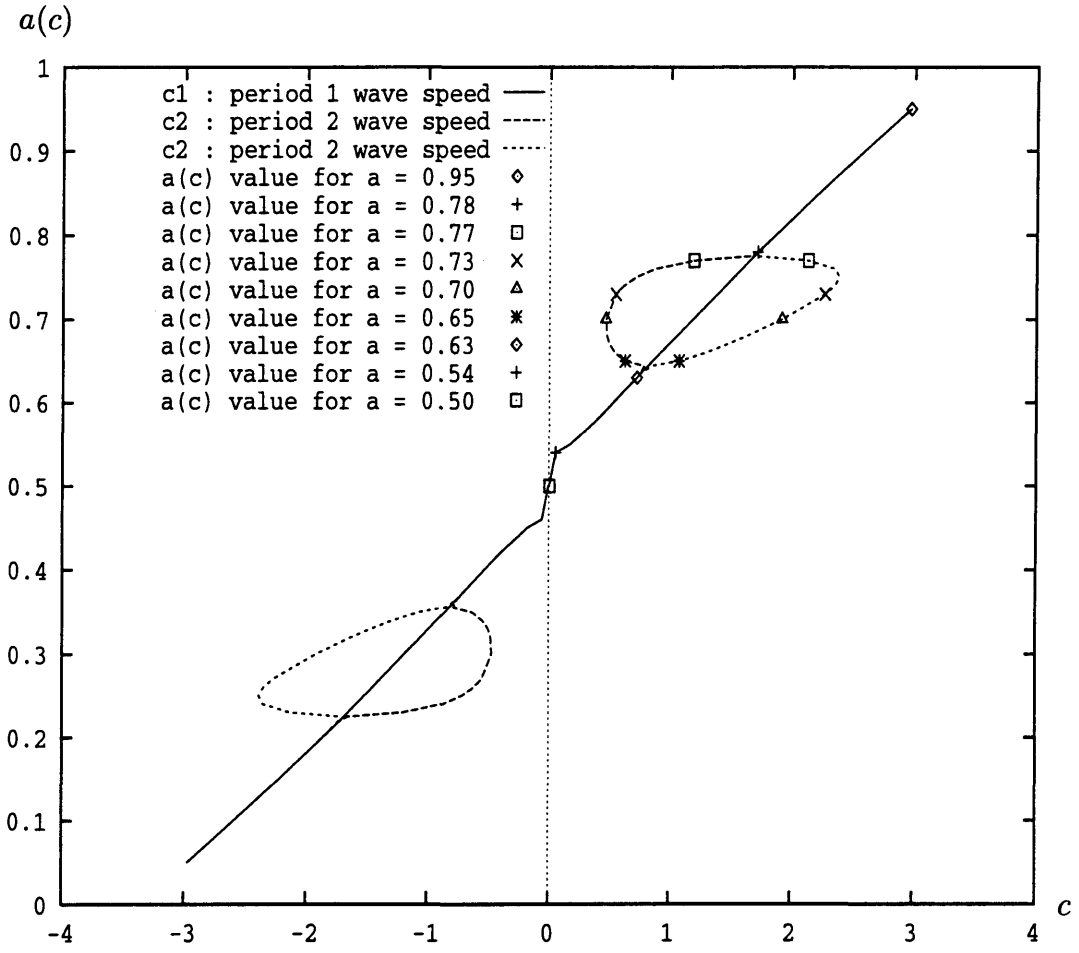

$$-c(\eta)\varphi'(\xi) - 10^{-3}\varphi''(\xi) = 1.6[\varphi(\xi+1) - 2\varphi(\xi) + \varphi(\xi-1)] - 15\varphi(\xi)(\varphi(\xi) - a)(\varphi(\xi) - 1)$$

Figure 5.5: Example 2: An $a(c)$ plot for a constant coefficient problem.

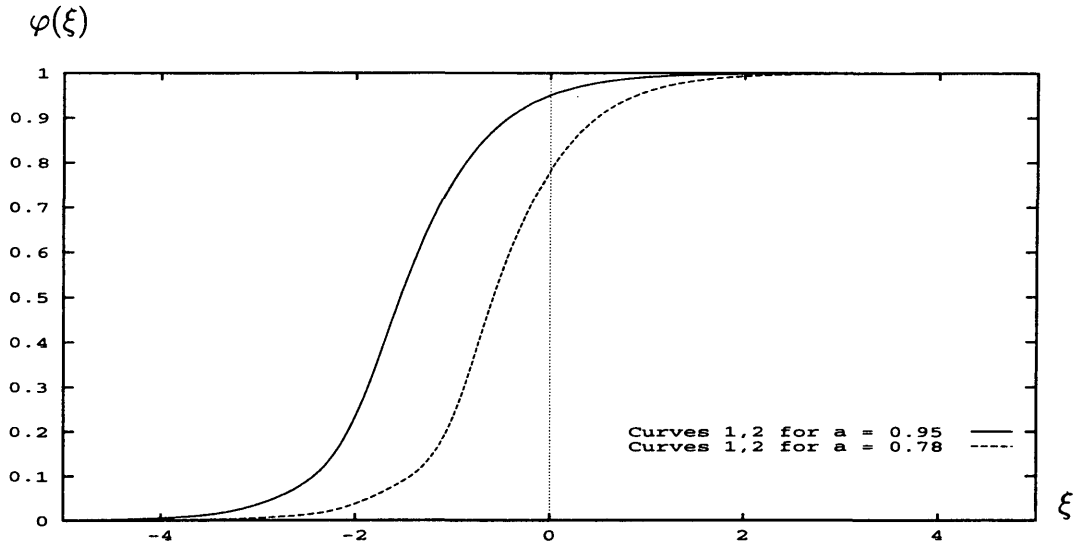

Figure 5.6: Example 2: Constant diffusion coefficients. No period splitting.

$$-c(\eta)\varphi'(\xi) - 10^{-3}\varphi''(\xi) = 1.6[\varphi(\xi+1) - 2\varphi(\xi) + \varphi(\xi-1)] - 15\varphi(\xi)(\varphi(\xi) - a)(\varphi(\xi) - 1)$$

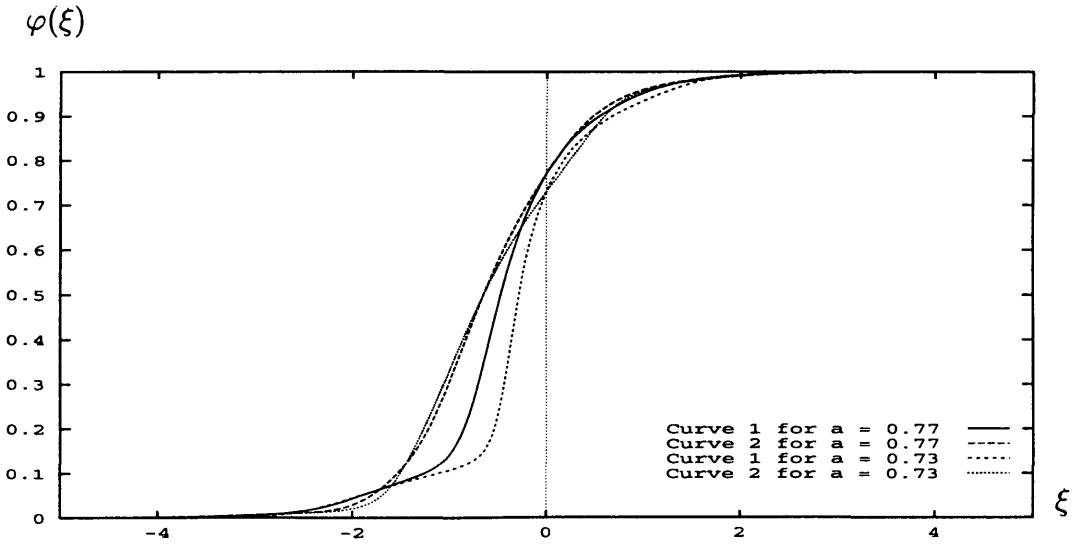

Figure 5.7: Example 2: Constant diffusion coefficients. Period splitting.

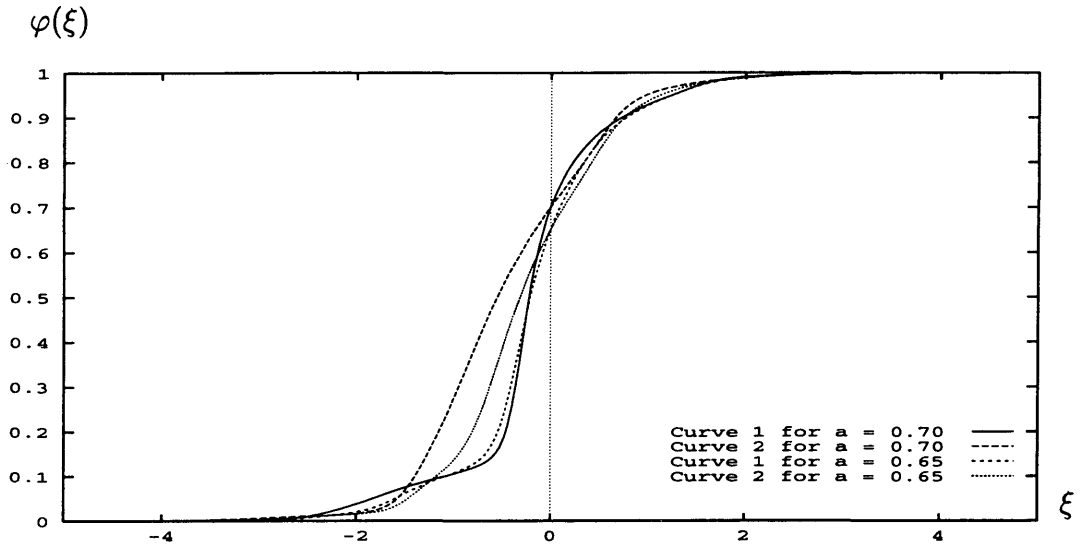

Figure 5.8: Example 2: Constant diffusion coefficients. Period splitting.

$$-c(\eta)\varphi'(\xi) - 10^{-3}\varphi''(\xi) = 1.6[\varphi(\xi+1) - 2\varphi(\xi) + \varphi(\xi-1)] - 15\varphi(\xi)(\varphi(\xi) - a)(\varphi(\xi) - 1)$$

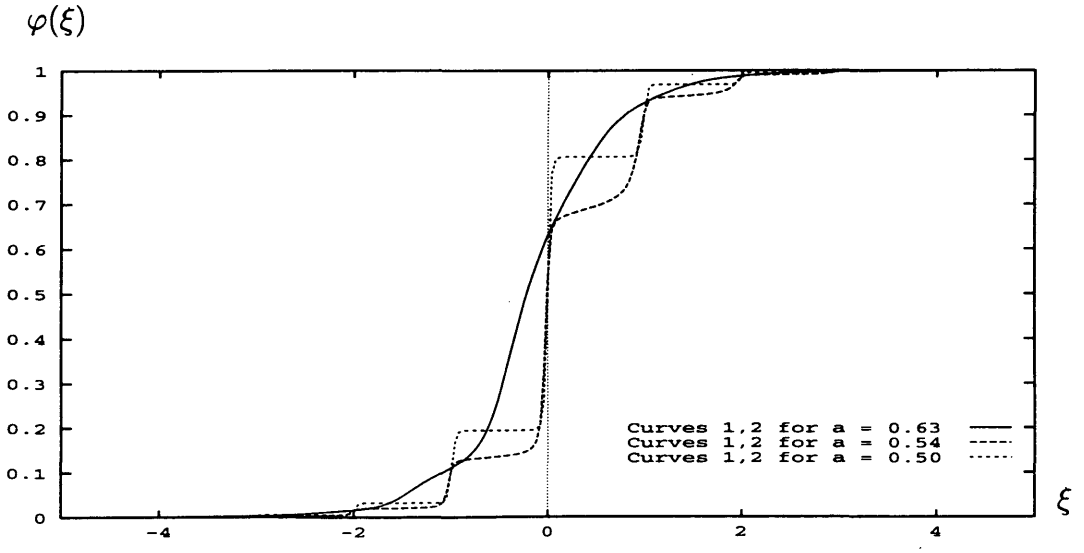

Figure 5.9: Example 2: Constant diffusion coefficients. No period splitting.

i) For each value of $a \neq 1/2$, *there exist two different values of* c, *both of which are the same sign.*

ii) There exists a "jump" in the c *values for some* $a \in (0.8466, 0.8470)$ *and for some* $a \in (0.1530, 0.1534)$.

iii) One of the pair of $a(c)$ *curves has a large interval for* a *in which* c *is small,* $|c| < 10^{-5}$, *while the other curve of the pair has no such nontrivial interval.*

Figures 5.11 through 5.17 are the corresponding solution plots. Starting with $a = 0.95$, Figure 5.11, we show how the pairs of solution curves associated with the $a(c)$ values progress as a decreases to 0.5, Figure 5.17.

Remark 5.2.3 *There exists a jump in the progression of the solution curves as* a *varies from* $a = 0.8470$ *to* $a = 0.8466$ *(Figures 5.12 and 5.13) corresponding to the jump in the wave speeds (Figure 5.10).*

Figure 5.18 consists of a set of various $a(c)$ curve pairs of the equation

$$- \; c(\eta)\varphi'(\xi) - 10^{-3}\varphi''(\xi) =$$

$$\alpha(\eta+1)[\varphi(\xi+1) - \varphi(\xi)] + \alpha(\eta)[\varphi(\xi-1) - \varphi(\xi)] - 15\varphi(\xi)(\varphi(\xi) - a)(\varphi(\xi) - 1)$$

for several sets of period two diffusion coefficients. The average of each pair of diffusion coefficients is 1.6.

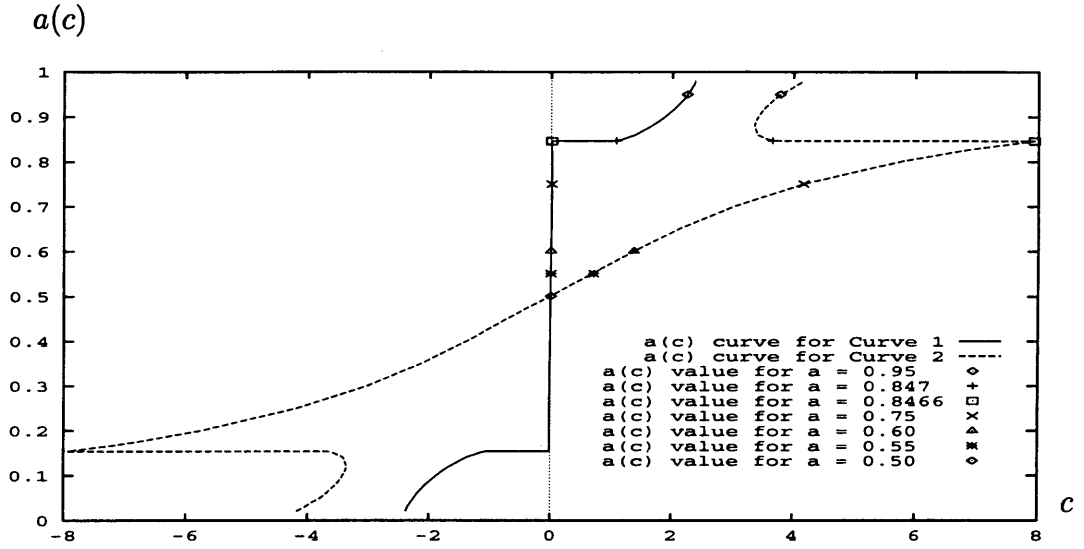

Figure 5.10: Example 2: An $a(c)$ plot for the period two pair of diffusion coefficients $\alpha = 1.3, 1.9$.

$$-c(\eta)\varphi'(\xi) - 10^{-3}\varphi''(\xi) =$$

$$\alpha(\eta+1)[\varphi(\xi+1) - \varphi(\xi)] + \alpha(\eta)[\varphi(\xi-1) - \varphi(\xi)] - 15\varphi(\xi)(\varphi(\xi) - a)(\varphi(\xi) - 1)$$

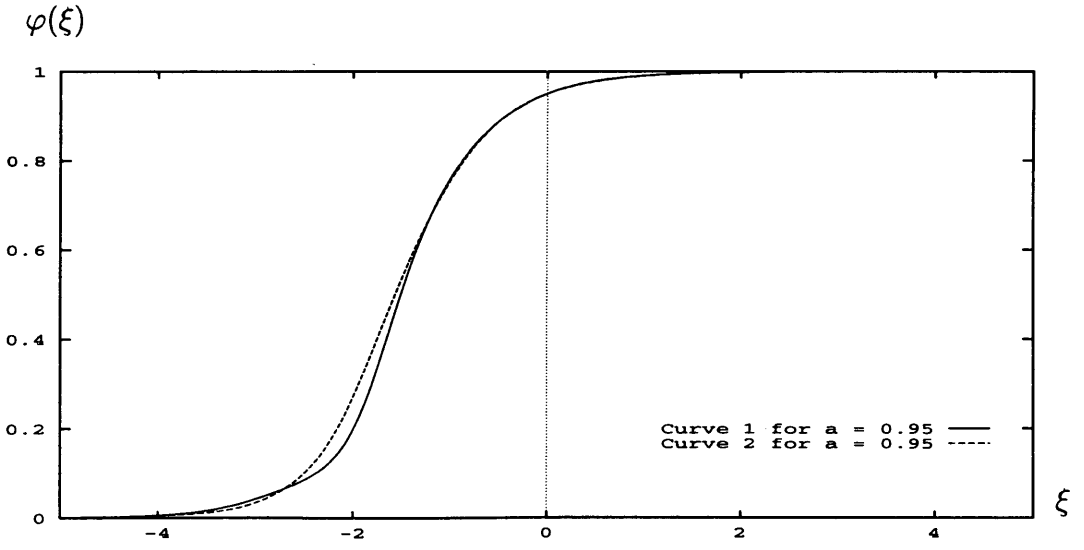

Figure 5.11: Example 2: A solution plot for the period two pair of diffusion coefficients $\alpha = 1.3, 1.9$.

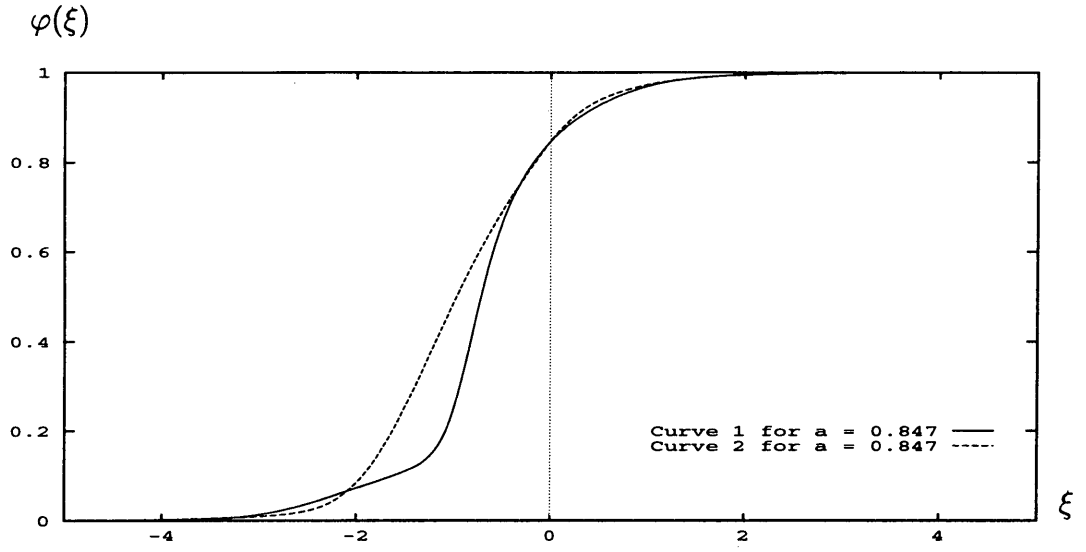

Figure 5.12: Example 2: A solution plot for the period two pair of diffusion coefficients $\alpha = 1.3, 1.9$.

$$-c(\eta)\varphi'(\xi) - 10^{-3}\varphi''(\xi) =$$
$$\alpha(\eta+1)[\varphi(\xi+1) - \varphi(\xi)] + \alpha(\eta)[\varphi(\xi-1) - \varphi(\xi)] - 15\varphi(\xi)(\varphi(\xi) - a)(\varphi(\xi) - 1)$$

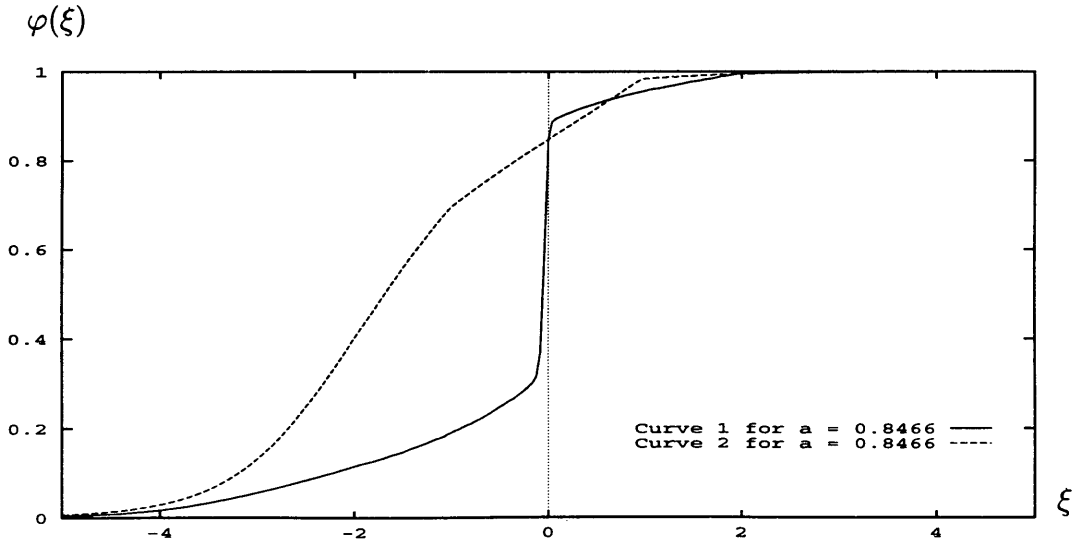

Figure 5.13: Example 2: A solution plot for the period two pair of diffusion coefficients $\alpha = 1.3, 1.9$.

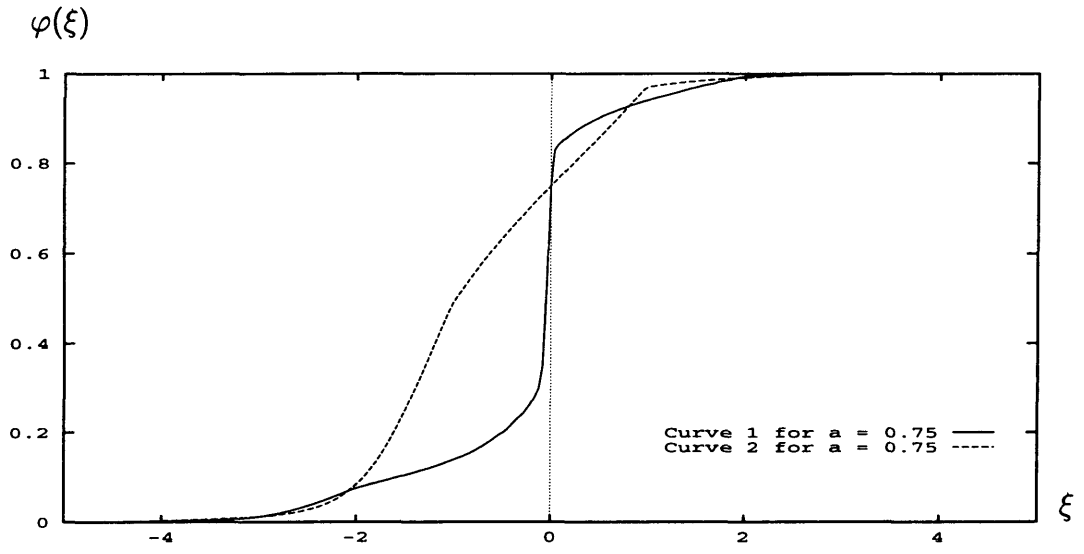

Figure 5.14: Example 2: A solution plot for the period two pair of diffusion coefficients $\alpha = 1.3, 1.9$.

$$-c(\eta)\varphi'(\xi) - 10^{-3}\varphi''(\xi) =$$
$$\alpha(\eta+1)[\varphi(\xi+1) - \varphi(\xi)] + \alpha(\eta)[\varphi(\xi-1) - \varphi(\xi)] - 15\varphi(\xi)(\varphi(\xi) - a)(\varphi(\xi) - 1)$$

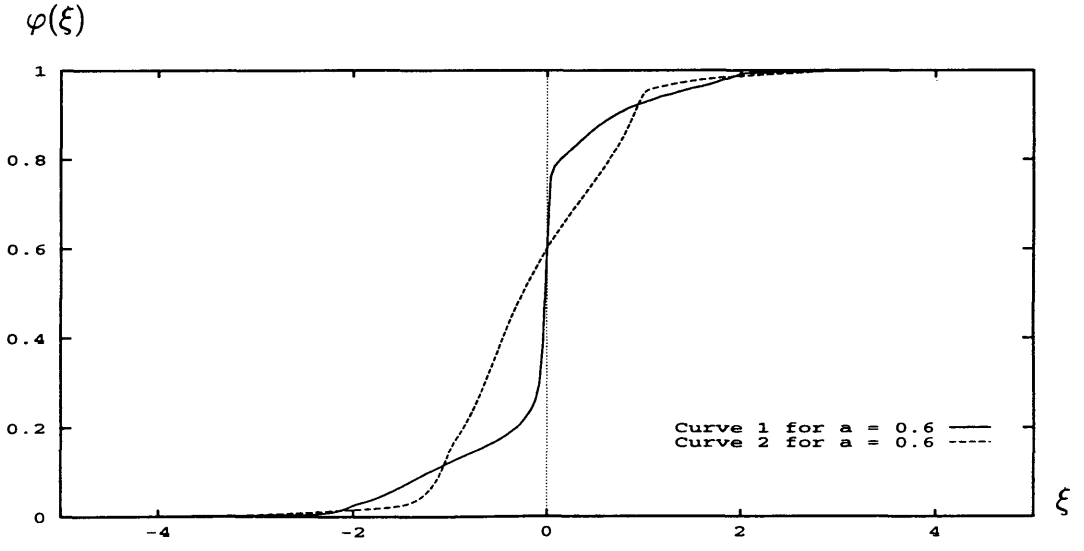

Figure 5.15: Example 2: A solution plot for the period two pair of diffusion coefficients $\alpha = 1.3, 1.9$.

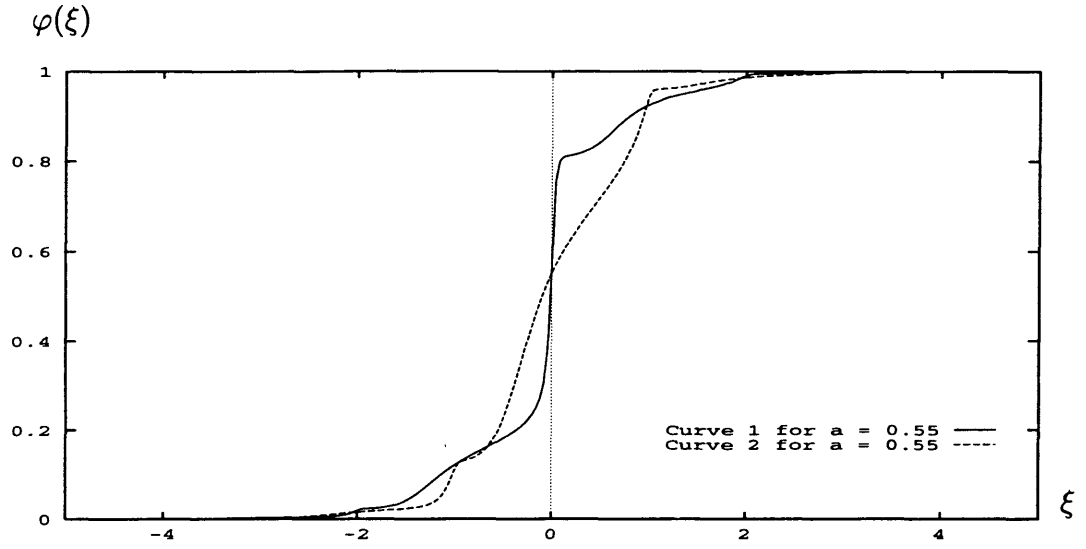

Figure 5.16: Example 2: A solution plot for the period two pair of diffusion coefficients $\alpha = 1.3, 1.9$.

$$-c(\eta)\varphi'(\xi) - 10^{-3}\varphi''(\xi) =$$
$$\alpha(\eta+1)[\varphi(\xi+1) - \varphi(\xi)] + \alpha(\eta)[\varphi(\xi-1) - \varphi(\xi)] - 15\varphi(\xi)(\varphi(\xi) - a)(\varphi(\xi) - 1)$$

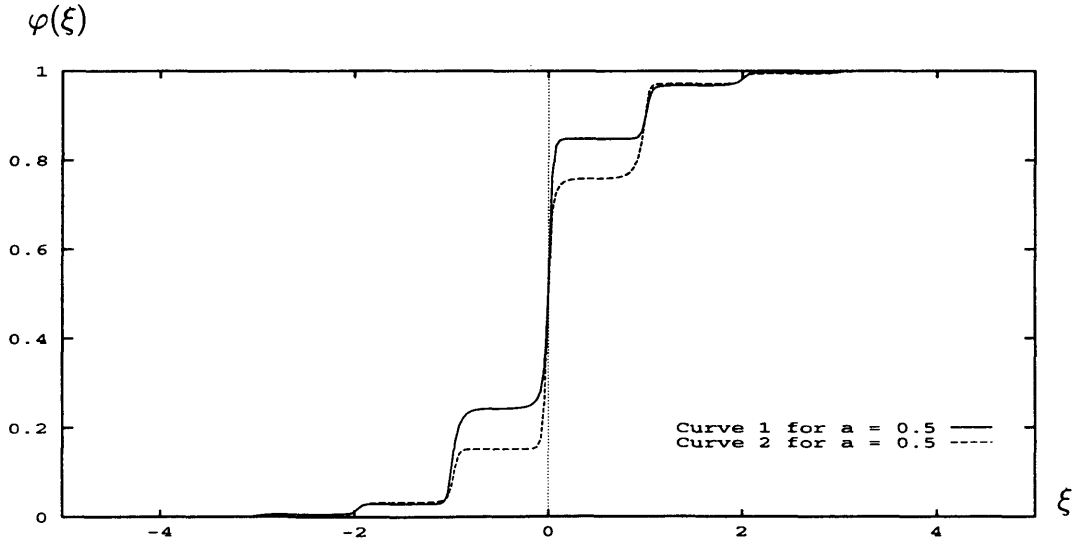

Figure 5.17: Example 2: A solution plot for the period two pair of diffusion coefficients $\alpha = 1.3, 1.9$.

Remark 5.2.4 *i) Starting with the $a(c)$ curves for $\alpha = (1.6, 1.6)$, we see in Figure 5.18, that as the distance between the two diffusion coefficient values increases, so does the distance between the two wave speeds.*

ii) There appears to be a vertical boundary, at $c = 0$, and two horizontal boundaries, at $a \approx 0.1532$ and $a \approx 0.8468$, which restrict the $a(c)$ curve pairs. This may imply a restriction on the magnitude of the difference in the two diffusion coefficient values.

The $a(c)$ plots of Figure 5.18 where found by applying our Newton's method to find the solution pair (φ, c) for various values of a.

5.3 Example 3: Inhomogeneous Equilibrium States

Thus far we have studied traveling wave solutions to problems that had constant or uniform equilibrium states, i.e., $\varphi(\eta - ct) \to 0$ as $\eta \to -\infty$ and $\varphi(\eta - ct) \to 1$ as $\eta \to \infty$. We now present a problem that we found in the conclusion of [10], in which the equilibrium states vary as the spatial variable $\eta \to \infty$. We consider

$$\dot{u}(\eta, t) - \gamma u_{\eta,\eta}(\eta, t) = L_D u(\eta, t) - f(u(\eta, t), a), \tag{5.3}$$

with $\eta \in \mathbb{Z}$,

$$L_D = \alpha[u(\eta + 1, t) - 2u(\eta, t) + u(\eta - 1, t)],$$

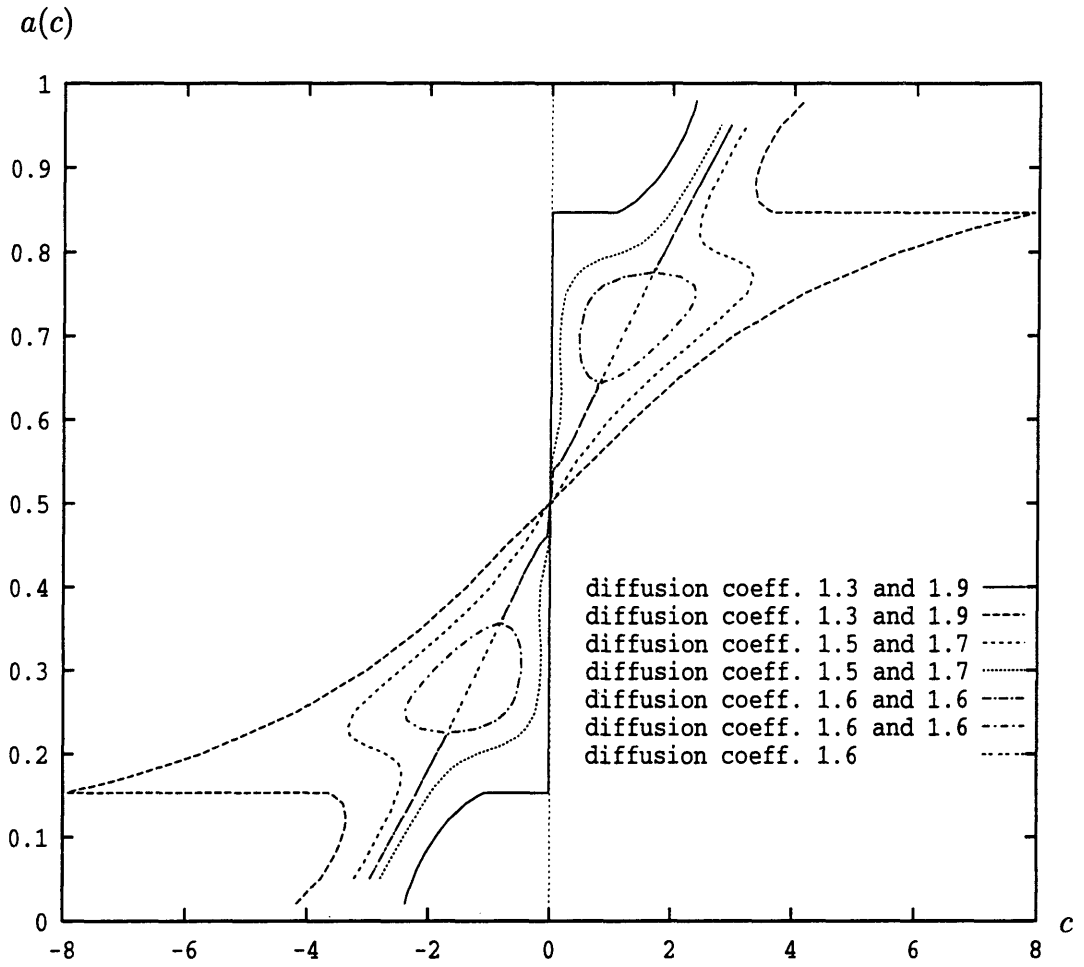

$$-c(\eta)\varphi'(\xi) - 10^{-3}\varphi''(\xi) =$$
$$\alpha(\eta+1)[\varphi(\xi+1) - \varphi(\xi)] + \alpha(\eta)[\varphi(\xi-1) - \varphi(\xi)] - 15\varphi(\xi)(\varphi(\xi) - a)(\varphi(\xi) - 1)$$

Figure 5.18: Example 2: A plot of $a(c)$ curves for various choices of period 2 diffusion coefficients. The average of each pair of coefficients is 1.6. The $a(c)$ curves appear in pairs.

and f is one of our bistable nonlinearities. Since for these f's, $f(0) = 0$, one equilibrium state is $u = 0$ for all η. Another equilibrium state is given by

$$u(\eta, t) = \begin{cases} k_e, & \eta \text{ even}, \\ k_o, & \eta \text{ odd}, \end{cases}$$

for particular values $k_e, k_o \in \mathbb{R}$. Since

$$L_D u(\eta, t) = \begin{cases} 2\alpha(k_o - k_e), & \eta \text{ even}, \\ 2\alpha(k_e - k_o), & \eta \text{ odd}, \end{cases}$$

by setting the right-hand side of (5.3) equal to zero, we obtain the conditions

$$f(k_e) = 2\alpha(k_o - k_e), \qquad f(k_o) = 2\alpha(k_e - k_o).$$

For $f = f_1$, (1.9), this means that for any a such that $k_o < a < k_e$,

$$k_e = \frac{1 + 2\alpha}{1 + 4\alpha}, \quad \text{and} \quad k_o = \frac{2\alpha}{1 + 4\alpha}.$$

In the spatial variable η, this equilibrium condition is like a one-dimensional checker board.

But we are interested in traveling wave solutions. Letting $\eta = 2j, j \in \mathbb{Z}$ we set

$$v(j,t) = u(\eta,t) \quad \text{and} \quad w(j,t) = u(\eta+1,t).$$

Then (5.3) may be rewritten as the system

$$\dot{v}(j,t) - \gamma v_{x,x}(j,t) = \alpha[w(j-1,t) + w(j,t) - 2v(j,t)] - f(v(j,t)),$$
$$\dot{w}(j,t) - \gamma w_{x,x}(j,t) = \alpha[v(j,t) + v(j+1,t) - 2w(j,t)] - f(w(j,t)),$$

and by substituting the pair of traveling wave ansatz,

$$v(j,t) = \varphi(j-ct), \qquad w(j,t) = \psi(j-ct),$$

we obtain the system of traveling wave equations

$$-c\varphi'(\xi) - \gamma\varphi''(\xi) = \alpha[\psi(\xi-1) + \psi(\xi) - 2\varphi(\xi)] - f(\varphi(\xi)),$$
$$-c\psi'(\xi) - \gamma\psi''(\xi) = \alpha[\varphi(\xi) + \varphi(\xi+1) - 2\psi(\xi)] - f(\psi(\xi)), \tag{5.4}$$

with $\xi = j - ct$ and boundary conditions

$$(\varphi,\psi)(-\infty) = (0,0), \qquad (\varphi,\psi)(\infty) = (k_e,k_o). \tag{5.5}$$

The following solution plots were obtained by solving the system (5.4) with boundary conditions (5.5) and nonlinearity f_1 using the fixed point method. Since we provide a and solve for φ, ψ, and c, the terms $-c\psi'$ and $-c\varphi'$ are nonlinear.

Figures 5.19 and 5.20 are each a solution set to the inhomogeneous problem. In Figure 5.19, $\gamma = 1$ and $\alpha = 1$. The continuous diffusion operator dominates in this solution, producing hyperbolic tangent shaped curves. In Figure 5.20, $\gamma = 10^{-9}$ and $\alpha = 1$. Here we see the solution behavior generated when the discrete diffusion term dominates, in particular, we see the familiar solution "kinks" caused by solving with the nonlinearity f_1.

Remark 5.3.1 *In both Figures 5.19 and 5.20, the detuning parameter* $a = 1/2$. *In the previous homogeneous equilibria problems we have studied, when* $a = 1/2$, *the wave speed* $c = 0$. *This is not true here. The value of the wave speed for the solution in Figure 5.19 is* $c \approx 1.006$ *and for the solution in Figure 5.20 is* $c \approx 0.516$. *This implies that waves in this case are not being propagated by an asymmetry of the potential, but by the relation between the equilibria and the potential.*

In Figures 5.21 and 5.22, we reexamine the problem of Figure 5.20 for various values of a. Figure 5.21 illustrates the upper member of the solution set and Figure 5.22 shows the lower.

Remark 5.3.2 *In Figures 5.21 and 5.22, for* $a = 0.46$, $c \approx 0.271$ *and for* $a = 0.54$,

$c \approx 0.810$. *In the previous homogeneous equilibria problems, the magnitude of* c *increased as the distance* $|a - 1/2|$ *increased. As we can see, this is not true here.*

5.4 Chapter Summary

We have solved a variety of problems in this chapter, showing some of the versatility of our numerical methods. The proof of Newton's method in Chapter 4 helped in producing numerical results by providing guidance in applying the method. Through these examples, we have seen that propagation failure is not an artifact of a discontinuous nonlinearity and that the slope at a affects the solution profile. The step-like solution behavior first exhibited in Chapter 2, when solving with nonlinearity f_1, also appears when solving with smooth nonlinearities. While solving the problem with period two diffusion, we discovered bifurcation points which appear in the solution pair $(\varphi(a), c(a))$ for the constant coefficient equation. In addition, for the period two diffusion problem, there seem to be limitations on the possible values of the diffusion coefficients such as their distance apart. We present an example of the reaction-diffusion equation applied to a system with inhomogeneous equilibria which demonstrates that a symmetric bistable nonlinearity can be associated with wave propagation.

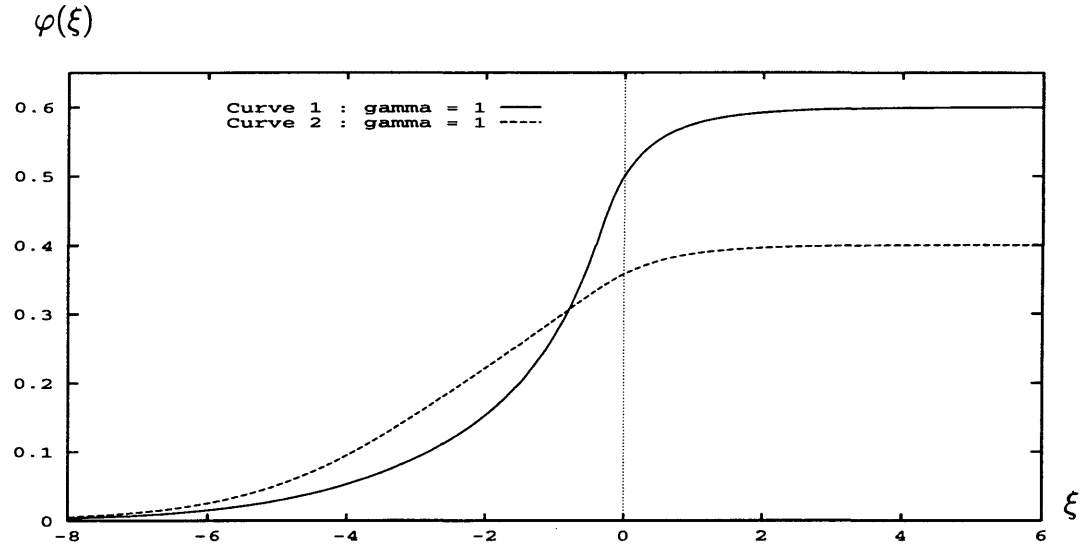

Figure 5.19: Example 3: A solution plot for the inhomogeneous equilibria $k_o = 0.4$ and $k_e = 0.6$ with $a = 0.5$ and $c \approx 1.006$.

$$-c\varphi'(\xi) - \gamma\varphi''(\xi) = [\psi(\xi - 1) + \psi(\xi) - 2\varphi(\xi)] - f_1(\varphi(\xi), 0.5)$$
$$-c\psi'(\xi) - \gamma\psi''(\xi) = [\varphi(\xi) + \varphi(\xi + 1) - 2\psi(\xi)] - f_1(\psi(\xi), 0.5)$$

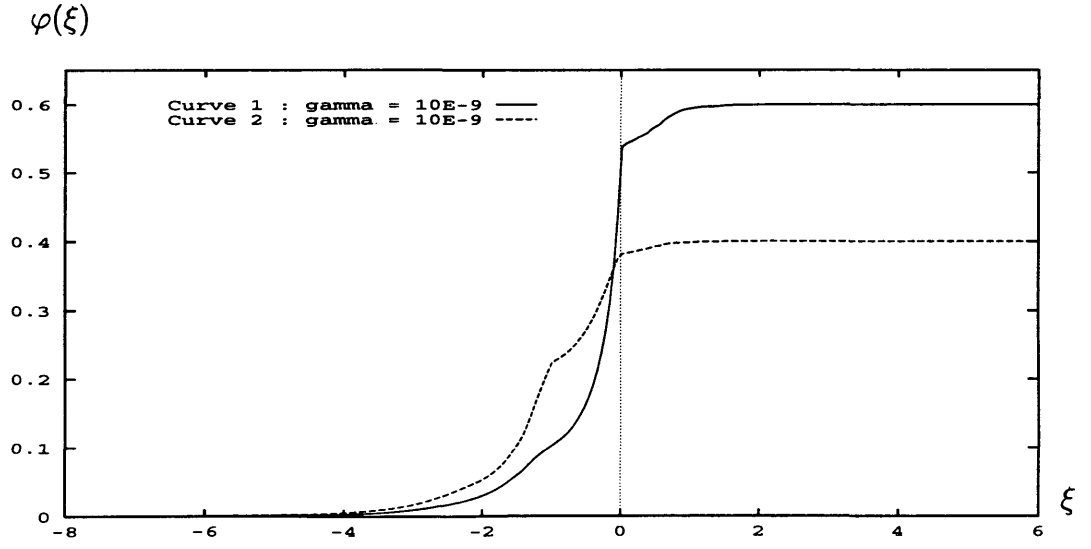

Figure 5.20: Example 3: A solution plot for the inhomogeneous equilibria $k_o = 0.4$ and $k_e = 0.6$ with $a = 0.5$ and $c \approx 0.516$.

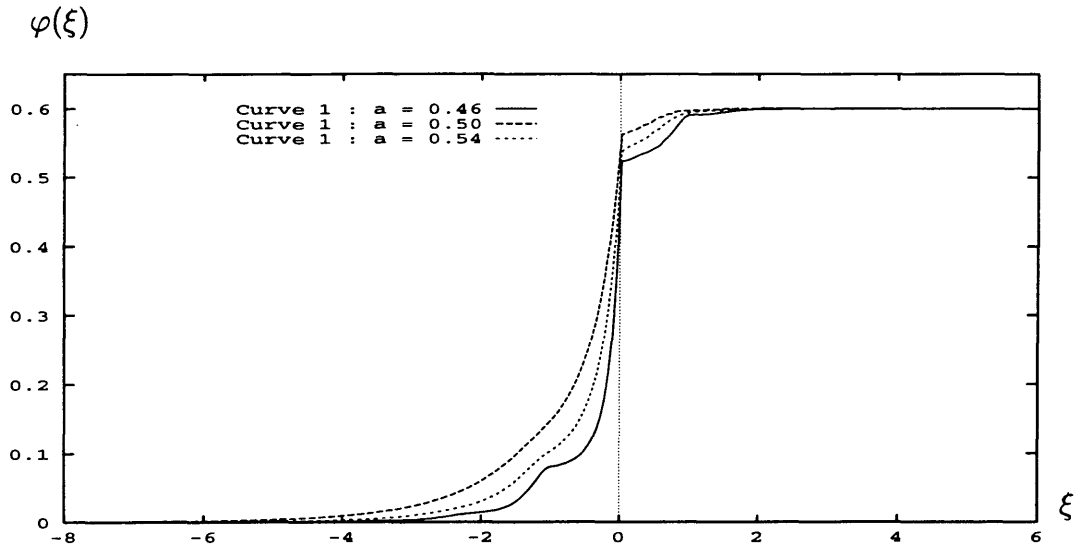

Figure 5.21: Example 3: The k_e curve for the inhomogeneous equilibria $k_o = 0.4$ and $k_e = 0.6$ for various values for a.

$$-c\varphi'(\xi) - 10^{-9}\varphi''(\xi) = [\psi(\xi - 1) + \psi(\xi) - 2\varphi(\xi)] - f_1(\varphi(\xi), a)$$
$$-c\psi'(\xi) - 10^{-9}\psi''(\xi) = [\varphi(\xi) + \varphi(\xi + 1) - 2\psi(\xi)] - f_1(\psi(\xi), a)$$

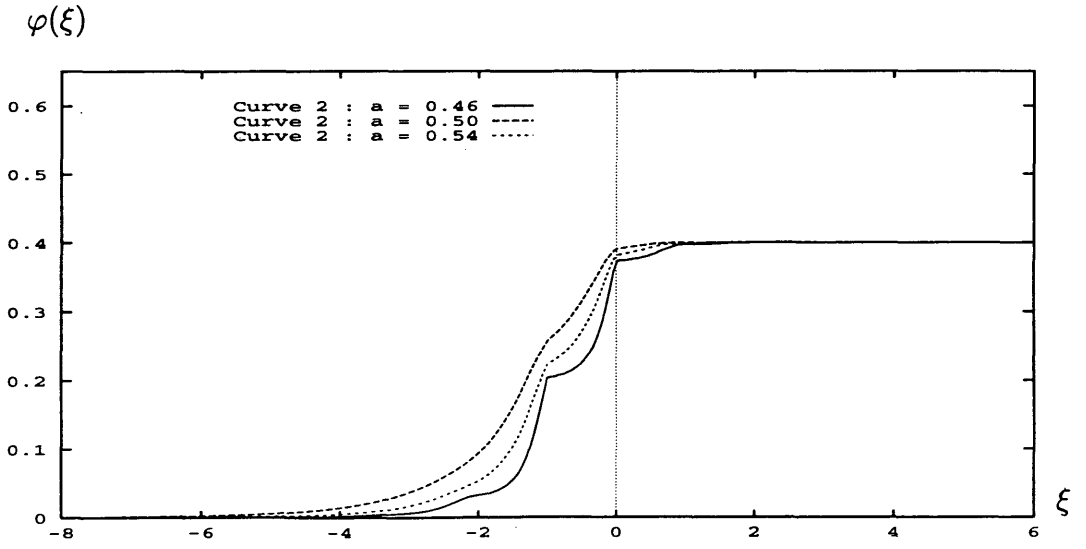

Figure 5.22: Example 3: The k_o curve for the inhomogeneous equilibria $k_o = 0.4$ and $k_e = 0.6$ for various values for a.

Chapter 6

CONCLUSIONS AND FUTURE DIRECTIONS

6.1 Conclusions

We presented an investigation of bistable differential-difference equations. In particular, we looked at traveling wave solutions, solutions that connect the two stable equilibria in an heteroclinic orbit. Our investigation focused on presenting explicit solutions to various differential-difference equations, where a solution for a particular nonlinearity and detuning parameter a, consisted of a wave-like function φ and the speed, c, of φ with respect to the underlying lattice. Although the analytical and numerical techniques used are based on the work of others, the specific applications and development of these techniques presented in this thesis was new.

6.2 Future Directions

This work opens up many possible directions for future work. Perhaps the key to any future continuation of the ideas here is the use of Fredholm theory for functional differential equations. Because of the behavior of these closed orbit equations, and because of the potentially high dimension of such systems, we feel further investigations should also consider using the Lyapunov-Schmidt reduction.

Recall that the traveling wave version of our differential-difference equations are highly directionally dependent, dependent on the underlying reference lattice, unlike the traveling wave version of the differential models of the same type. We intend to develop a numerical method for solving the partial differential-difference equations, not their traveling wave form, to see if the same directional dependence appears as in the traveling wave formulations. Hopefully, this will support the concept of constructing general solutions from traveling wave solutions.

The Newton's method we present, and its convergence proof, appears to be generalizable to general parameterized dynamical systems represented by differential-difference equations that possess connecting orbit solutions (traveling wave solutions are connecting orbit solutions).

One of the main interests in exploring variable diffusion problems is to deal with the problem of finding a traveling wave solution across a single interface between two materials, between two lattice domains that possess different properties.

The domain of the traveling wave equations we study is all of $\mathbb{R}$. In all of our numerical applications we truncate this interval, then solve, approximating the "tails" of our solutions with asymptotic boundary conditions (with exponentially decaying functions). Because of the strong attraction of the stable equilibria in our equations, this is an effective solution. As we increase the variations in the type of equations being considered, the need for allowing the truncation interval to vary as part of the numerical solution process may become apparent.

Additional directions include: discovering the full bifurcation maps for the (φ, c) pair of various constant coefficient equations; using other phase conditions, such as minimizing the change in solution between successive iterations; and using more sophisticated damping terms instead of the viscous damping term used here.

BIBLIOGRAPHY

[1] S. Allen and J.W. Cahn, A Microscopic Theory for Antiphase Boundary Motion and its Application to Antiphase Domain Coarsening, *Acta Metallurgica* **27** (1979) 1084–1095.

[2] U. Ascher, J. Christiansen, and R.D. Russell, Collocation Software for Boundary-Value Odes, *Acm Trans. Math Software 7* (1981), 209-222.

[3] U. Ascher, J. Christiansen, and R.D. Russell, Colsys - A Collocation Code for BoundaryValue Problems, *Acm Trans. Math Software 7* (1981), 209-222.

[4] U. Ascher, R. M. Mattheij, and R.D. Russell, *Numerical Solution of Boundary Value Problems for Ordinary Differential Equations* (Prentice Hall, Englewood Cliffs, N.J., 1988).

[5] J. Bell, Some Threshold Results for Models of Myelinated Nerves, *Math. Biosciences* **54** (1981) 181–190.

[6] J. Bell and C. Cosner, Threshold Behavior and Propagation for Nonlinear Differential-Difference Systems Motivated by Modeling Myelinated Axons, *Quart. Appl. Math.* **42** (1984) 1–114.

[7] W.J. Beyn, The Numerical Computation of Connecting Orbits in Dynamical Systems, *IMA J. Numer. Anal.* **9** (1990) 379–405.

[8] J.W. Cahn, Theory of Crystal Growth and Interface Motion in Crystalline Materials, *Acta Metallurgica* **8** (1960) 554–562.

[9] J.W. Cahn, S.-N. Chow, and E.S. Van Vleck, Spatially Discrete Nonlinear Diffusion Equations, *Rocky Mountain J. Math.* **25** (1995) 87–117.

[10] J.W. Cahn, J. Mallet-Paret, and E.S. Van Vleck, Traveling Wave Solutions for Systems of ODE's on a Two-Dimensional Spatial Lattice, *to appear in SIAM J. Appld. Math.*

[11] J.R. Cash, G. Moore, and R.W. Wright, An Automatic Continuation Strategy for the Solution of Singularly Perturbed Linear Two-Point Boundary Value Problems, *J. Comp. Phys.* **122** (1995), 266–279.

[12] J.R. Cash, G. Moore, and R.W. Wright, An Automatic Continuation Strategy for the Solution of Singularly Perturbed Nonlinear Two-Point Boundary Value Problems, *to appear.*

[13] H. Chi, J. Bell, and B. Hassard, Numerical Solution of a Nonlinear Advance-Delay-Differential Equation from Nerve Conduction Theory, *J. Math. Biol.* **24** (1986) 583-601.

[14] S.-N. Chow and W. Shen, Stability and Bifurcation of Traveling Wave Solutions in Coupled Map Lattices, *Dyn. Syst. Appl.* **4** (1995) 1–26.

[15] L.O. Chua and T. Roska, The CNN Paradigm, *IEEE Trans. Circuits Syst.* **40** (1993) 147–156.

[16] L.O. Chua and L. Yang, Cellular Neural Networks: Theory, *IEEE Trans. Circuits Syst.* **35** (1988) 1257–1272.

[17] L.O. Chua and L. Yang, Cellular Neural Networks: Applications, *IEEE Trans. Circuits Syst.* **35** (1988) 1273–1290.

[18] H.E. Cook, D. de Fontaine, and J.E. Hilliard, A Model for Diffusion on Cubic Lattices and its Application to the Early Stages of Ordering, *Acta Metallurgica* **17** (1969) 765–773.

[19] E.J. Doedel and M.J. Friedman, Numerical Computation of Heteroclinic Orbits, *J. Comp. Appl. Math.* **25** (1989) 155–171.

[20] D.B. Duncan and M.A.M. Lynch, Jacobi Iteration in Implicit Difference Schemes for the Wave Equation, *SIAM J. Numer. Anal.* **28** (1991) 1661–1679.

[21] C.E. Elmer and E.S. Van Vleck, Computation of Traveling Wave Solutions for Spatially Discrete Bistable Reaction-Diffusion Equations, *Appld. Numer. Math.* **20** (1996) 157–169.

[22] G.B. Ermentrout, Stable Periodic Solutions to Discrete and Continuum Arrays of Weakly Coupled Nonlinear Oscillators, *SIAM J. Appl. Math.* **52** (1992) 1665–1687.

[23] G.B. Ermentrout and N. Kopell, Inhibition-produced Patterning in Chains of Coupled Nonlinear Oscillators, *SIAM J. Appl. Math.* **54** (1994) 478–507.

[24] T. Erneux and G. Nicolis, Propagating Waves in Discrete Bistable Reaction-Diffusion Systems, *Physica D* **67** (1993) 237–244.

[25] P.C. Fife and L. Hsiao, The Generation and Propagation of Internal Layers, *Num. Anal. TMA* **12** (1988) 19–41.

[26] P. Fife and J. McLeod, The Approach of Solutions of Nonlinear Diffusion Equations to Traveling Front Solutions, *Arch. Rat. Mech. Anal.* **65** (1977) 333–361.

[27] W.J. Firth, Optical Memory and Spatial Chaos, *Phys. Rev. Lett.* **61** (1988) 329–332.

[28] M.J. Friedman and E.J. Doedel, Numerical Computation and Continuation of Invariant Manifolds Connecting Fixed Points, *SIAM J. Numer. Anal.* **28** (1991) 789–808.

[29] F.N. Fritsch and R.E. Carlson, Monotone Piecewise Cubic Interpolation, *SIAM J. Numer. Anal.* **17** (1980) 238–246.

[30] W.-Z. Gao, Threshold Behavior and Propagation for a Differential-Difference System, *SIAM J. Math. Anal.* **24** (1993) 89–115.

[31] G.H. Golub and C. Van Loan, *Matrix Computations* (Johns Hopkins University Press, Baltimore, MD, 1989).

[32] C.P. Grant and E.S. Van Vleck, Slowly-Migrating Transition Layers for the Discrete Allen-Cahn and Cahn-Hillard Equations, *Nonlinearity* **8** (1995) 861–876.

[33] W. Hackbusch, *Iterative Solution of Large Sparse Systems of Equations* (Springer-Verlag, New York, 1994).

[34] J.K. Hale, *Theory of Functional Differential Equations* (Springer-Verlag, New York, NY, 1977).

[35] J.K. Hale, *Ordinary Differential Equations* (Krieger, Malabar, FL, 1980).

[36] D. Hankerson and B. Zinner, Wavefronts for a Cooperative Tridiagonal System of Differential Equations, *J. Dyn. Diff. Eq.* **5** (1993) 359–373.

[37] M. Hillert, A Solid-Solution Model for Inhomogeneous Systems, *Acta Metallurgica* **9** (1961) 525–535.

[38] M.E. Johnston, Bifurcations of Coupled Bistable Maps, *Physics Letters A* (1997).

[39] M.E. Johnston, Bifurcations Associated with Wave Propagation and its Failure in Chains of Bistable Units, *Preprint.*

[40] J.P. Keener, Propagation and its Failure in Coupled Systems of Discrete Excitable Cells, *SIAM J. Appl. Math.* **22** (1987) 556–572.

[41] J.P. Keener, The Effects of Discrete Gap Junction Coupling on Propagation in Myocardium, *J. Theor. Biol.* **148** (1991) 49–82.

[42] N. Kopell, G.B. Ermentrout, and T.L. Williams, On Chains of Oscillators Forced at One End, *SIAM J. Appl. Math.* **51** (1991) 1397–1417.

[43] J.P. Laplante and T. Erneux, Propagation Failure in Arrays of Coupled Bistable Chemical Reactors, *J. Phys. Chem.* **96** (1992) 4931–4934.

[44] M. Lentini and H.B. Keller, Boundary Value Problems on Problems on Semi-Infinite Intervals and Their Numerical Solution, *SIAM J. Numer. Anal.* **17** (1980) 577–604.

[45] R.S. Mackay and J.-A. Sepulchre, Multistability in Networks of Weakly Coupled Bistable Units, *Physica D,* **82** (1995) 243–254.

[46] J. Mallet-Paret, The Fredholm Alternative for Functional Differential Equations of Mixed Type, *preprint.*

[47] J. Mallet-Paret, The Global Structure of Traveling Waves in Spatially Discrete Dynamical Systems, *preprint.*

[48] H. McKean, Nagumo's Equation, *Adv. Math.* **4** (1970) 209–223.

[49] J. Ortega and W. Rheinboldt, *Iterative Solution of Nonlinear Equations in Several Variables* (Academic Press, San Diego, CA, 1970)

[50] K.J. Palmer, Exponential Dichotomies and Transversal Homoclinic Points, *J. Differ. Eqns.* **55** (1984) 225–256.

[51] T. Roska and L.O. Chua, The CNN Universal Machine: an Analogic Array Computer, *IEEE Trans. Circuits Syst.* **40** (1993) 163–173.

[52] W. Rudin, *Principles of Mathematical Analysis* (McGraw-Hill Publishing Company, New York, N.Y., 1976).

[53] W. Rudin, *Functional Analysis* (McGraw-Hill Publishing Company, New York, N.Y., 1991).

[54] A. Rustichini, Functional Differential Equations of Mixed Type: the Linear Autonomous Case, *J. Dyn. Diff. Eq.* **1** (1989), 121-143.

[55] A. Rustichini, Hopf Bifurcations for Functional Differential Equations of Mixed Type, *J. Dyn. Diff. Eq.* **113** (1994), 145-177.

[56] L.I. Schiff, Nonlinear Menson Theory of Nuclear Forces, I, *Phys. Rev.* **84** (1951) 1–9.

[57] I.E. Segal, The Global Cauchy Problem for a Relativistic Scalar Field with Power Interaction, *Bull. Soc. Math. France* **91** (1963) 129–135.

[58] I.E. Segal, Nonlinear Relativistic Partial Differential Equations, *Proc. Int. Congress Math. Moscow* (1966) 681–690.

[59] L.F. Shampine, R.C. Allen Jr., S. Pruess, *Fundamentals of Numerical Computing* (J. Wiley and Sons, New York, N.Y., 1997).

[60] W. Shen, Traveling Waves in Time Almost Periodic Structures Governed by Bistable Nonlinearities I. Stability and Uniqueness, *preprint.*

[61] W. Shen, Traveling Waves in Time Almost Periodic Structures Governed by Bistable Nonlinearities II. Existence, *preprint.*

[62] R. Temam, *Infinite-Dimensional Dynamical Systems in Mechanics and Physics* (Springer-Verlag, New York, N.Y., 1988).

[63] P. Thiran, K.R. Crounse, L.O. Chua, and M. Hasler, Pattern Formation Properties of Autonomous Cellular Neural Networks, *IEEE Trans. Circuits Syst.* **42** (1995) 757–774.

[64] A.I. Volpert, V.A. Volpert, and V.A. Volpert, *Traveling Wave Solutions of Parabolic Systems* (American Mathematical Society, Providence, RI, 1994)

[65] R.L. Winslow, A.L. Kimball, and A. Varghese, Simulating Cardiac Sinus and Atrial Network Dynamics on the Connection Machine, *Physica D* **64** (1993) 281–298.

[66] R. Wright, J. Cash, and G. Moore, Mesh Selection for Stiff Two-Point Boundary Value Problems, *Numer. Algorithms* **7** (1994), 205–224.

[67] B. Zinner, Stability of Traveling Wavefronts for the Discrete Nagumo Equation, *SIAM J. Math. Anal.*, **22** (1991) 1016–1020.

[68] B. Zinner, Existence of Traveling Wavefront Solutions for the Discrete Nagumo Equation, *J. Diff. Eq.* **96** (1992) 1–27.

[69] B. Zinner, G. Harris, and W. Hudson, Traveling Wavefronts for the Discrete Fisher's Equation, *J. Diff. Eq.* **105** (1993) 46–62.